Pharmacological Screening and Evaluation of Novel Chemical Entities in Cardiometabolic Disorders

A synopsis submitted to

THE MAHARAJA SAYAJIRAO UNIVERSITY OF BARODA

For the partial fulfillment of degree of

DOCTOR OF PHILOSOPHY
in
PHARMACY

By

SAGAR PIYUSHKUMAR PATEL

Under the guidance of

DR. KIRTI. V. PATEL
Associate Professor & Head
Faculty of Pharmacy

Faculty of Pharmacy
The Maharaja Sayajirao University of Baroda
Vadodara - 390 001

July 2022

TABLE OF CONTENTS

1. INTRODUCTION

Cardiometabolic disorders (CMets) have turned into an epidemic represented by constellation of metabolic dysfunction characterized by insulin resistance with hyperglycemia, hypertension, atherogenic dyslipidemia, intra-abdominal adiposity, hypercoagulability and pro-inflammatory stage(1).Repercussions of CMets include Atherosclerotic Cardiovascular Diseases (ASCVDs), diabetes mellitus and chronic renal failure. Statistics from the World Health Organization reflects that only cardiovascular mortality accounts for 18.5 million death (around 32.8%) globally(2). Among them ischemic heart disease (49.2%), ischemic stroke disease (17.7%), hypertensive heart disease and circulatory disease (9.5%) contribute to be the leading causes (3). Statistics from India are also in line with these staggering numbers reflecting 1.63 million deaths in India (4). Individuals at risk of CVD may demonstrate raised blood pressure, glucose and lipids as well as overweight and obesity. Recent clinical studies have demonstrated that hypertension and metabolic syndrome play significant role in initiation and progression of cardiovascular events either alone or in combination leading to significant increase in risk of sudden cardiac death(5),(6).

Hypertension is one of the major modifiable risk factors of the cardiovascular associated events (7). Definitions of hypertension have been revised over time owing to clinical studies in diverse populations and research elaborating the etiopathology of hypertension(8). It can be generalized on the basis of recent guidelines of ACC/AHA 2020 that an individual is hypertensive if his/her blood pressure (BP) is above 130/80 mm Hg(9). The etiology of hypertension involves the complex interplay of environmental and pathophysiological factors as well as genetic predisposition that affect multiple systems. The regulation of BP is a very complex physiological function, which depends on a continuum of actions of cardiovascular, neural, renal and endocrine systems. Briefly, sympathetic and parasympathetic regulation constitute neural control, renin angiotensin aldosterone system (RAAS) represents renal control while local endothelium derived factors such as nitric oxide, bradykinin, substance P make up the endocrine system. These systems work in tandem to maintain the hemostasis of blood pressure (10).

Sympathetic nervous system (SNS) and RAAS are recognized as the major governing regulatory mechanism for maintenance of BP. SNS handles wide spectrum of responses ranging from mild to massive and from acute to chronic changes in BP(11). Release of catecholamines upon SNS stimulation leads to vasoconstriction in the peripheral beds,

along with an increase in the chronotropic and inotropic action of the heart(12). The SNS is the only system of the body capable of both momentary and sustained regulation of BP. On the other hand, RAAS maintains the blood pressure both directly and indirectly. Directly, through the vasoconstrictive action of the octapeptide angiotensin II (AngII) released upon ACE-mediated hydrolysis of angiotensin I and indirectly, through stimulating aldosterone release leading to sodium-water retention contributing to increase in total blood volume.

Moreover, there are ample evidences suggesting that these two systems do not only work independently but are connected in extricable and reciprocal manner(13). It is reported that heightened activation of sympathetic flow promotes activation of RAAS system by increasing renin secretion and aldosterone production in renal tubule ultimately causing increased blood volume. Simultaneously, release of renin from juxtaglomerular cells stimulates release of catecholamines from presynaptic nerve terminals. At molecular level, norepinephrine modulates AngII receptors via interaction with α_1 adrenergic receptors (14, 15) while intracerebral injection of AngII may trigger a sympathetically mediated rise in blood pressure (16-18). Stimulation of presynaptic AngII receptors can stimulate norepinephrine release from nerve terminals (18-20) and AngII may amplify vasoconstrictor responses affected by the α_1 receptors.

Hypertension is also an integral part, usually associated with other metabolic abnormalities such as insulin resistance, glucose intolerance, obesity and dyslipidemia. Impact of mentioned risk factors either independently or collectively increase global burden of cardiovascular morbidity and mortality. Around 91.3% of the hypertensive patients had at least one associated metabolic or cardiovascular risk factor(21). People with cardiometabolic syndrome are two times more likely to die from coronary heart disease and three times more likely to have heart attack and stroke(22). The relationship between HTN and CMets is complex and encompasses many interactive dysfunctional regulatory systems that all contribute to increased CVDs(23). It involves not only vascular and hemodynamic changes that accompany HTN, but also a myriad of complex metabolic abnormalities that collectively constitute CMets. Activation of overwhelming RAAS activity is reported in metabolic patients depicting the role of AngII in insulin resistance, body weight regulation and oxidative stress(24),(25).Multiple studies have supported the role of sympathetic nervous system (SNS) activation in obesity-related HTN(26),(27).Persistent hypertension also induces sympatho-toxication which leads to diminished insulin signaling, insulin

resistance and lipid abnormalities. Over activation of SNS in turn activates RAAS which advances the vicious loop of metabolic disturbances. The coexistence of insulin resistance and hypertension can be viewed as a cause-effect relationship (insulin resistance as a cause of hypertension or vice versa) or as a non-causal association (28). Insulin can increase blood pressure via several mechanisms: increased renal sodium reabsorption, activation of the sympathetic nervous system, alteration of transmembrane ion transport and hypertrophy of resistance vessels (29),(30). On the other hand, hypertension can cause insulin resistance by altering the delivery of insulin and glucose to skeletal muscle cells, resulting in impaired glucose uptake.

Controlling of hypertension and metabolic disorder mainly involves lifestyle modifications (exercises and diet modifications) and pharmacological therapy. However, lifestyle medications prove inefficient for the control and progression of disease and combination therapy is mainly prescribed to regulate these conditions. Usually, two or more pills are prescribed for the control of hypertension (31),(32) and if the metabolic anomalies are present with HTN, it further increases the pill burden, renders poor adherence, adverse effects and unpredictable PK-PD relationships.

Recently, it is being recognized that deliberately designed multitargeted ligands (DML) can provide superior therapeutic alternative for the treatment of multifactorial diseases such as cancer, neurological disorders and multiple cardiovascular complications. In cardiovascular disease, despite a plethora of available treatment options, a substantial portion of the hypertensive population has uncontrolled blood pressure. The unmet need of controlling blood pressure in this population may be addressed, in part, by developing new drugs and devices/procedures to treat hypertension and its co-morbidities. The deliberately designed multifunctional ligands certainly will provide superior therapeutic efficacy, predictable pharmacokinetic properties, lesser off target effects and ultimately enhanced patient compliance. Different complimentary systems have been targeted to develop multitargeted ligands such as angiotensin-converting enzyme/neutral endopeptidase inhibitors(33), neutral endopeptidase/endothelin-converting enzyme inhibitors, angiotensin-converting enzyme/neutral endopeptidase/endothelin-converting enzyme inhibitors(34), dual angiotensin/endothelin receptor(35),(36).

In the quest of developing DMLs for multifactorial complex disease such as hypertension and cardiometabolic disorders, there are certain primary requirements that have to be taken into consideration such as selection of targets, identification of leads/hits, rational design

of small molecules, balance modulation of desirable targets and eliminating off target effects(37). Regarding the first issue at hand, it is still a challenge to choose the right combination of targets for the disease of interest in both multi-target drugs and therapeutic combinations. It requires good understanding of target-disease associations, pathway-target-drug-disease relationships and adverse events profiling(38). Furthermore, the selection should be based on whether or not modulating the selected targets could lead to additive or synergistic effects. Particularly, additive effects can be obtained when the targets belong to the same pathway, whereas synergism can be achieved only if the selected targets are located on functionally complementary pathways. Secondly, design of DMLs involves integration of pharmacophores with suitable linkers. These involve size, druggability and solubility of molecules under investigation(39).

This is one of the few studies utilizing interlink between two major governing systems i.e. RAAS and SNS and their involvement on hypertension and metabolic abnormalities. In line with this notion, the novel dual receptor antagonists were synthesized by Medicinal Chemistry Laboratory, Faculty of Pharmacy, The Maharaja Sayajirao University of Baroda. Subsequently, screening of a series of new chemical entities for potential dual-antagonist activity on the AT_1 and α_1 receptors was evaluated. These compounds belong to a series of 6,7-dimethoxyquinazolines with different substitutions using framework combination involving prazosin and losartan as parent molecules and were assumed to show a balanced modulation of both the receptors in question.

Newly synthesized compounds were pharmacologically evaluated by *in-vitro* screening on aorta and were further evaluated for their toxicological and pharmacokinetic profile. Compounds exhibited potent and balance modulations at the targets and were further explored for their potential in *in-vivo* animal models of hypertension.

Current series of DMLs were initially designed and studied for its potential role in treatment of hypertension. However, as discussed earlier, involvement of plethora of mechanisms involved in CMets sparked an idea to explore the role of novel molecules in the management of CMets. This hierarchal approach and detailed investigation can provide superior therapeutic alternative for the management of CMets.

The current research is also focused on another important risk factor i.e., Coagulation and Thrombosis, involved in CVDs mortality. As mentioned earlier, hypertension and MetS are well recognized risk factors of cardiovascular disease (40),(41). Given the evidence of hypercoagulability, hypofibrinolysis and endothelial dysfunction as the carriers of the

MetS, there is a rationale to hypothesize that the MetS may also predispose patients to develop venous thromboembolism (VTE) (42),(43).

Attributes of CMets are closely related for the development of arterial and venous thrombosis to the varying degree. Presence of metabolic triad, Hypertension, insulin resistance and the metabolic syndrome increases the risk of CVD by multifold (44), (45). Recently, one of largest cohort study on deep vein thrombosis have shown percent recurrence increased in a stepwise fashion with each additional MetS component, ranging from 7% recurrence in patients without any MetS comorbidities to 37% recurrence in those with all 4 components (46). Increasing clinical and laboratory evidence suggests that hypertension per se may confer a prothrombotic or hypercoagulable state. This may explain in part why, despite exposure of the blood vessels to high pressures, the main complications of hypertension are paradoxically thrombotic in nature rather than hemorrhagic(47). Some individual components of the metabolic syndrome have been associated with VTE mainly dyslipoproteinemia involving high triglyceride (TG) levels, small LDL particles and low HDL particles (48),(49). A recent metanalysis assessed the association between cardiovascular risk factors and VTE. A total of 63,552 subjects met the inclusion criteria representing the largest study conducted for the association of MetS and VTE. Compared with control subjects the risk of VTE was 2.33 for obesity and 1.42 for diabetes mellitus. HDL cholesterol was inversely and consistently correlated with VTE, and triglycerides were on average 21 mg/dl higher in patients with VTE than in controls (46).

Blood clotting is a complex process that has been well explained by the cascade model (2). As per the cascade model, coagulation process is coordinated by two parallel pathways, the extrinsic and intrinsic pathways (50) - both intersecting at the point of activation of FXa. The activated FXa forms a complex with the FVa to bring about cleavage of prothrombin to generate thrombin, which then activates soluble fibrinogen to produce insoluble fibrin. Following this, the polymerized fibrin sheets and activated platelets form a stable clot at the injury site (51).

To regulate blood coagulation, various enzymes involved in blood coagulation process have gained great attention as potential target for the development of new antithrombotic agents. Various clinical and preclinical studies have proven the effectiveness of conventional anticoagulants such as vitamin K antagonists (VKAs), unfractionated heparin (UFH), low-molecular-weight heparins (LMWHs), dabigataran, in the prevention and treatment of a diverse set of thromboembolic arterial and venous diseases (52). The use of

warfarin and other VKAs is particularly troubling, despite the convenience of oral administration offered by these anticoagulants. Unfortunately, warfarin has been found to be involved with numerous drug and food interactions, slow recovery with vitamin K antidote, unpredictable pharmacokinetic (PK) and pharmacodynamic (PD) profile and considerable intra/inter-patient variability in drug response. As a direct consequence, the appropriate therapeutic dose differs, requiring constant monitoring and regular dose adjustment. Regular supervision of warfarin therapy is important due to this uncertainty in response and relatively narrow therapeutic index, which often results in subtherapeutic anticoagulant action and a higher risk of thromboembolism or prolonged anticoagulant action and greater risk of bleeding (53).

Short-term anticoagulant agents usually involve UFH, LMWHs, fondaparinux (as indirect FXa inhibitor), argatroban, bivalirudin and hirudin (as direct thrombin inhibitors) (54). These medications need intravenous administration that creates a problem for their use outside the hospital and causes clot formation at the site of injection. Heparin analogues like UFH and LMWHs bear the risk of thrombocytopenia and as they are isolated from animal tissue, they sometimes exhibit serious complications like immunological reactions, uncontrolled bleeding. Besides, UFH has an uncertain PK profile and anticoagulant reactions that require monitoring(55). These drawbacks of parenteral anticoagulants pose concern regarding their use and safety in clinical setting. Dabigatran, an oral thrombin inhibitor has been found to cause uncontrolled bleeding which could prove fatal at high doses (56). These clinical limitations in the existing drugs prompt researchers to develop new orally bioavailable antithrombotic drugs with a better safety profile.

Efforts have been made to develop strategies for selective inhibition of target specific enzymes within the coagulation cascade. Two serine proteases, factor Xa (FXa) and factor IIa (thrombin) have particularly emerged as promising targets. Amongst these two targets, FXa is placed at a very critical juncture of blood hemostasis cascade and acts as a rate limiting step in clot formation. Direct inhibition of FXa has appeared as the most effective strategy to achieve anticoagulation with minimal bleeding risks by maintaining the normal hemostasis. Factor Xa inhibitors are small molecules that selectively and reversibly bind to the active site of activated factor Xa, which blocks the interaction with its substrate in a rapid and competitive fashion. They inhibit both free factor Xa in solution and within a clot, and have no direct effect on platelet aggregation(57). Due to its upstream position in the amplification cascade and limited function outside the cascade, direct inhibition of FXa

is more effective than direct inhibition of thrombin. Selective inhibition of FXa displays less bleeding risks because it does not affect normal existing thrombin level, and activation and aggregation of platelets. Several preclinical studies revealed that FXa inhibitors displayed a larger therapeutic window than direct thrombin inhibitors (58),(59). Thus, FXa has received great attention of researchers to develop novel antithrombotic drugs due to its significant role in coagulation cascade.

In line with this notion, novel compounds were screened for their FXa inhibitory potential, specificity and anticoagulant activity. Selected NCEs were studied for their toxicity and pharmacokinetic profile. Finally, compounds were studied for their *in-vivo* antithrombotic potential by ferric chloride and arteriovenous shunt induced thrombosis in rats.

2. AIM AND OBJECTIVE

2.1 Aim

Pharmacological Screening and Evaluation of Novel Chemical Entities in Cardiometabolic Disorders.

2.2 Objectives for designed multitargeted ligands for hypertension and cardiometabolic disorder

- Pharmacological screening and evaluation of novel dual receptor antagonists by functional antagonism assay on rat abdominal aorta (pA_2 value determination) and by invasive blood pressure measurement for their antihypertensive effect.
- To develop structure activity relationships, molecular dynamics and docking simulation of potent NCEs with α_1 and AT_1 receptors.
- Docking studies of compound **(18)** and **(24)** with selected targets (DPP4 and PPARγ) for cardiometabolic disorder.
- To predict and evaluate ADMET properties of compound **(18)** and **(24)**.
- To study the toxicity of compound **(18)** and **(24)** as per the OECD guidelines
- To study the pharmacokinetic profile of compound **(18)** and **(24)**
- Evaluation of compound **(18)** and **(24)** in unilateral nephrectomy and DOCA salt induced hypertension in rats.
- Evaluation of compound **(18)** and **(24)** in L-NAME induced hypertension in rats.
- Evaluation of compound **(18)** and **(24)** in 20 % fructose induced cardiometabolic disorder in rats.

2.3 Objectives for novel Factor Xa (FXa) inhibitors for anticoagulant and antithrombotic activity

- Pharmacological screening of NCEs for Factor Xa inhibition by human Factor Xa enzyme inhibition assay.
- Development of structure activity relationships and molecular docking of selected NCEs.
- To assess the effect of compound **(14)** and **(50)** on intrinsic and extrinsic pathway of coagulation by prothrombin time (PT) and activated partial thromboplastin (aPTT) time measurement.

- To study the specificity of compound **(14)** and **(50)** by human thrombin enzyme inhibition assay.
- To predict and evaluate physicochemical and ADMET properties of compound **(14)** and **(50)**.
- To study the toxicity ofcompound **(14)** and **(50)** by OECD guidelines.
- To study the efficacy of compound **(14)** and **(50)** in ferric chloride ($FeCl_3$) and artereovenous shunt (AV shunt) induced thrombosis.

3. MATERIAL AND METHODS

3.1 Material

Novel test compounds were synthesized by the Medicinal Chemistry Laboratory, Pharmacy Department, Faculty of Pharmacy, The Maharaja Sayajirao University of Baroda. Phenylephrine hydrochloride, angiotensin II, acetylcholine chloride, deoxycorticosterone acetate were procured from Merck (Sigma Aldrich) St. Louis, MO, USA. L-Nitroarginine Methyl Ester (L-NAME) was procured from TCI chemical, Tokyo, Japan. Prazosin, Valsartan, and Losartan potassium were kind gifts from Alembic and Zydus Pharmaceuticals. Heparin, ketamine, diazepam, tramadol, Amoxicillin, doxazosin and terazosin were purchased from Adhyamaheshwar medical store, Vadodara, Gujarat. Protein kinase C, Phospho-Akt, Tumour necrosis factor-alpha (TNF-α), interleukin-6 (IL-6), nuclear factor kappa-β, renin, adiponectin, leptin, ELISA kits were purchased from Krishgen Biosystems, Mumbai, India. Insulin ELISA kit was purchased from Genxbio health services Pvt. Ltd., New Delhi, India. Cell cultures (HEK 293 and H9C2) were procured from National Cell culture (NCCS), Pune, India. Dulbecco's minimum essential medium (DMEM, High Glucose), Trypsin: EDTA solution, Fetal bovine serum, Antibiotic-antimycotic solution, tissue culture flasks (T-25 and T-75), MTT and lyophilized phosphate buffered saline (PBS, *p*H 7.2) were procured from HiMedia, Mumbai, India.

Human FXa enzyme and substrate S-2765 were procured from Molecular Innovations, USA. Thrombin assay kit was purchased from Biophen DTI, Anira Biosciences (USA). Prothrombin time and activated partial prothrombin time was measured by commercial kits purchased from Tulip diagnostics, India. Apixaban and Rivaroxaban were kind gifts from Zydus Cadila Healthcare Ltd., Dabhasa, Vadodara. Other routinely utilized chemicals were of analytical grade and purchased from companies like Himedia, Lobachemie, Sulab chemicals etc.

3.2 Animals

Animals were procured from licensed animal breeders. Animals were housed in an air-conditioned room (25±2 °C, 50-65 % RH) in plastic cages having corncorb bedding (Shree Dutt Agro Pvt. Ltd., Vadodara, India) with 12 hr. light-12 hr. dark cycles. They had free access to pelleted diet (Pranav Agro Foods Pvt. Ltd., Pune, India) and RO water. All experimental protocols were approved by the Institutional Animal Ethics Committee (IAEC) of Pharmacy Department, Faculty of Pharmacy, The M. S. University of Baroda,

Vadodara (Protocol No: MSU/IAEC/2016-17/1602, MSU/IAEC/2018-19/1828, MSU/IAEC/2019-20/1907). All the experimental procedures were carried out as per the CPCSEA guidelines.

3.3 Methods for screening and evaluation of designed multitargeted ligands in hypertension and cardiometabolic disorders

3.3.1 Functional antagonism assay using isolated rat thoracic aorta preparation

This assay was selected to determine the antagonistic effect of synthesized compounds against ang II and phenylephrine mediated contractions of rat aortic strips. Male Wistar rats (14-16 weeks old; 200-250 g) were used for the study. They were sacrificed by euthanasia using sodium pentobarbital (120mg/kg; i.p); immediately descending thoracic aortas were removed and placed in ice-cold Kreb's bicarbonate solution of the following composition (mM): NaCl 112, $NaHCO_3$ 12, glucose 11.1, KCl 5.0, $MgSO_4$ 1.2, KH_2PO_4 1.0 and $CaCl_2$ 2.5.The *p*H of the Krebs's solution was 7.4 and maintained at 37°±1C using a thermostat. The tissue was aerated with carbogen (95% O_2 and 5% CO_2) continuously. Peri-adventitious tissue was removed, taking care not to stretch the tissue. A spinal needle was inserted in the tissue and rotated gently to denude the endothelium. Following this, the tissue was cut spirally into a helical strip using a surgical blade No.10. The strip was tied at both ends using a cotton thread and suspended in a 25 ml organ tube under an initial resting tension of 2 g. The Krebs's solution in the organ tube was changed at every 15 minutes during an equilibration period of about 90 minutes. Denudation of the endothelium was confirmed by observing the "absence of relaxation" on strips precontracted with phenylephrine. Isometric contractions were recorded using a force transducer (MLT002 Isometric force transducer, AD Instrument, Australia). Contractions were induced in rat aortic strips with graded, cumulative concentrations of phenylephrine or ang II. Standard drugs or test compound was added to organ tubes 30 minutes prior to recording of the addition of phenylephrine. Similar procedure was followed to record graded cumulative response curves of AngII. Control strips were incubated with solvent [DMSO (0.5%) or normal saline] for 30 minutes before recording the concentration response curves. pA_2 values were calculated by the method described by Arunlakshana and Schild(60),(61).

3.3.2 *In-vivo* pressor response by invasive blood pressure measurement of compound (18) and (24)

3.3.2.1 *In-vivo* pressor response evaluation under unmasked condition

Male Wistar rats of 12 weeks weighing 250±20gwere anesthetized by ketamine 80mg/kg, i.p; xylazine 20 mg/kg, i.p. After confirming the anesthesia, a blunt dissection was performed on the ventral neck region and sternohyoid muscles were removed to expose the trachea. To facilitate the respiration, A partial transverse cut was put between the cartilaginous regions and a small piece of pediatric Ryle's tube was inserted in the trachea. The left jugular vein was cannulated using polyethylene (PE) catheter for administration of standard drugs and test compound dissolved in isotonic saline with 0.5% DMSO. Following this, vagotomy was performed to exclude the effect of vagus nerve. The carotid artery was isolated and cannulated with a PE catheter attached to a pressure transducer (MLT 844 pressure transducer, AD Instrument, Australia) for measurement of intra-arterial blood pressure. The silicone membrane dome and cannula were filled with heparinized saline (100 IU/ml) to prevent clotting of blood inside cannula. The transducer was connected to Powerlab-4/35 data acquisition system (AD Instruments, Australia) for recording of the blood pressure. Baseline blood pressure was recorded for 15 minutes following which pressor responses to phenylephrine (5 µg/kg, i.v. bolus) and AngII (5µg/kg, i.v. bolus) were observed in absence and presence of standard drugs or test compound in different set of experiment. Inhibition of pressor response was observed at 2 dose levels; 10µg/kg and 50µg/kg for α_1 receptor inhibition and 100µg/kg and 200µg/kg for AT_1 receptors inhibition. Reduction in blood pressure with antagonist treatments were normalised and statistically evaluated using one way ANOVA(62).

3.3.2.2 *In-vivo* pressor response evaluation under masked conditions

As mentioned above, surgical procedure is performed to measure invasive blood pressure. Further it was planned to evaluate the pressor-inhibition potential of selected NCE under masked conditions. *In-vivo* inhibition of selected test compounds against phenylephrine mediated arterial pressor response was measured in those animals to which 200 µg/kg losartan was pre-administered. The idea behind such a protocol was to mask the effects of test compound upon AT_1 receptor. Similarly, the other set involved measurement of inhibition of Ang II mediated arterial pressor response in those animals to which 50 µg/kg terazosin was pre-administered to mask the effect test compound upon α_1 receptors. Change

in blood pressure with antagonists were normalized against agonist response and statically evaluated using one way ANOVA.

3.3.3 Docking study of compound (18) and (24) with α_1 and AT_1 receptor

To understand the molecular mechanism of dual acting anti-hypertensive agents with α1 and AT_1 receptors antagonism, docking studies of the synthesized compounds were performed within the active sites of the respective α_1 and AT_1 receptors obtained by homology modeling.

For docking purpose Glide offers three different levels of docking precision: HTVS (high-throughput virtual screening), SP (standard precision), and XP (extra precision). The docking studies were performed by using Glide module with XP mode. The 3D structures of ligand molecules were built within Maestro using the Build module and a single low energy conformation search was carried out for all molecules under study using OPLS2e force field at physiological *p*H condition using LigPrep module of Schrödinger while keeping other parameters at standard value. Docking interactions were studies for compound **(18)** and **(24)** on the active site of α_1 and AT_1 receptor

3.3.4 Cytotoxicity assay of compound (18) and (24) on HEK 293 cell culture

This assay involved treatment of cells with the test compounds at different concentrations and evaluation of cytotoxic potential on HEK293 (kidney epithelial cell line) cell culture by means of reaction with MTT. For this purpose, after reaching to the required confluency, cells were trypsinized, washed with sterile PBS and counted. The final quantity of cells was adjusted with media, such that 200 µl suspensions of cells contained nearly 10^4 cells/well. This final suspension was seeded onto different wells of a sterile 96-well tissue culture plate and the plate was placed in the incubator to allow adherence of cells for 24 hours. Stock solution of test compound **(18)** and **(24)** were prepared in DMSO and further dilutions (0.01µM to 1000µM) were prepared in serum deprived medium. The concentration of the aliquots was adjusted in such a way that 200 µl of the medium contained the required concentration of compound **(18)** and **(24)** without exceeding the total concentration limit of DMSO (3%). A concentration range of 0.01µM to 1000 µM was utilized for the assay. After a 24-hr incubation period, the complete media was removed from the wells by inverting the plate on a tissue paper. Serum deprived medium containing the test compound was added in different wells with appropriate controls for DMSO in

triplicates. The cells were allowed to remain in contact with the test compounds for 12 hrs after which the media was removed and 200 µl of complete media containing MTT (500 µg/ml) was added to each well. The plate was then put inside the incubator and MTT was allowed to react with the cells for 4 hrs. Mitochondrial dehydrogenases from live cells metabolize MTT to insoluble formazan crystals. After 4 hrs. of incubation, the medium is removed and 200 µl DMSO (filtered through a 0.22 µm syringe filter) is added to each well to solubilize the formazan crystals. The plate is covered and shaken on a plate-shaker for 3 minutes. The lid is then removed and the purple color developed is read at 570 nm with a correction applied at 620 nm to account for unmetabolized MTT that may be present in the wells. Higher absorbance is directly proportional to the number of live cells present in each well. % Survival in each well was calculated by the following formula:

% Survival = (OD of test compound well/OD of Control well) × 100

3.3.5 Evaluation of antihypertensive activity of compound (18) and (24) in unilateral nephrectomy (UNX) and DOCA salt induced hypertension in rats

Unilateral nephrectomy was performed as per the protocol with minor modifications. Adult Wistar rats (20-24 weeks; 200-250 g) were utilized for the study and they were anesthetized by ketamine (80mg/kg,i.p) and xylazine (20 mg/kg,i.p) Briefly, after confirming anesthesia through loss of righting reflex and pinching response, peritoneal laparotomy was performed around 1.2 cm dorsolateral to the diaphragm line. The left kidney was identified in peritoneum and gently brought out by holding the surrounding fat. The adhering fat and periadventitious tissue was separated using a pointed forceps. The kidney was gently pulled towards the exterior side of the peritoneal cavity to expose the ureter, renal vein and renal artery. They were clipped together using a hemostatic forceps and tied towards the kidney with 2 silk sutures (no.4), one distal and the other proximal. The kidney was now severed away from the knot and the remaining portion was allowed to retract by removing the haemostatic forceps. The incision was closed by ethicon® braided-silk sutures. Since ketamine also acts as a preemptive analgesic, immediate post-surgical anesthesia was not required, however, after recovery from anesthesia a dose of tramadol (12.5 mg/kg, i.p.) was administered as post-surgical analgesic and amoxicillin (50mg/kg;i.p.) were given as antibiotic during recovery period. The animals were allowed to recover from surgery for one week. After the recovery period animals were divided into different groups.

Group I (normal control) and II (sham control) provided with normal RO water and food *ad-libitum* throughout the study period. Animals of group III-VIII underwent unilateral nephrectomy followed by DOCA salt treatment. Group II was subjected to surgical procedure of unilateral nephrectomy but kidney was kept intact in animals. Group III rats received 25mg/kg DOCA salt via s.c route twice a week for six weeks with 1% NaCl+ 0.2%KCl in drinking water. G-III served as the hypertensive control. Animals of group IV and V received 5 and 10mg/kg of compound **(18)** combined with hypertensive treatment. While group VI and VII treated with compound **(24)** at 5 and 10 mg/kg respectively with hypertensive treatment. Group VIII served as standard control group received losartan and terazosin (5mg/kg each; p.o; once a day) for six weeks along DOCA salt and salt administration.(63).

Table 3.1: Evaluation of compound (18) and (24) UNX+DOCA salt induced hypertension in rats

Group	No. of animals	Group	Treatment
I	9	Normal control	Normal RO water
II	9	Sham control	Sham surgical procedure
III	9	UNX+ DOCA salt [Disease Control (DC)]	25mg/kg; s.c.; twice in a week for 6 weeks
IV	9	DC + Compound **(18)**	5mg/kg Oral; Once daily for 6 weeks
V	9	DC + Compound **(18)**	10mg/kg Oral; Once daily for 6 weeks
VI	9	DC + Compound **(24)**	5mg/kg Oral; Once daily for 6 weeks
VII	9	DC + Compound **(24)**	10mg/kg Oral; Once daily for 6 weeks
VIII	9	DC+ Losartan + Terazosin	5mg/kg each; once daily for 6 weeks

3.3.6 Collection, processing and storage of samples

- **Collection of blood**

On the penultimate day of the study, rats were fasted overnight and the blood samples were withdrawn from retro-orbital plexus under light anesthesia added to centrifuge tubes. Samples were divided in two parts where one tube contained 2 % EDTA solution and while other tube is without EDTA solution for collection of plasma and serum samples respectively. Blood samples were centrifuged at 2200-2500 rpm for 10 minutes. The plasma and serum obtained was kept at -70ºC until used. Samples were analyzed for various biochemical parameters.

Plasma samples were utilized for interleukin-6 (Il-6), tumor Necrosis Factor-α (TNF-α), renin by rat specific sandwich ELISA immunoassay kit as described by manufacturer (Krishgen Biosystems) using BIO RAD Elisa plate reader 680XR.

Serum samples were used for the measurement of metabolic parameters such as glucose, triglycerides, total cholesterol, LDL, HDL by colorimetric kits as recommended by manufacturer (Span diagnostics Pvt. Ltd., India) using UV spectrophotometer Shimadzu 1800.

- **Collection of urine**

On the penultimate day of the study, rats were fasted overnight and kept individually into metabolic cages with access to water. After 24 hours the urine was collected and filtered through syringe filters and stored for further urine analysis.

Urine samples were analysed for various biochemical parameters such as uric acid, creatinine, sodium, potassium, albumin and were measured by colorimetry as recommended by manufacturer (Span diagnostics Pvt. Ltd., India) using an UV Spectrophotometer shimadzu1800.

3.3.7 Measurement of Hemodynamic parameters

3.3.7.1 Invasive blood pressure measurement

Invasive blood pressure was measured as explained in *in-vivo* pressor evaluation section.

3.3.7.2 Electrocardiogram

Rats were anesthetized by injecting ketamine (80 mg/kg) and xylazine (20 mg/kg) intraperitoneally. The electrocardiograms were recorded using Power lab 4/35 (AD instrument, Australia) connected to animal bio amp and signal amplifier. After confirming anesthesia, positive (left upper limb), negative (right lower limb) and earthing (right upper limb) electrodes were inserted subcutaneously*(64)*.

3.3.8 Endothelial dysfunction

Endothelial dysfunction was measured by the relaxation of aortic strips from different groups of animals by acetylcholine. Briefly, after dissecting the aorta from the animal, periadventitious fat was removed and care was taken to preserve the endothelium in intact form while preparing the strips. The strips were mounted as mentioned in the *'functional antagonism assay'* section. Endothelial dysfunction was evaluated by means of graded,

Ach-mediated relaxations on strips precontracted with phenylephrine as compared to sodium nitroprusside mediated relaxations on the same strips(65).

3.3.9 Blood and Urine parameters

3.3.9.1 Blood plasma parameters

3.3.9.1.1 Tumor necrosis factor-α (TNF-α)

TNF-α level in plasma samples were analysed by rat specific sandwich ELISA kit from Krishgen Biosystems. (Cat No: KB3145)

Reagent preparation

1) Wash buffer (1X) was prepared by adding 5 ml of Wash Buffer (20X) to 95 ml of Distilled water. This was labelled as working solution.
2) Assay diluent (1X) was prepared by adding 1 ml of assay diluent (5X) to 4 ml of distilled water. This was labelled as working solution.
3) Standard (Rat TNF-α, Lyophilized): Reconstitution: Lyophilized Rat TNF-α standard was reconstituted with 1.2 ml of distilled water to achieve final concentration 2000 pg/ml. Mixed gently and allowed to stand for 30 min before further dilution.
4) Dilutions: Reconstituted standard was used directly as a top standard (2000 pg/ml) and serial dilution was performed in assay diluent (1X) to prepare the standard range.
5) Detection Antibody Dilution 1:200, Detection Antibody solution of 20 µl was added to 4980 µl of assay diluent (1X) to make final volume to 5 ml.
6) Streptavidin-HRP Dilution 1:200, 20 µl of Streptavidin added: HRP solution added to 4980 µl of assay diluent (1X) to make final volume to 5 ml.

Procedure

1) 100 µl/well of Standards and Samples were added to the plate either in duplicate or triplicate. Six two-fold serial dilutions of the 2000 pg/ml top standard were performed, either within the plate or in separate tubes. Thus, the Rat TNF alpha standard concentrations were 2000 pg/ml, 1000 pg/ml, 500 pg/ml, 250 pg/ml, 125 pg/ml and 62.5 pg/ml. Assay Diluent (1X) served as a blank.
2) Plates were sealed and incubated for 2 hours at Room Temperature (18-25 °C).
3) Plates were aspirated and washed 4 times with Wash Buffer (1X) and blotted for residual buffer by firmly tapping plate upside down on absorbent paper. Any liquid from the bottom outside of the microtiter wells was wiped off as any residue can interfere in the reading step. All the washes were performed similarly.

4) 100µl of diluted Detection Antibody solution was added to each well; plate was sealed and incubated for 2 hours at Room temperature (18-25 °C).
5) Plate was washed 4 times with Wash Buffer (1X) as in step 3.
6) 100µl of diluted Streptavidin-HRP solution was added to each well; plate was sealed and incubated for 30 minutes at room temperature (18-25 °C).
7) Plate was washed 4 times with Wash Buffer (1X) as in step 3. For this final wash, wells were soaked in wash buffer for 30 seconds to 1 minute for each wash. This helped in minimizing the background.
8) 100 µl of TMB Substrate solution was added and the plate was incubated in the dark for 15 minutes. Positive wells turned bluish. It was not necessary to seal the plate during this step.
9) Reaction was stopped by adding 100µl of Stop Solution to each well. Positive wells turned from blue to yellow.
10) Absorbance at 450 nm was measured within 30 minutes of stopping the reaction.
11) Concentration of samples was measured by generating calibration curve using standard TNF-α.

3.3.9.1.2 Interleukin-6 (IL-6)

IL-6 level in plasma samples were analysed by rat specific sandwich ELISA kit from Krishgen Biosystems. (Cat No: KB1068)

Reagent preparation

1) Wash buffer (1X) was prepared by adding 5ml of Wash Buffer (20X) to 95 ml of Distilled water. It was labeled as working solution
2) Assay diluent (1X): Dilution: It was ready to be used.
3) Detection Antibody Dilution was prepared by adding 28 µl of detection antibody solution to 2472 µl of assay diluent to make the final volume to 2.5 ml.
4) Streptavidin-HRP Dilution was prepared by adding 25 µl of Streptavidin-HRP solution to 4975 µl of Assay Diluent to make final volume to 5 ml.
5) Standard (Recombinant Rat IL-6; 440 ng/ml) upon first use, 440 ng/ml tube of recombinant standard was thawed and quick-spun; aliquots were made in polypropylene vials, and stored at -20 °C. The assay was done by thawing and diluting the recombinant protein by adding 9 µl of the standard solution in 991 µl of assay

diluent to prepare the top standard solution (4000 pg/ml) to make up the final volume to 1 ml.

Procedure

1) Same procedure was followed for **Interleukin-6 as per section 3.3.9.1.1.**
2) Concentration of samples was measured by generating calibration curve using standard IL-6.

3.3.9.1.3 Renin

Renin level in plasma samples were analysed by rat specific sandwich ELISA kit from Krishgen Biosystems (Catalogue No: KLR0548).

Procedure

1) 50 µl of standards and 40 µl samples were pipetted into the respective wells as mentioned in the work list. Sample, biotin conjugate and streptavidin-HRP were not added to the blank well.
2) 10µl of biotin conjugate was pipetted out into each sample well. Biotin conjugate was not added into the blank and standards wells.
3) 50µl of HRP conjugate was pipetted into each sample and standards well. HRP conjugate was not added to the blank well.
4) The plate was covered and incubated for 1 hour at 37 °C in the incubator.
5) Plate was aspirated and washed 4 times with 1X Wash Buffer and blotted for residual buffer by firmly tapping plate upside down on absorbent paper. Any liquid from the bottom outside of the microtiter wells were wiped off as any residue can interfere in the reading step. All the washes were performed similarly. 50µl substrate B was added to each well including blank well. Gently mixed, incubated for 10 minutes at 37 °C in dark.
6) 50 µl of Stop Solution was added resulted into change in color from blue to yellow which is measured at 450nm.
7) Concentration of samples was measured by generating calibration curve using standard renin.

3.3.9.1.4 Estimation of Protein kinase C (PKC) and phospho-Akt (p-Akt) in aorta

PKC (Cat No: KLR0203) and p-Akt (Cat No: KLR1201) were analysed by rat specific sandwich ELISA kit from Krishgen Biosystems.

Procedure

1) 50 µl of standards and 40 µl samples were pipetted into the respective wells as mentioned in the work list. Sample, biotin conjugate and streptavidin-HRP were not added to the blank well.
2) 10 µl of biotin conjugate was pipetted out into each sample well. Biotin conjugate was not added into the blank and standards wells.
3) 50 µl of HRP conjugate was pipetted into each sample and standards well. HRP conjugate was not added to the blank well.
4) The plate was covered and incubated for 1 hour at 37 °C in the incubator.
5) Plate was aspirated and washed 4 times with 1X Wash Buffer and blotted for residual buffer by firmly tapping plate upside down on absorbent paper. Any liquid from the bottom outside of the microtiter wells were wiped off as any residue can interfere in the reading step. All the washes were performed similarly. 50 µl substrate B was added to each well including blank well. Gently mixed, incubated for 10 minutes at 37 °C in dark.
6) 50 µl of Stop Solution was added resulted into change in color from blue to yellow which is measured at 450 nm.
7) Concentration of samples was measured by generating calibration curve using respective standard.

3.3.9.2 Blood serum parameters

3.3.9.2.1 Fasting serum glucose (GOD-POD end point assay)

Determination of glucose level in blood serum was done by using enzymatic assay kit(66) (Span or Reckon diagnostics Pvt. Ltd., India).

Procedure

1) 20 µl of either serum samples or standard were taken to labeled 2 ml microcentrifuge tubes.
2) 1.5 ml of working glucose solution was added to all the tubes.
3) All the above solutions were mixed well and incubated at 37 °C for 10 min.
4) Spectrophotometer was set to zero by blank solution of working glucose solution.
5) After incubation absorbance was measured at 505 nm**.**

Calculation:

Glucose (mg/dL) = (Absorbance of Test/ Absorbance of Standard) *100

3.3.9.2.2 Cholesterol

Determination of the quantity of cholesterol in serum was done using enzymatic kit (Span or Reckon diagnostics Pvt. Ltd., India).

Procedure

1) 10 µl of serum samples and standard cholesterol was pipette into microcentrifuge tubes.
2) 0.5 ml enzyme reagent was added into each tube allowed for 10 minutes incubation at 37^0C.
3) After incubation 1 ml of distilled water was added to each tube and mix well.
4) For the preparation of blank, only enzyme reagent and distilled water was mixed and spectrophotometer was adjusted to zero with blank sample.
5) After incubation, absorbance was measured at 505nm and total cholesterol content was calculated by following formula.

Calculation:

Total Cholesterol (mg/dl) = (OD of T / OD of S) *200

3.3.9.2.3 HDL-cholesterol (CHOD/POD-Phosphotungstate method)

Quantitative determination of the activity of HDL-cholesterol in serum was done using enzymatic kit (Span or Reckon diagnostics Pvt. Ltd., India). Estimation of cholesterol was performed in two steps. First steps involved the preparation of samples from serum followed by estimation.

Procedure

Step 1

1) 0.2 ml of clear serum samples were pipetted into labeled microcentrifuge tubes and 0.3 ml of precipitating reagent was added to each tube.
2) Samples were vortexed and incubated at 25 °C for 10 minutes.
3) The samples were centrifuged at 3000 rpm for 10 minutes to get clear supernatant. If the supernatant was not clear (high TG level) the samples were diluted in 1:1 ratio with normal saline.

Step 2

1) After separating the clear supernatant, 0.5ml of enzyme reagent was added to each microcentrifuge tube containing 20µl serum samples.
2) Standard was prepared by adding 1ml of enzyme regent to 10µl of cholesterol standard.

3) After addition, tubes were incubated at 370C for 5 minutes and 1ml of distilled water was added to each tube.
4) Spectrophotometer was set to auto zero by blank solution containing 0.5ml of enzyme regent and 1ml of distilled water.
5) Absorbance was measured at 505nm and HDL content was measured as per the following formula(67)**.**

Calculation:

HDL Cholesterol (mg/dl) = (Abs. of T / Abs. of S) * 50

3.3.9.2.4 Triglycerides (GPO method)

Quantitative measurement of triglyceride concentration in serum was done by using kit (span or reckon diagnostics Pvt. Ltd.)

Procedure

1) 10 µl of either serum samples or standard were taken to labelled microcentrifuge tubes.
2) 0.75 ml of working reagent solution was added to microcentrifuge tubes.
3) Tubes were incubated for 15 minutes at 37 °C.
4) 0.75 ml of distilled water was added to each tube and mixed well with vortexing.
5) Spectrophotometer was set to zero by blank solution of working reagent and distilled water.
6) After incubation absorbance was measured at 546nm and triglyceride content was calculated as per the following formula(68).

Calculation:

Triglycerides (mg/dl) = (Abs. of Test/ Abs. of Std.) *50

3.3.9.3 Urine sample analysis

3.3.9.3.1 Creatinine

Procedure

1) 100µl of urine samples and standard were pipetted into microcentrifuge tubes.
2) 1 ml of creatinine working reagent was added to each tube.
3) Mixed well and aspirated immediately for measurement**.**
4) The analyzer was blanked with purified water and samples were measured at 520 nm

5) Initial absorbances of the standard and test samples were measured was measured i.e. for test samples: AT_1 after 30 seconds and final absorbance (AT2) after an interval of another 120 seconds(69). (Similar procedure was followed for standard)

3.3.9.3.2 Uric Acid

Procedure

1) 20µl of urine samples or standard was pipette into microcentrifuge tubes.
2) 1ml of uric acid monoreagent was added to each tube and
3) Solutions were mixed well and incubated at 37 ºC for 5 minutes.
4) The analyzer was blanked with purified water.
5) Absorbance of Standard was measured followed by the test samples at 520 nm
6) Results were calculated as per given calculation formula(70).

Calculation:

$$\text{Serum / Plasma Uric acid (mg/dL)} = \frac{\text{Absorbance of test}}{\text{Absorbance of Standard}} \times 6$$

Urine Uric acid (mg/day)

$$= \frac{\text{Absorbance of test}}{\text{Absorbance of Standard}} \times 6 \times \text{dilution factor} \times \text{24 hours urine volume in dL}$$

CONVERSION FACTOR
Uric acid concentration in mmol/L = Uric acid concentration in mg/dL×0.059

3.3.9.3.3 Sodium

Measurement of sodium was carried out in two steps as mentioned below:

Step 1: Precipitation

1) 20µl of urine samples and standard sample were pipette into microcentrifuge tubes.
2) 1ml of sodium precipitating reagent (L1) was added to each tube.
3) Solutions were mixed well and kept at room temperature for 5 min. with occasional shaking.
4) Samples were centrifuged at 2500 to 3000 RPM to obtain a clear supernatant.

Step 2: Color development

1) 20 µl of supernatant samples and standard sample were added into microcentrifuge tubes.
2) 1 ml of acid reagent (L2) was added to each tube and mixed well

3) 100 µl of colour reagent was added each tube and incubated at room temperature for 5 minutes.
4) Blank sample was prepared by adding regents without sample or standard and spectrophotometer was set to auto zero with blank.
5) Absorbance was read at 546 nm and sodium content in urine samples were calculated by following formula(71).

Calculation:

$$\text{Sodium in mmol} = \frac{\text{Abs.B - Abs.T}}{\text{Abs.B - Abs.S}} \times 150$$

3.3.9.3.4 Potassium

Measurement of potassium was carried as steps mentioned below:

Procedure

1) 20 µl of urine samples (T) and standard sample (S) were pipette into microcentrifuge tubes.
2) 1 ml of potassium reagent was added to each tube.
3) Solutions were mixed well and kept at room temperature for 5 min. with occasional shaking.
4) Absorbance was measured at 630 nm within 15 minutes and concentration was determined by the given formula.

Calculation:

Potassium (mmol/l) = [Abs.(T) / Abs.(S)] * 5

3.3.9.3.5 Urea

Measurement of urea was carried out as steps mentioned below:

Procedure

1) 100 µl of urine samples (T) and standard sample (S) were pipetted into microcentrifuge tubes.
2) 2.5 ml of solution I was added to each tube.
3) Solutions were mixed well and kept in boiling water for 10 minutes.
4) Samples were cooled down immediately with running water at brought down to room temperature with occasional shaking.
5) Absorbance was measured at 490 nm within 10 minutes.

6) Concentration was determined as per the given the formula.

Calculation:

Urea (g/day) = [Abs.(T) / Abs.(S)] * 30 * dilution factor * 24 hrs. urine volume in dl

3.3.9.3.6 Albumin

Measurement of albumin was carried out as steps mentioned below:

Procedure

1) 100 µl of urine samples (T) and standard sample (S) (Reagent 2) were pipette into microcentrifuge tubes.
2) 1 ml of reagent 1 was added to each tube.
3) Solutions were mixed well and kept in cold condition (15-30^{0}C) for 1 minute.
4) Absorbance was measured at 630 nm and Concentration was determined as per the given the formula.

Calculation:

Albumin (g/dl) = [Abs.(T) / Abs.(S)] * 4

3.3.9.3.7 Creatinine clearance

Creatinine clearance was calculated by following formula:

Creatinine clearance = [{(Urea creatinine×Urine output)/serum creatinine}×(1000/Body weight)/1440]

3.3.10 Estimation of oxidative stress parameters in heart and kidney homogenates

Reperfused heart and kidneys homogenate were prepared in 10% w/v of ice-cold Phosphate buffer solution pH 7.4 using tissue homogenizer and centrifuged at 7000 rpm for 15 minutes at 4^0 C. Supernatants were collected and analyzed for oxidative stress parameters.

3.3.10.1 Total protein content (72)

Total NO was determined by measuring its stable metabolites, particularly, nitrite ($NO2^-$) and nitrate ($NO3^-$) based on the method of Miranda et al. (2001).

Reagents

1) Ortho- phosphoric acid (OPA) (2.5% v/v): 2.5 ml of OPA was made upto100 ml of distilled water.
2) Sulfanilamide (1% w/v): 1.0 g of sulfanilamide was dissolved in 50 ml of OPA.

3) Naphthylethylenediaminedihydrochloride (0.1% w/v): 0.1 g of NEDA was dissolved in 50 ml of OPA.
4) Griess reagent: prepare 100 ml of Griess reagent by mixing sulfanilamide (1% w/v), NEDA (0.1% w/v) and ortho- phosphoric acid (OPA) (2.5% v/v)
5) Standard sodium nitrite: 10 mg of sodium nitrite in 100 ml of distilled water.

Procedure

To freshly prepared 1ml of Griess reagent, 1 ml of tissue homogenate was added and solution was incubated for 30 min at room temperature. The absorbance was measured at 540 nm and compared to those of known concentrations of sodium nitrite. The levels of tissue nitrite were expressed as µmoles/g of protein.

3.3.10.2 Nitric oxide (73)

Total NO was determined by measuring its stable metabolites, particularly, nitrite ($NO2^-$) and nitrate ($NO3^-$) based on the method of Miranda et al. (2001).

Reagents

1) Ortho-phosphoric acid (OPA) (2.5% v/v): 2.5 ml of OPA was made upto 100 ml of distilled water.
2) Sulfanilamide (1% w/v): 1.0 g of sulfanilamide was dissolved in 50 ml of OPA.
3) Naphthylethylenediaminedihydrochloride (0.1% w/v): 0.1 g of NEDA was dissolved in 50 ml of OPA.
4) Griess reagent: prepare 100 ml of Griess reagent by mixing sulfanilamide (1% w/v), NEDA (0.1% w/v) and ortho- phosphoric acid (OPA) (2.5% v/v)
5) Standard sodium nitrite: 10 mg of sodium nitrite in 100 ml of distilled water.

Procedure

To freshly prepared 1ml of Griess reagent, 1 ml of tissue homogenate was added and solution was incubated for 30 min at room temperature. The absorbance was measured at 540 nm and compared to those of known concentrations of sodium nitrite. The levels of tissue nitrite were expressed as µmoles/g of protein.

3.3.10.3 Malondialdehyde (MDA) (74)

The determination of the levels of lipid peroxides, expressed as malondialdehyde (MDA), was carried out according to the thiobarbituric acid assay of Slater and Sawyer (1971).

Reagents

1) Thiobarbituric acid (0.67% w/v): 0.67 g of thiobarbituric acid was dissolved in 50 ml of hot distilled water and the final volume was made up to 100 ml with hot distilled water.
2) Trichloroacetic acid (10% w/v):10 g of trichloroacetic acid (TCA) was dissolved in 60 ml of distilled water and the final volume was made up to 100 ml with distilled water.
3) Standard Malonedialdehyde stock solution: A standard MDA stock solution was prepared by mixing 25 µl of 1, 1′, 3, 3′-tetraethoxypropane with 10 ml with distilled water. 1.0 ml of this stock solution was diluted up to 100 ml to get solution containing 23µg of malondialdehyde/ml. One ml of this stock solution was diluted up to 100 ml to prepare a working standard solution containing 23ng of malondialdehyde/ml.

Procedure

2.0 ml of the tissue homogenate (supernatant) was added to 2.0 ml of freshly prepared TCA and the mixture was allowed to stand in an ice bath for 15 minutes. After 15 minutes, the precipitate was separated by centrifugation at 3000 rpm for 15 min at 4 °C and 2.0 ml of clear supernatant solution was mixed with 2.0 ml of freshly prepared TBA. The resulting solution was heated in a boiling water bath for 10 minutes. It was then immediately cooled in an ice bath for 5 minutes. The color developed was measured at 532 nm against reagent blank. Different concentrations (0-23 nM) of standard MDA were taken and processed as above for standard graph. The values were expressed as nmol of MDA/mg protein.

3.3.10.4 Reduced glutathione (GSH) (75)

Reduced glutathione level was determined as previously described by Moron and Depierre (1979).

Reagents

1) Tri-chloroacetic acid (20% w/v): 20 g of TCA was dissolved in sufficient quantity of distilled water and the final volume was made up to 100 ml with distilled water.
2) Phosphate Buffer (0.2 M, pH 8.0): 0.2 M sodium phosphate was prepared by dissolving 31.2 g sodium phosphate ($Na_2HPO_4*2H_2O$) in 600 ml of distilled water, the pH was adjusted to 8.0 with 0.2 M sodium hydroxidesolution and the final volume was adjusted up to 1000 ml with distilled water.

3) DTNB reagent (0.6mM): 23.76 mg of 5, 5'-dithiobis (2-nitro benzoic acid) was dissolved in 50 ml of Phosphate buffer and the final volume was adjusted to 100 ml with Phosphate buffer.
4) Standard Glutathione: 10mg of reduced glutathione was dissolved in 60 ml of distilled water and the final volume was made up to 100 ml with distilled water

Procedure

Equal volumes of tissue homogenate (supernatant) and 20% TCA were mixed. The precipitated fraction was centrifuged at 4000 rpm for 10 min at 4 °C and to 0.25ml of supernatant, 2ml of DTNB reagent was added. The final volume was made up to 3ml with phosphate buffer. The colour developed was read at 412 nm against reagent blank. Different concentrations (10-50µg) of standard glutathione were taken and processed as above for standard graph. The amount of reduced glutathione was expressed as µg of GSH/mg protein

3.3.10.5 Super oxide dismutase (SOD) (76)

Superoxide dismutase was estimated using the method described by Mishra and Fridovich (1972).

Reagents

1) Potassium Phosphate buffer (0.02 M, at 25 °C pH 7.5):
2) Carbonate Buffer (0.05 M, pH 10.2): 16.8 g of sodium bicarbonate and 22 g of sodium carbonate was dissolved in 500 ml of distilled water and the volume was made up to 1000 ml with distilled water.
3) Ethylenediaminetetraacetic acid (EDTA-Na) solution (0.49mM):182 mg of EDTA-Na was dissolved in 200 ml of distilled water and the volume was made up to 1000 ml with distilled water.
4) Hydrochloric acid (0.1 N): 8.33 ml of conc. hydrochloric acid was mixed with 500 ml of distilled water and the volume was made up to 1000 ml with distilled water.
5) Epinephrine solution (3 mM): 0.99 g epinephrine bitartarate was dissolved in 100 ml of 0.1 N hydrochloric acid and the volume was adjusted to 1000 ml with 0.1 N hydrochloric acid.
6) Superoxide Dismutase (SOD) standard (1000 U/ml): 98µL from primary stock solution (7.3 mg/1.46 m) (14965 U/1.46 ml) of SOD from bovine liver was taken and the volume was made up to1 ml with Potassium Phosphate buffer. Stored at -20 °C. (Bottle contain 7.3 mg powder, 2050 U/mg solid, 2554 U/ mg protein).

Procedure

0.5 ml of tissue homogenate was diluted with 0.5 ml of distilled water, to which 0.25 ml of ice-cold ethanol and 0.15 ml of ice-cold chloroform was added. The mixture was mixed well using vortex for 5 minutes and centrifuged at 2500 rpm for 10 min at 4 °C. To 0.5 ml of supernatant, 1.5 ml of carbonate buffer and 0.5 ml of EDTA solution were added. The reaction was initiated by the addition of 0.4 ml of epinephrine and the change in optical density/minute was measured at 480 nm against reagent blank. SOD activity was expressed as units/mg protein. Change in optical density per minute at 50% inhibition of epinephrine to adrenochrome transition by the enzyme is taken as the enzyme unit. Calibration curve was prepared by using 5-160 units of SOD

3.3.10.6 Catalase (77)

It was estimated by the method of Hugo Aebi as given by Colowiek *et al.* (1984).

Reagents

1) Phosphate Buffer (50 mmol/l, pH 7.0): (a) 6.81 g of potassium dihydxogen orthophosphate (KH_2PO_4) was dissolved in distilled water and made up to 1000 ml. (b) 8.90 g of disodium hydrogen orthophosphate (Na_2HP0_4) was dissolved in distilled water and made up to 1000 ml. The solutions (a) and (b) were mixed in the proportion of 1:1.5 (v/v).
2) Hydrogen Peroxide (30mmol/1): 0.34ml of 30% hydrogen peroxide was diluted with phosphate buffer to 100 ml. This solution was prepared fresh each day.
3) Catalase standard (65,000 U/mg protein; 1mg protein/ml): Crystalline beef-liver catalase suspension was centrifuged to isolate the crystals of the enzyme that was dissolved in 0.01M phosphate buffer (pH 7.0) to give a final concentration of l.0 mg protein/ml. Before assay, it was diluted with distilled water to obtain 1000 U/ml.

Procedure

Dilute homogenate 20 times with phosphate buffer (50 mmol/l; pH 7.0). To 2 ml of diluted sample, 1ml of hydrogen peroxide (30mmol/l) was added to initiate the reaction. The blank was prepared by mixing 2 ml of diluted sample (similar dilution) with 1 ml of phosphate buffer (50 mmol/l; pH 7.0). The dilution should be such that the initial absorbance should be approximately 0.500. The decrease in absorbance was measured at 240 nm. Catalase activity was expressed as µmoles of H_2O_2 consumed/min/mg protein.

3.4 Methods for screening and evaluation of novel FXa inhibitors for anticoagulant and antithrombotic activity

3.4.1 *In-vitro* inhibition assay

3.4.1.1 *In-vitro* FXa inhibition assay

FXa inhibition study was performed using a *p*H 6.5 buffer containing 50 mM Tris-HCl, 150mM NaCl, 0.1% w/v bovine serum albumin. 10µl of potential FXa inhibitor (test compounds or solvent reference) and 10µl of FXa (1µM) (FXa Human, Molecular Innovations, USA) were consecutively added. After incubating at 37 °C for 10 minutes, 20µl of FXa substrate (3 mM) (S-2765, Molecular Innovations, USA) was rapidly, added and 70µl of Tris buffer was added to make the volume upto 100µl *p*H 6.5 buffer was added to the wells, and the absorbance was measured at 405 nm using Biorad microplate reader 682XR(78).

3.4.1.2 *In-vitro* thrombin inhibition assay

In-vitro thrombin inhibition was studied by BIOPHEN DTI kit from Anira biosciences. Human thrombin enzyme and thrombin specific chromogenic substrate was prepared according to instruction manual by adding 2.5 ml distill water to enzyme and substrate vial. Solutions of standard drug and NCEs were made from 100nM-100µM. 50µl of standard drug or NCEs dilution was incubated with 50µl of thrombin specific chromogenic substrate for 10 minutes at 37^0C. 50µl of human thrombin enzyme was added and incubated for 2minutes with mild shaking. Reaction was stopped by adding 100µl of 2% citric acid and immediately measured at 405 nm in Biorad microplate ELISA reader 680XR.

3.4.1.3 *In-vitro* anticoagulant activity by PT and aPTT measurement

Clotting time was determined by standard one-stage recalcification assay with a BBL Fibrosystemfibrometer (Bectone Dickinson, Sparles, MD). For PT assay thromboplastin was reconstituted and warmed at 37 ^{0}C as per the manufacturer's directions. 2.5 µL of FXa inhibitor (test compound), with the desired concentration (1 mM) made up to 25 µL using citrated human plasma, was incubated for 30 sec at 37 ^{0}C followed by addition of 50 µL of pre-warmed thromboplastin. For the aPTT assay, 25 µL of pre-warmed aPTT reagent (0.2% ellagic acid) was mixed with 2.5 µL of inhibitor and 22.5 µL of citrated human plasma and kept for incubation at 37 ^{0}C for 4 minutes. Thereafter, immediate addition of 25 µL of pre-warmed 25 mM calcium chloride caused clotting and the clotting time was noted. Similar

procedure was followed in the absence of FXa inhibitor using 2.5 µL of organic vehicle or saline***(79)***.

3.4.2 Docking studies of novel FXa inhibitors

The novel FXa inhibitors were designed on the basis of existing active site knowledge. Here, different structure-based approach was applied to design potential active molecules; these compounds were designed on basis of literature review and the knowledge of receptor active site and the biologically most active molecules were reanalyzed with the help of docking study.

Docking studies were executed with Glide module of Schrodinger Suite 2019.Glide is projected for screening of probable ligands based on binding mode and affinity for a given receptor molecule. It performs grid-based ligand docking and searches for promising interactions between ligand molecules and a macro molecule, typically a protein.

For docking purpose Glide offers three different levels of docking precision: HTVS (high-throughput virtual screening), SP (standard precision), and XP (extra precision). The 3D structures of ligand molecules were built within Maestro using the Build module and a single low energy conformation search was carried out for all molecules under study using OPLS2e force field at physiological *p*H condition using LigPrep module of Schrödinger, here all the parameters were kept to standard value.

The receptor crystal structure for FXa obtained from Protein data bank (PDB code: 2P16) were optimized and prepared using protein preparation wizard, using standard parameters in protein preparation wizard. The grid was generated on active site of respective receptor structure and was validated by re-docking the pre-existing co-crystallized ligand structures. Here the docking study was performed in XP mode and interactions were visualized in visual interface.

3.4.3 Cyotoxicity assay of compound (14) and (50) on H9C2 cardiacmyocytes

MTT assay for the compound **(14)** and **(50)** on H9C2 cardiacmyocytes were performed according to the procedure mentioned in 3.3.4.

3.4.4 *In-vivo* evaluation of antithrombotic activity of compound (14) and (50) in $FeCl_3$ induced arterial thrombosis

Male rats (weight 200-250 g) were treated orally with selected NCEs of 15 and 30 mg/kg dose suspended in 0.5%Na-CMC and then subjected to $FeCl_3$-induced arterial thrombosis after 2 h of administration. Rats were anesthetized with ketamine and xylazine (80mg/kg, 20mg/kg respectively, intraperitoneally). A midline cervical incision was made on the ventral side of the neck, and left carotid artery was isolated. A 2*3 mm strip of Whatman filter paper no. #1 saturated with 35% (w/v) $FeCl_3$ was kept on the carotid artery for 5 min. One hour after removal of the filter paper, the arterial thrombus was excised, blotted of excess blood and immediately weighed(79).

Table 3.2: Effect of compound (14) and (50) in $FeCl_3$ induced thrombosis in rats

Groups	No. of animals	Group	Treatment
I	6	Sham control	Equivalent volume
II	6	$FeCl_3$ (Positive Control)	35% $FeCl_3$
III	6	Positive control + Compound **(14)**	15mg/kg;p.o.
IV	6	Positive control + Compound **(14)**	30mg/kg;p.o.
V	6	Positive control + Compound **(50)**	15mg/kg;p.o.
VI	6	Positive control + Compound **(50)**	30mg/kg;p.o.
VII	6	Positive control + Apixaban	15mg/kg;p.o.
VIII	6	Positive control + Apixaban	30mg/kg;p.o.

4. RESULTS AND DISCUSSION

4.1 Functional antagonism assay of standards and synthesized multitargeted ligands

4.1.1 Establishing baseline values for agonists and studies with standard antagonists of α_1 and AT_1 receptor

The primary aim of the studies was to identify a potential candidate that showed balanced inhibition of the α_1 and the ang II receptors. This was brought about by studying the antagonistic ability of different test compounds against phenylephrine and ang II mediated contractions of the rat thoracic aorta. Similar studies were also performed with the standard compounds for the purpose of direct comparison. The studies were initiated with the evaluation of terazosin against phenylephrine mediated contractions. Phenylephrine initiated contractions in the rat aortic strips at concentrations ranging from 5 nM or higher. It was observed that addition of 10µM terazosin caused a rightward parallel shift in the concentration-response-curve of phenylephrine. pA_2 calculations revealed a value of **8.97 ± 0.14** which was in line with previously reported value on rat aorta(80). Hence, this value was considered as the standard value for further studies and reported accordingly. This study allowed establishment of baseline values for phenylephrine and simultaneously permitted calculation of pA_2 value of NCEs against α_1 receptors.

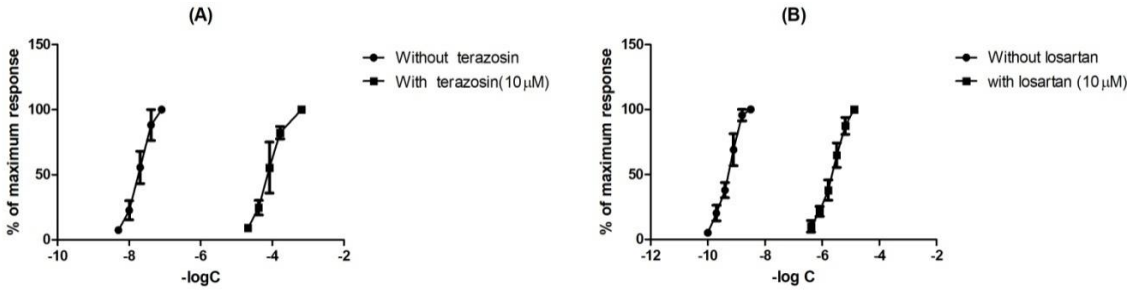

Figure 4.1: Concentration response curves to **(A)** phenylephrine and **(B)** angiotensin II in presence of standard drugs at 10 µM (n=3).

Similar studies were performed on separate set of aortic strips using angiotensin II as the agonist where losartan was used as the standard antagonist. Concentration Response Curve (CRC) was obtained with ang II at concentrations ranging from 1 nM and higher. Incubation of losartan (0.1 µM) or higher concentrations (10 µM) resulted in a rightward parallel shift of the CRC of ang II with pA_2 value being **8.63 ± 0.08**.

4.1.2 Screening of potential compounds for dual antagonism of α_1 and AT_1 receptors

After establishing the pA_2 value for standards drugs against their respective agonists, it was decided to evaluate the potency of newly synthesized NCEs for their balance antagonistic potential against α_1 and AT_1 receptors. Various novel compounds bearing 6,7 dimethoxyquinazoline and 7,8 dimethoxyquinazoline as parent scaffolds were screened by functional antagonism assay using rat aorta, pA_2 of NCEs are mentioned in tables 4.1-4.9 according to their scaffold, linker moiety and substitutions.

Series I

Table 4.1: pA_2 value of compounds of series I

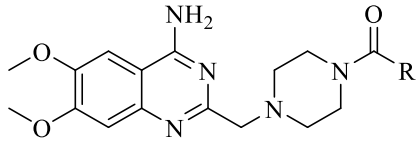

Compound	*Where –R is*	*p*A_2 values	
		α_1	AT_1
1	-C_6H_5	5.95 ± 0.83	4.75 ± 0.72
2	-C_6H_4F (o)	5.66±1.06	**7.75±0.49**
3	-C_6H_4OMe(o)	6.46±0.19	5.37±0.94
4	-C_6H_4OMe(m)	-	-
5	-C_6H_4Cl(m)	2.14±0.22	4.36±0.35
6	C_6H_4Br(m)	3.45±0.12	4.67±0.2
7	-$C_6H_3Cl_2$(o,m)	-	6.61±1.12
8	-$C_6H_3OMe_2$(o,m)	-	6.34±1.07
9	-C_6H_4Me(m)	-	-
10	-C_6H_4F(p)	3.28±0.87	2.15±0.21
11	-C_6H_4CN(p)	**6.93±0.47**	**6.87±0.60**
12	-CH_2-C_6H_5	1.98±0.34	3.03±0.45
13	-CH_2-C_6H_4Cl(m)	4.05±0.43	5.41±0.52
14	-CH_2-C_6H_4OMe(p)	-	-

(-) = Did not show any activity

Compounds **(1-14)** were designed and synthesized by having a methylene spacer between the 4-amino-6,7-dimethoxyquinazoline scaffold and the piperazine ring. Phenyl derivatives were attached with piperazine ring by carbonyl linker (-C=O). Test compounds were evaluated for functional antagonism assay. pA_2 values did not revealed comparable potency with standard drugs. Compound **(2)** showed considerable activity for AT_1 receptor while compound **(11)** displayed balanced modulation at both receptors but having sub level potency compared to standard drugs. Conversion of phenyl(piperazinyl)methanone moiety **(12)** to phenyl(piperazinyl)ethenone **(14)** as in compounds (**12-14**) also failed to produce significant inhibition on both the receptors as compared to standard drugs.

Series II

Table 4.2: pA_2 value of compounds of series II

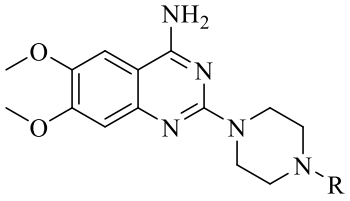

Compound	*Where –R is*	*p*A_2 values	
		α_1	**AT_1**
15	-CH_3	**9.23 ± 0.12**	5.75 ± 0.07
16	-CH_2CH_3	**10.41 ± 0.12**	5.08 ± 0.08
17	-C_6H_5	8.74 ± 0.08	3.31 ± 0.13
18	-C_6H_4CN (*o*)	**9.47 ± 0.06**	**8.54 ± 0.07**
19	-$C_6H_4OCH_3$ (*o*)	7.26 ± 0.12	6.54 ± 0.51
20	-C_5H_4N	6.95 ± 0.08	5.09 ± 0.12
21	-$CH(C_6H_5)_2$	**7.09 ± 0.15**	**7.59 ± 0.58**

Series II designed by substituted phenyl derivatives attached directly to piperazine linker resulted into improved activity especially at α_1 receptor. Compound **(15-21)** showed good to excellent inhibition for α_1 receptor, with similar to higher activity when compared to terazosin (**15-21)**. However, compound **(15-17)** failed to exhibit significant AT_1 receptor antagonism. From the results it was speculated that absence of aromatic moiety is responsible for absence of AT_1 receptor antagonism. Substitution with benzene moiety in **(16)** resulted into compound **(17)** and substitution with different phenyl derivatives in **(16)** resulted into compound **(18-21).** As suspected, replacement with aromatic moiety resulted into improvement in AT_1 receptor blocking potency **(18-21).** Compound **(18)** showed excellent potency for α_1 and AT_1 receptor (pA_2 for **α_1=9.47±0.06, AT_1= 8.54±0.07**) (Table 4.2). Compound **(21)** also showed balance modulation at both the receptors compared to standard drugs.

Series III

Table 4.3: pA_2 value of compounds of series III

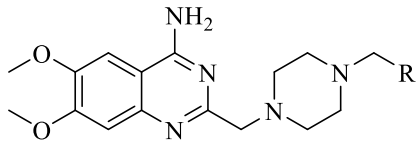

Compound	*Where –R is*	*p*A_2 values	
		α_1	AT_1
22	-C_6H_5	4.55±0.43	5.41±0.52
23	-$C_6H_4CF_3$(o)	-	6.10±0.97
24	-C_6H_4Me(o)	**8.34±0.14**	**8.73 ±0.10**
25	-C_6H_4Br(o)	5.08±0.84	-
27	-C_6H_4CN (o)	5.89±0.90	-
28	-C_6H_4Br(p)	5.91±0.81	6.49±0.77
29	-C_6H_4Me(p)	5.91±0.35	6.12±0.72
30	-C_6H_4OMe(p)	**7.19±0.56**	-
31	-C_6H_4-t-butyl(p)	**7.50±0.69**	6.58±0.84
32	-C_6H_4-C-C_6H_4CN(o)	4.64±0.56	-
33	-naphtyl	6.32±0.62	6.95±0.37
34	-benzhydryl	**7.44±1.10**	**7.26±1.03**
35	-cyclohexyl	-	6.95±0.37

(-) = Did not show any activity

Series III designed by placing methylene bridge on the either side of piperazine ring. Further compounds were synthesized by different aromatic ring substitution at 2nd and 4th positions resulted into compounds **(22-35).** Compounds (**22, 23, 25-29**) reflected poor antagonism at both the targeted receptors. Compound **(24)** exhibited excellent antagonism at the target sites reflected by its superior pA_2 values. (pA_2 for **α_1=8.55±0.13, AT_1= 8.68 ±0.02)**. Replacement of substituted benzyl with benzhydryl in **(34)** also revealed balance modulation with comparable potency. (Table 4.3). Loss of aromaticity in compound **(35)** having cyclohexyl substitution resulted into diminished inhibition at both the target site.

Series IV

Table 4.4: pA_2 value of compounds of series IV

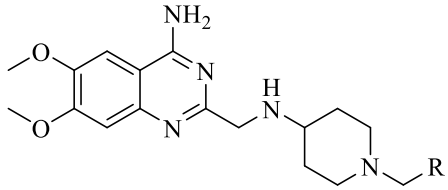

Compound	*Where –R is*	***p*A$_2$ values**	
		α_1	**AT_1**
36	-C_6H_5(o)	4.95±0.42	5.51±1.01
37	-C_6H_4Br(o)	6.43±0.05	-
38	-C_6H_4CN(o)	6.55±1.01	5.78±0.78
39	-C_6H_4Me(o)	6.79±0.20	5.66±0.25
40	-C_6H_4OMe(m)	6.75±0.22	5.96±0.12
41	-C_6H_4Me (p)	6.79±0.14	6.52±0.08

(-) = Did not show any activity

Series IV was explored with a view to study the effect of heterocyclic substitution on biological activity. To achieve the same, piperazine linker was replaced with piperadine ring. However, this attempt resulted into loss of potency as depicted in table 4.4. Compound **(36-41)** showed loss of activity compared to series III. Compound **(36-41)** showed mild activity at α_1 receptor (pA_2= 6-6.8) but resulted into absence of AT_1 antagonism.

Series V

Table 4.5: pA2 value of compounds of series V

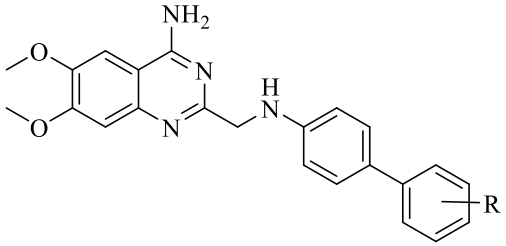

Compound	*Where –R is*	*p*A_2 values	
		α_1	AT_1
42	-C_6H_5(o)	**7.82±0.06**	**7.99±0.10**
43	-C_6H_4Cl(o)	6.39±0.06	**7.20±0.20**
44	-C_6H_4Me(o)	**6.92±0.16**	**6.90±0.12**
45	-C_6H_4CN(p)	6.37±0.19	6.92±0.20
46	-C_6H_4SMe(p)	6.10±0.14	**7.71±0.08**
47	-$C_6H_4C(CH_3)_3$ (p)	6.32±0.1	5.31±0.22

Series V constituted by substituted biphenyl at 2nd or 4th position resulted into compound **(42-47)** with comparable potency exhibited at both the receptor. Compound **(42)** (pA_2 α_1=**7.82±0.06,** AT_1= **7.99±0.10**) displayed excellent blockade of α_1 and AT_1 receptor. Compound **(43-47)** showed mild to considerable antagonistic activity at both the target with pA_2 value ranging from 6-7.7 Compound **(44)** also showed balance antagonism by substitution at 2nd position with methyl group in compound **(42).** The results were encouraging as substitution with biphenyl derivatives offered balance modulation which support the notion of impact of aromaticity on AT_1 antagonism.

Series VI

Table 4.6: pA2 value of compounds of series VI

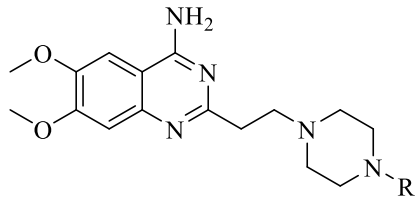

Compound	*Where –R is*	*p*A$_2$ values	
		α_1	**AT_1**
48	-C_6H_4Cl(o)	**9.24±0.07**	**7.00±0.09**
49	-C_6H_4CN(o)	**8.81±0.18**	**7.13±0.21**
50	-C_6H_4OMe(o)	**9.29±0.18**	4.99±0.04
51	-C_6H_4Me(o)	**9.27±0.09**	6.02±0.12
52	-pyridyl	-	-
53	-benzhydryl	**6.81±0.21**	**8.71±0.09**

(-) = Did not show any activity

Compound **(48-53)** synthesized by linking 6,7 dimethoxyquinazoline and substituted phenylpiperazine with ethyl linker which resulted into excellent antagonist activity at both the receptors. Compound **(48)** and **(49)** possessed superior α_1 antagonism **9.24±0.07, 8.81±0.18** respectively with considerable activity at AT_1 receptor (**7.00±0.09, 7.13±0.21)**. Substitution at 2nd position with methoxy **(50)** and methyl group **(51)** resulted in suppression of AT_1 receptor antagonism but α_1 antagonistic activity was retained as shown in table 4.6. Heterocyclic ring substitution with pyridyl in **(48)** resulted into **(52)** which revealed the loss of activity at both the receptors. The novel synthesized compounds superior antagonism compared to terazosin with noteworthy antagonism of AT_1 receptor. These results also provide leads for future development of similar multitargeted ligands.

Series VII

Table 4.7: pA2 value of compounds of series VII

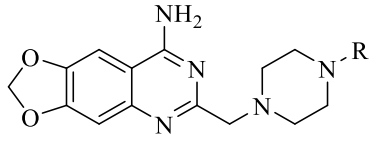

Compound	*Where –R is*	pA_2 values	
		α_1	**AT_1**
54	-C_6H_5	5.82±0.12	6.7±0.11
55	-C_6H_4F(o)	6.16±0.07	-
56	-C_6H_4CN(o)	**8.33±0.16**	5.80±0.06
57	-C_6H_4OMe(o)	6.37±0.05	4.70±0.19
58	-$C_6H_4NO_2$(p)	6.06±0.32	5.95±0.12
59	-C_6H_4Me(p)	6.07±0.23	5.96±0.27
60	-C_6H_4-butyl	6.06±0.28	5.42±0.28
61	-pyridine	6.59±0.23	5.31±0.21
62	-pyrimidine	5.68±0.11	-
63	-Napthyl	**7.57±0.21**	5.25±0.10
64	-Benzhydryl	6.22±0.28	6.08
65	-Cyclohexane	4.51±0.08	5.43±0.11
66	-CH_2-C_6H_4Br(o)	6.17± 0.15	6.07±0.21
67	-CH_2-C_6H_4Me(o)	6.23±0.24	6.21±0.09
68	-CH_2-C_6H_4OMe(p)	5.06±0.06	-
69	-CH_2-C_6H_4-t-butyl	6.52±0.30	**6.80±0.14**
70	-CH_2-Napthyl	6.69±0.14	5.66±0.10

(-) = Did not show any activity

In order to evaluate the effect parent scaffold on biological activity, 6,7-dimethoxy group on quinazoline scaffold linked to form cyclic diether resulting into compound **(54-70)**. As mentioned in table 4.7, changing in the parent scaffold resulted into decreased potency of compounds where only compound **(56)** and **(63)** showed considerable α_1 receptor blocking potential, however they failed to display considerable AT_1 receptor blocking action. pA_2 value for other NCEs were only between 5-6.80 suggesting inferiority of developed NCE.

Series VIII

Table 4.8: pA2 value of compounds of series VIII

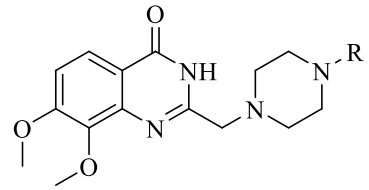

Compound	*Where –R is*	*p*A_2 values	
		α_1	AT_1
71	-C_6H_5	6.23±0.01	4.46±0.31
72	-C_6H_4Cl(o)	7.05±0.05	5.62±0.2
73	-C_6H_4CN(o)	**6.93±0.06**	**6.82±0.05**
74	-C_6H_4OMe(o)	6.61±0.17	5.46±0.13
75	-$C_6H_4NO_2$(p)	5.28±0.09	6.1±0.02
76	-t-butyl	5.56±0.15	6.02±0.09
77	-pyridine	6.00±0.28	5.80±0.11

Series IX

Table 4.9: pA2 value of compounds of series IX

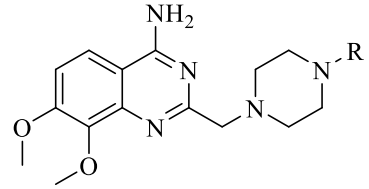

Compound	*Where –R is*	*p*A_2 values	
		α_1	AT_1
78	-C_6H_5	6.42±0.12	4.46±0.31
79	-C_6H_4Cl(o)	**7.05±0.27**	5.26±0.30
80	-C_6H_4CN(o)	**7.04±0.15**	**6.92±0.07**
81	-C_6H_4OMe(o)	6.8±0.12	5.67±0.09
82	-C_6H_4Me(o)	**7.87±0.05**	**7.35±0.2**
83	-$C_6H_4NO_2$(p)	**8.08±0.66**	6.25±0.24
84	-pyridine	5.44±0.12	5.97±0.1
85	-pyrimidine	5.68±0.24	6.00±0.21
86	-Napthyl	**7.07±0.04**	5.42±0.14
87	-benzhydryl	**7.37±0.30**	5.83±0.14
88	-CH_2-C_6H_5	6.39±0.31	5.82±0.20
89	-CH_2-C_6H_4CN(o)	5.38±0.21	-
90	-CH_2-C_6H_4Me(o)	**8.34±0.21**	**6.63±0.09**

Series VIII and IX were designed by using 7,8 dimethoxyquinazoline as a parent scaffold with different substitutions made at 2nd and 4th positions. Compound with carbonyl (C=O) group in parent moiety resulted into mild to moderate potency of developed NCE where compound **(71-77)** revealed pA2 value ranging from 5.5 – 7 (Table 4.8). These results emphasized the role of 4-NH_2 in the parent scaffold which provide important interaction site within the target site of the receptor. While in series IX with 4 –amino 7,8 – dimethoxyquinazoline derivatives **(78-90)** produced compounds with significant improvement in potency compare to series VIII (Table 4.9). Compound **(82)** possessed balance modulation with good pA_2 value. Substitution with more aromatic group resulted into loss of AT_1 receptor blocking action however α_1 antagonism was still preserved in compound **(86), (87)**. Addition of one carbon spacer to compound **(82)** resulted into **(90)** with enhanced α_1 blocking activity however activity towards AT_1 receptor was slightly compromised.

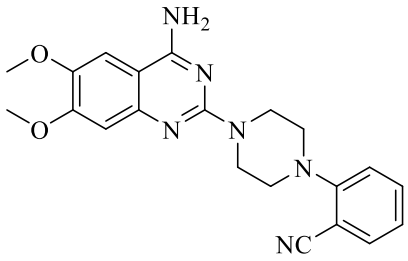

Compound (18)

2-(4-(4-amino-6,7-dimethoxyquinazolin-2-yl)piperazin-1-yl) benzonitrile

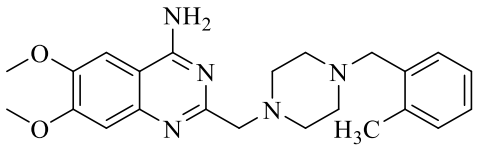

Compound (24)

6,7-dimethoxy-2-((4-(2-methylbenzyl)piperazin-1-yl)methyl)quinazolin-4-amine

After the extensive screening of developed NCEs, it was concluded that 6,7 dimethoxyquinazoline scaffolds with appropriate aromatic substitution with piperzine as linker can provide balance blocking activity at α_1 and AT_1 receptor.

From the above results, it was concluded that compound **(18) pA2 for α_1= 9.47±0.06, AT_1= 8.54±0.07)** and compound **(24) (pA_2 for α_1=8.55±0.13, AT_1= 8.68 ±0.02)** displayed potent

and balance inhibition at both target sites and hence, were explored for further study of activity, toxicity and *in-vivo* model of rat hypertension and cardiometabolic disorders.

4.1.3 Elaborated functional antagonism assay of potent compound (18) and (24)

The antagonism afforded by compound **(18)** and **(24)** on rat aortic strips was evaluated at 3 different concentrations (0.1, 1, 10 µM) to find that each higher concentration resulted in a further rightward parallel shift in the CRC of phenylephrine as well as Ang II. It has been suggested that if a series of antagonist concentrations yield linear Schild regression with a slope of unity, then obtained pA_2 value may be considered as the actual affinity of the ligand to the receptor(81). The pA_2 value calculated at different concentrations of compound **(18)** remained the same as that observed in preliminary studies. Accordingly, the pA_2 value of compound **(18)** against phenylephrine mediated contractions were 8.52±0.08 at 0.1µM, 8.81±0.06, at 1 µM, 8.34±0.14 at 10 µM with mean value of **8.55±0.13** for **α_1** and **8.68 ±0.02** for **AT_1** (8.67±0.09 at 0.1µM, 8.64±0.17 at 1µM, 8.73±0.10 at 10µM).

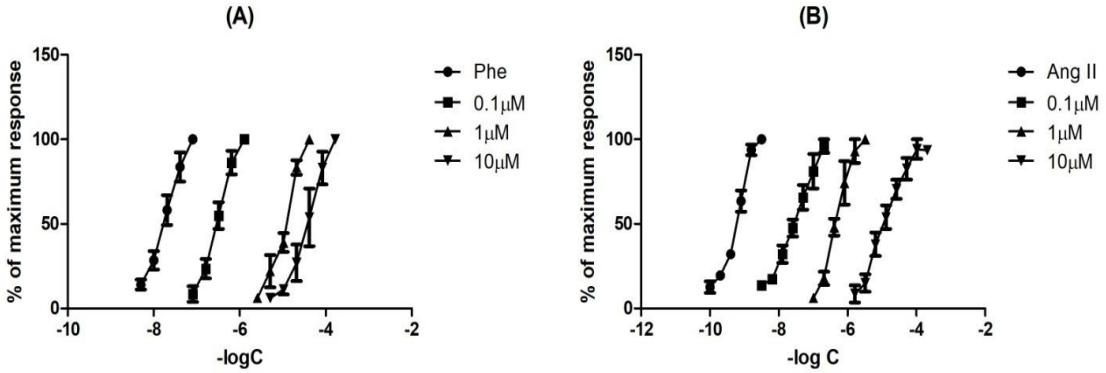

Figure 4.2: Concentration response curves of phenylephrine **(A)** and angiotensin II **(B)** in presence of different concentrations of compound **(18)** at 0.1, 1, 10 µM.

Similar experiments were also performed for compound **(24)** and results showed rightward parallel shifts were observed at each concentration and no significant deviation was observed in pA_2 value at different concentration range from 0.1µM to 10µM. For α_1 receptor, mean pA_2 value was found to be **9.47±0.06**(9.35±0.04 at 0.1µM, 9.50±0.07 at 1µM, 9.57±0.06 at 10µM) while at AT_1 receptor, pA_2value is **8.54±0.07**(8.44±0.08 at 0.1µM, 8.69±0.05 at 1µM, 8.48±0.01 at 10µM). These results also suggested competitive antagonism as similar pA_2 values were obtained at different concentrations.

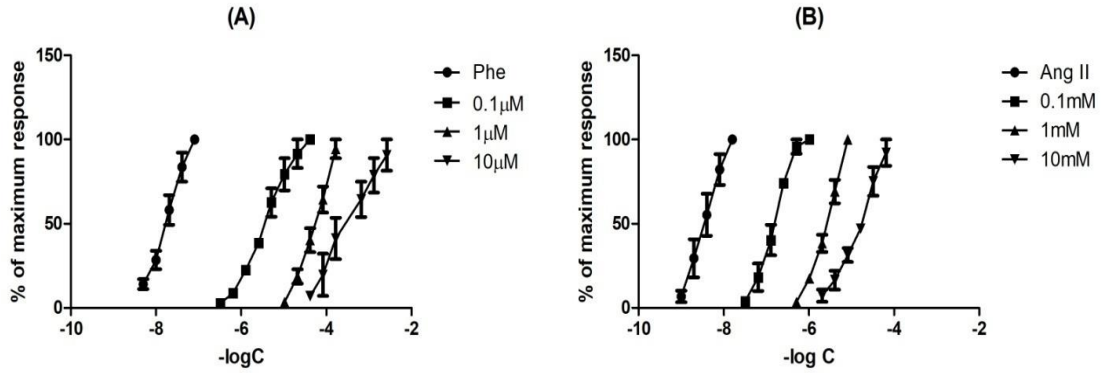

Figure 4.3: Concentration response curves of phenylephrine **(A)** and angiotensin II **(B)** in presence of different concentrations of compound **(24)** (0.1, 1, 10 μM).

4.2 *In-vivo* pressor response evaluation of compound (18) and (24) in anesthetized rats

4.2.1 Unmasked pressor response

The effects of **(18)** and **(24)** in *in-vitro* study were so profound that it was decided to challenge it against the *in-vivo* effects of phenylephrine and AngII on rat arterial blood pressure. Intact animals have been utilized by different research groups to evaluate the effects of AngII (82),(83) and phenylephrine(84) on arterial blood pressure. This method involves measurement of arterial blood pressure via cannulation of the carotid artery and offers a direct measurement of blood pressure. This method may also be utilized to study arterial reactivity of different vasoactive substances. Accordingly, two dose levels were chosen and the effects of **(18)** and **(24)** were evaluated against intravenous injections of phenylephrine and AngII (5μg/kg, i.v. each).

The effects were compared with similar doses of terazosin and losartan as standards. Phenylephrine produced increase in BP (ΔP= 40.66±8.12mmHg). It was found that terazosin-mediated effects were stronger as compared to **(18)** and **(24)** in inhibiting the pressor response to phenylephrine. At a lower dose of 10μg/kg, terazosin exhibited near 50% inhibition (50.27±4.64%) of pressor response to phenylephrine whereas compound **(18)** showed 19.55±1.28 % and compound **(24)** showed 22.75±2.32% inhibition of pressor response against phenylephrine which was significantly less as compared to terazosin ($p<0.001$).

At higher doses (50 μg/kg), the effects were more prominent and terazosin almost completely blocked the pressor effects of phenylephrine. Similarly compound **(18)** and **(24)**

at 50 µg/kg offered 46.19±5.47% and 55.74±4.93% inhibition of pressor effect of phenylephrine, respectively [Figure 4.4 (A)].

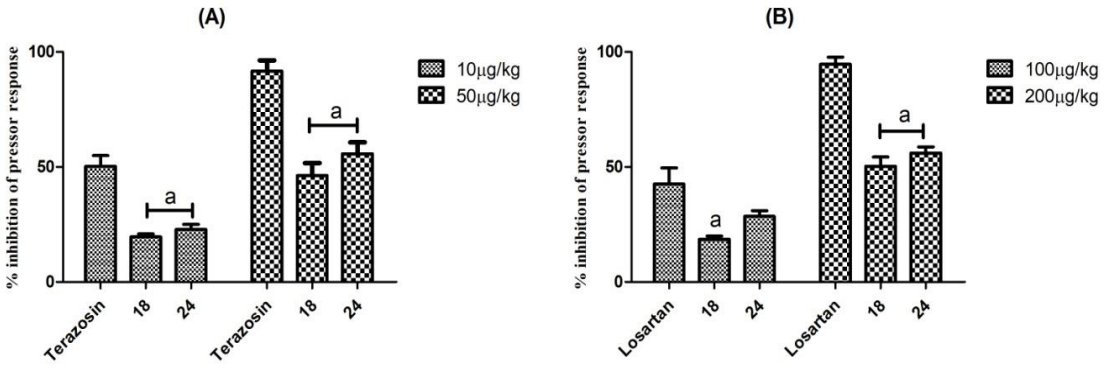

Figure 4.4: (A) Inhibition of mean arterial pressor response of phenylephrine in animals (n=3) previously dosed with compounds **(18)** and **(24)**, or terazosin. (**B**) Inhibition of mean arterial pressor response of Ang II in animals (n=4) previously dosed with compounds **(18)** and **(24)**, or losartan. Results are expressed as Mean± SEM values. Values were considered significant when $p<0.05$.a= compare to standard drug, b=compare to compound **(18).**

Separate dose levels were employed for the evaluation of antagonistic effects against AngII. Administration of i.v bolus of AngII (5 µg/kg) produced increase in MAP ($\Delta P=66.47\pm0.47$). It was more than observed by phenylephrine. Evaluation of mean arterial pressures revealed that losartan at a dose level of 100 µg/kg produced 42.55±6.99% inhibition of pressor response to AngII. At similar dose level, the response of compounds **(18)** and **(24)** was found to be considerably feeble and produced only about 20% inhibition of Ang-II pressor response. Administration of 200 µg/kg losartan prior to AngII challenge brought about a complete inhibition of AngII mediated rise in blood pressure. However, compounds **(18)** and **(24)** were only able to inhibit 50.28±2.99% and 56.03±2.66% respectively ($p<0.001$ vs. losartan) [Figure 4.4 (B)]. The results were unanticipated since there was a vast difference between the *in-vitro* data and preliminary *in-vivo* investigations. *In-vitro* data showed quite encouraging potency of the test compound however *in-vivo* studies did not reflect the same. This disparity in the results could be due to different in metabolism and pharmacokinetic profile of NCEs. However, it was unlikely as compounds were administered via i.v bolus and effects were observed immediately as in the case of standard drugs.

While considering these alternatives, it was speculated that since developed NCEs show dual action *in-vitro*, it is possible that the actual concentration of the drug reaching at a

particular receptor was lesser compare to standards at equal dose level. The reasons for such an abridged response may therefore be the distribution of the drug upon both the receptors in question suggesting that only a fraction of dose is available at a given time to act upon a particular population of receptors when challenged against specific agonist.

4.2.2 Masked pressor response

To evaluate the hypothesis proposed above, it was planned to evaluate the pressor-inhibition potential of **(18)** and **(24)** under masked conditions. *In-vivo* inhibition of phenylephrine mediated arterial pressor response was measured in those animals in which 200 µg/kg losartan was pre-administered. The idea behind such a protocol was to mask the effects of investigational NCEs on AT_1 receptor. Dose of losartan was selected on the basis of previous study [Figure 4.4 (B)] as 200 µg/kg showed more than 90% inhibition. Similarly, the other set involved measurement of inhibition of AngII mediated arterial pressor response in those animals in which 50 µg/kg terazosin [dose selected as per figure 4.4 (A)] was pre-administered to mask the effects of **(18)** and **(24)** upon α_1 receptors.

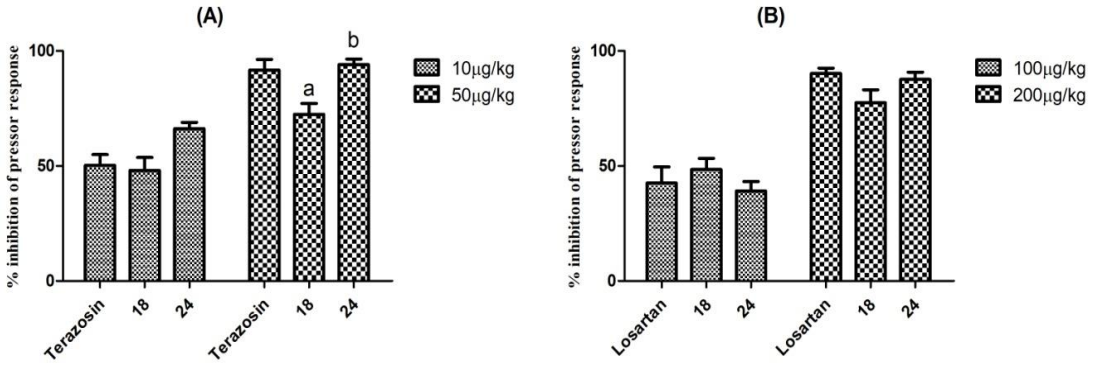

Figure 4.5: Mean arterial pressor responses under masking conditions. **(A)** effect of **(18)** and **(24)** against phenylephrine under losartan masking and **(B)** to ang II under terazosin masking. Results are expressed as Mean± SEM values (n=3). Values were considered significant when $p<0.05$. a= compare to terazosin, b=compare to compound **(18).**

It can be observed that [figure 4.5 (A)], previous administration of losartan (200 µg/kg) greatly increase the potential inhibition of **(18)** and **(24)** as there was no significant difference was observed between terazosin and NCEs. At 10ug/kg, compound **(18)** and **(24)** exhibited 48.00±5.58% and 66.13±2.84% respectively. At higher dose level of 50µg/kg, terazosin was able to show around 90% inhibition while **(18)** showed around 70% (72.36±4.78%, $p<0.05$ vs. terazosin) and **(24)** exhibited 94.01±2.46% inhibition.

In the different set of experiments as depicted in figure 4.5 (B), pre-administration of terazosin 50 µg/kg, produced profound increase in inhibition offered by **(18)** and **(24)** against AngII. At low dose of 100 µg/kg, compound **(18)** and **(24)** produced 43.37±5.32% while at 200 µg/kg, 85.10±3.71 % inhibition was achieved against pressor effect of AngII. There was no significant difference at both dose level compared to standard and investigational entities.

The results clearly shed light on the multiple effects shown by drugs used in clinical practice. The results suggest that the drugs used in clinical practice may have certain off-target effects not known at present. Simultaneously, it is also evident that it is possible to design ligands which have multiple targets for action. Such compounds may form the basis for favorable management of complex disorders like hypertension and other cardiovascular diseases.

4.3 Molecular modeling and Docking study of compound (18) and (24) with α_1 and AT_1 Receptor

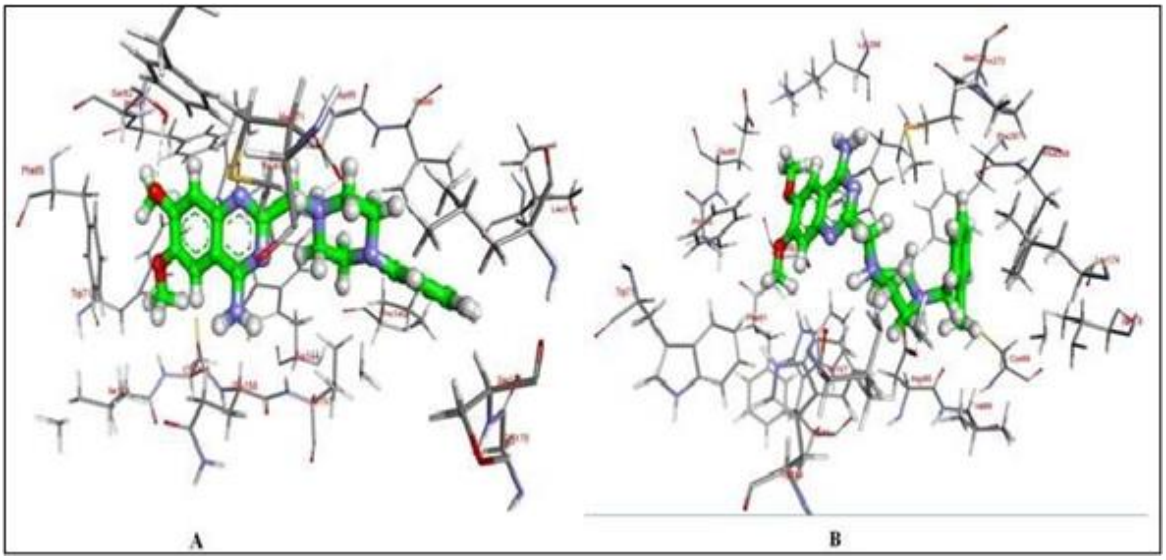

Figure 4.6: Docking interactions of compound **(A) 18** and **(B) 24** with the α_1-receptor

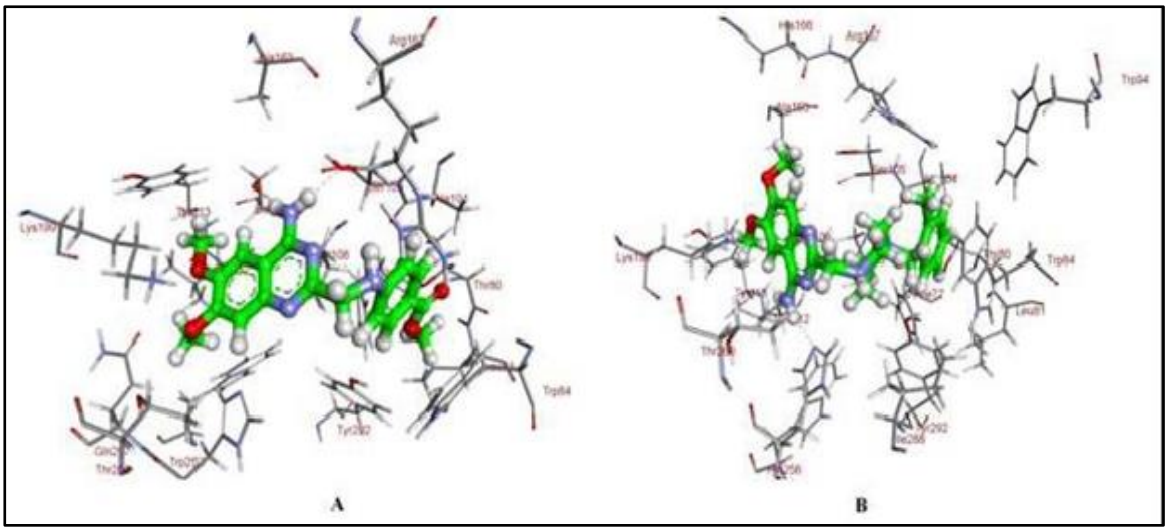

Figure 4.7: Docking interactions of compound **(A) 18** and **(B) 24** with the AT_1 receptor

After performing *in-vitro* and *in-vivo* experiments, two potential compounds **(18)** and **(24)** exhibited dual antagonism at both the target receptors. Using the available data of biological activity in hand for the synthesized compounds, highly predictive pharmacophore and 3D-QSAR models were developed to support the findings obtained from animal experiments. Docking interactions of compounds **(18)** and **(24)** are displayed in figure 4.6 and 4.7.

- **Docking of compound (18) and (24) with α_1 receptor**

In case of compound **(18)**, the protonated NH of piperazine forms a salt bridge with Asp85. One of the methoxy groups of dimethoxyquinazoline ring formed H bonding with Ser62. The aromatic ring of quinazoline offered further stability to the receptor ligand complex by showing π-π stacking with Trp81 [Figure 4.6 (A)]. For compound **(24)**, a similar type of salt bridge was observed with Asp85. Additionally, the *o*-methylbenzyl group was observed to be present into the hydrophobic pocket of Cys89, Phe267, Phe268, Met271 and Pro272. The quinazoline part was found to be stabilized by hydrophobic interactions with Phe65, Trp71 and Phe291 [Figure 4.6 (B)].

- **Docking of compound (18) and (24) with AT_1 receptor**

Docking interactions of compounds **(18)** and **(24)** were studied similarly within the active site of AT1-receptor. The aromatic ring of quinazoline was found to be stabilized by hydrophobic interactions with Leu112, Tyr113 and Trp253. The anilino part of the ligand

lent stability to the receptor-ligand complex by forming π-π stacking interaction with Trp84. The amino group of quinazoline ring offered further stability by having H-bonding with Ser105 and Ser109 [Figure 4.7 (A)].

In the case of compound **(24)**, the π-cation interaction of the aromatic ring of quinazoline and H-bonding of the amino group with His256 offered stability to the complex. But the orientation of *o*-methylbenzyl group towards Arg167 may be causing non-favorable interactions at this end as one part is polar and the other is hydrophobic in nature [Figure 4.7 (B)].

4.4 Cytotoxicity assay of compound (18) and (24) in HEK293 cell

In-vitro cytotoxicity assays have been used extensively to study the effect of NCEs or drugs on cell viability. It is necessary to evaluate the cytotoxic potential of developed NCE during preclinical studies, as it can become cause of failure in the later stages if not studied. After confirming *in-vitro* activity, developed NCEs were tested in HEK 293 kidney epithelial cell culture. Compounds **(18)** and **(24)** did not produce cell death as survival was found to be >80% at most of the concentrations

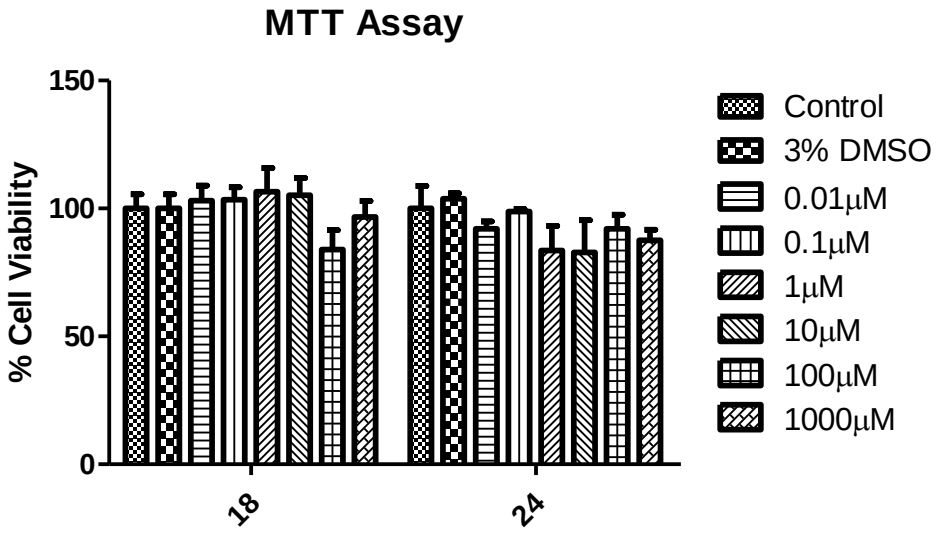

Figure 4.8: Survival of cells post-incubation with different concentrations of compounds **(18), (24)**, 3% DMSO (vehicle) and control cells in HEK293 cells (n=3). Statistical analysis did not find any significant difference between the groups.

4.5 Evaluation of compound (18) and (24) in UNX+DOCA salt induced hypertension

Recent studies in human and animal studies indicate that hypertension and associated CVS anomalies often stems from an overactive sympathetic nervous system(85) and an

imbalance in the renin- angiotensin system (RAS). The deoxycorticosterone acetate (DOCA)-salt model is ideal for defining the role of these two major pathways that are critical in essential hypertension pathogenesis. The DOCA-salt hypertensive rat is an established model of malignant mineralocorticoid hypertension with renal dysfunction(86). The administration of DOCA, in combination with salt loading, induces increased renal sodium reabsorption, resulting in hypervolemia(87). These conditions lead to symphatho-excitation and a rise in blood pressure due to increased vessel smooth muscle tone and peripheral vascular resistance. The hypertension induced by these factors later leads to endothelial dysfunction, cardiovascular remodelling, left ventricle hypertrophy, fibrosis, and heart failure. Additionally, kidney damage with glomerulosclerosis and tubular fibrosis are also the hallmark feature of DOCA salt induced hypertension. Evidences also suggested pathomechanism of DOCA-salt evoked volume-dependent hypertension and end organ damage, increased oxidative stress and inflammation are highly involved. Accordingly, this model emphasizes the role of the sympathetic nervous system, activation of RAAS, reactive oxygen species (ROS) and inflammation in the development of renal and cardiovascular remodeling. This study highlighted the effect of persistent salt loading induced hypertension and role of developed multitargeted ligands **(18)** and **(24**) in the amelioration of developed anomalies.

4.5.1 Effect of compound (18) and (24) on physiological parameters in UNX+DOCA salt induced hypertension

Table 4.10: Effect of compound (18) and (24) on physiological parameters in UNX+DOCA salt induced hypertension

Groups	Weight (gm)		Water intake (ml/rat)	Food intake (g/rat)
	0^{th} day	42^{nd} day		
NC	235.33±6.64	262.00±3.48	24±0.93	11.66±0.88
SC	236.33±5.24	254.00±1.63	24.66±0.80	10.83±1.01
UNX+DOCA (DC)	244.33±2.60	286.33±8.41	$71.83\pm2.21^{\#\#\#}$	11.66±1.45
DC+ Compound (18) (5 mg/kg)	225.00±0.81	252.00±2.44	$39.66\pm1.62^{***}$	13.00±1.15
DC+ Compound (18) (10 mg/kg)	229.05±5.52	266.66±3.33	$29\pm1.78^{***,\$\$}$	13.33±1.20
DC+ Compound (24) (5 mg/kg)	237.00±4.04	249.00±3.69	$42.33\pm2.66^{***}$	12.66±0.88

Groups	Weight (gm)		Water intake (ml/rat)	Food intake (g/rat)
	0th day	42nd day		
DC+ Compound (24) (10 mg/kg)	234.00±1.00	245.33±6.22	39.66±1.66***	13.00±1.52
DC+Los+Tera	243.5±6.94	252.5±6.12	33.16±2.16***	11.33±1.20

Effect of compound (18) and (24) on Physiological parameters. Values are expressed as mean±SEM (n=6). Data was analysed by one way ANOVA followed by Dunnet post hoc test. #= compare to sham control. *= compare to UNX+DOCA, $= compared to Los+ Tera, $$, **=p<0.01, ###,***=p<0.001

All the groups underwent unilateral nephrectomy followed by DOCA salt and 1% NaCl administration except normal and sham control animals for six weeks. Surgical intervention did not cause detrimental effect on weight and food intake of animals. There was no significant difference observed amongst groups. There was significant increase in water intake of UNX+DOCA salt treated rats compare to NC and SC rats (SC vs. DC; 24.66±0.80ml vs. 71.83±2.21ml, p<0.0001). As depicted in table 4.10, there was no difference in weight of animals amongst groups is observed suggesting surgical intervention did not interfere with normal growth process. Some of the studies have reported weight loss in DOCA salt treated rats as study progresses. Contrary, we have found slight weight gain, it was speculated that it may be due to dramatic increase in water intake in hypertensive rats. Administration of DOCA salt and 1% salt loading resulted into increase water intake as the study progresses resulted into significant elevation in water intake(88) as shown in table 4.10.

Reports have shown that consumption of sodium causes sensation of osmotic Na^+ receptors and increase in plasma osmolality. Changes in plasma osmolality serve as a signal for induction of thirst; increase water intake and set the loop in motion(89). It is also reported that increase salt consumption combined with fluid retention produce activation of RAAS and SNS nerve activity, vasopressin and endothelin release(90),(91). This global response of vasoconstriction resulted into initiation and maintenance of hypertension. Treatment with (18) and (24) caused reversal of this effect by inhibiting RAAS and SNS system and put halt to this feedback mechanism. Combination of standard drug also produced comparable effect compare to NCEs

4.5.2 Effect of compound (18) and (24) on hypertrophic response in UNX+DOCA salt induced hypertension

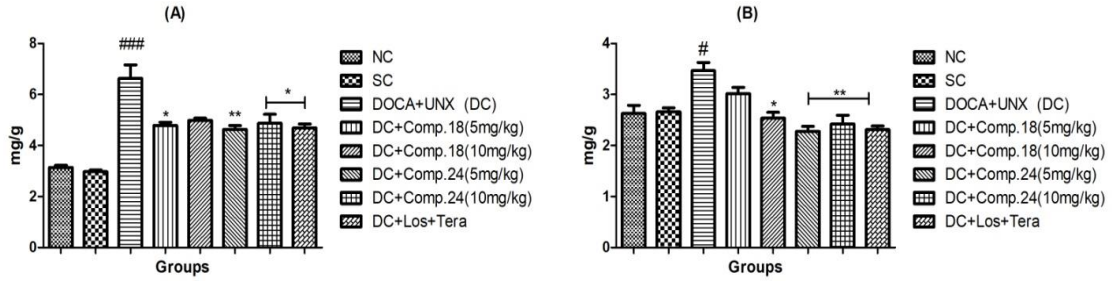

Figure 4.9: Effect of Comp (18) and (24) on **(A)** kidney odema index (KOI) **(B)** heart odema index (HOI). Values are expressed as mean±SEM (n=6). Data was analysed by one way ANOVA followed by Dunnet post hoc test. #= compare to sham control. *= compare to UNX+DOCA. #,*=p<0.05, ##, **=p<0.01, ###,***=p<0.001

Uninephrectomized rats underwent DOCA treatment and salt administration showed marked elevation in kidney weight in previous investigations(86). Our results are in accordance with previous findings as evident in figure 4.9 (A) Hpertensive rats showed almost 3 fold increase (p<0.001 vs. NC) in KW/BW ratio compare to normotensive rats. This observation can be attributed to increased workload implicated on the solitary kidney resulted into hypertrophic response. Treatment with compound **(18)** and **(24)** abrogated this damage resulted into significantly reduced Kidney Oedema Index (KOI) in dose dependent manner. Previous investigations also reported prevention in KOI by losartan and other ARB drugs. Standard drugs also exhibited similar degree of beneficial effect.

Sustained hypertension also produces significant increase in cardiac mass revealed by significantly increase Heart Oedema Index (HOI) in hypertensive rats. Chronic activation of AngII and epinephrine is reported to increase left ventricular mass and diameter suggested cardiac remodeling, increase end diastolic pressure, and elevations in hypertrophic factor in heart(92),(93). Administration of Compound **(18**) at 5mg/kg did not show improvement (p>0.05) in HOI while 10mg/kg and Compound **(24)** at both doses exhibited their preventive potential in dose dependent manner (p<0.001) compared to DC rats.

4.5.3 Effect of compound (18) and (24) on hemodynamic alterations in UNX+DOCA salt induced hypertension

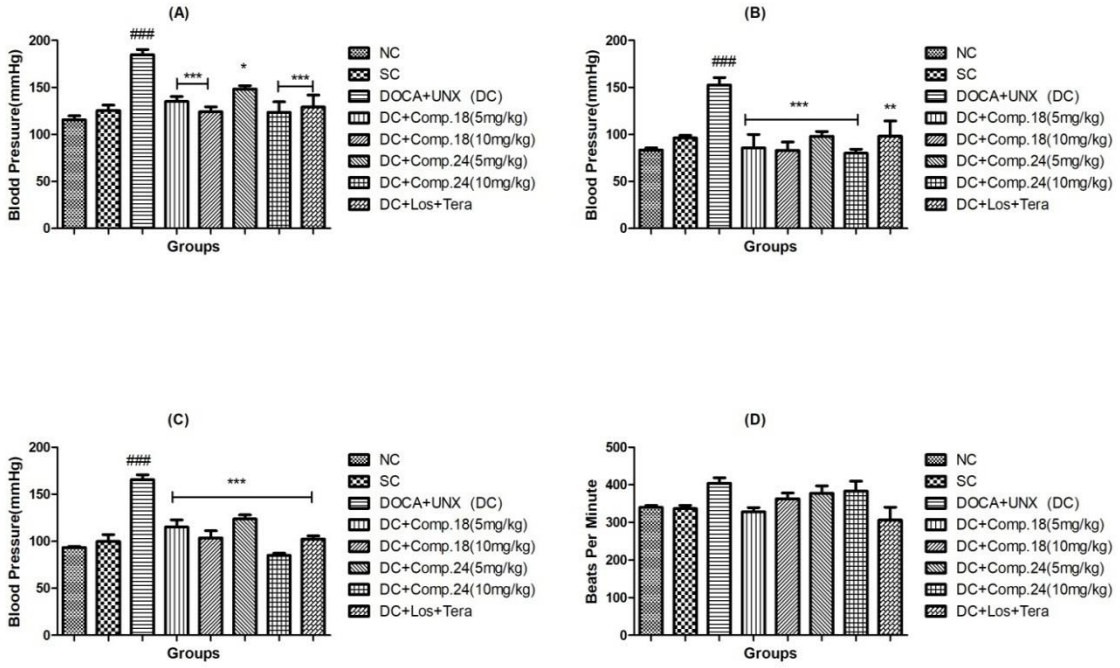

Figure 4.10: Effect of (18) and (24) on hemodynamic parameters. (A) SBP (B) DBP (C) MABP (D) Heart rate. Values are expressed as mean±SEM (n=6). Data was analysed by one way ANOVA followed by Dunnet post hoc test. #= compare to sham control. *= compare to UNX+DOCA. *=p<0.05, ##, **=p<0.01, ###,***=p<0.001 ns= non-significant. SBP= Systolic blood pressure, DBP=Diastolic blood pressure, MABP= Mean arterial blood pressure

UNX+DOCA treatment caused marked increase in SBP and DBP as depicted in figure 4.10 (A) by significant increase (NC vs. DC, 115.75±3.94 vs. 186.78±5.64, p<0.0001) as compare to normal and sham control animals. Treatment with compound (18) at both the doses produced excellent reduction in SBP [5 mg/kg (135.03±5.25), p<0.0001 vs. DC] and [10 mg/kg (122.32±5.22) p<0.0001 vs. DC]. While administration of compound **(24)** [5 mg/kg (148.42±3.06), p<0.05 vs. DC] and [10 mg/kg (123.34±11.42) p<0.0001 vs. DC] also produced potent antihypertensive effect by significant fall in BP. Combination of standard drugs showed comparable reduction in SBP (129.05±12.85, p<0.0001 vs. DC) to compound **(18)** and **(24)**. Treatment with compound **(18)** and **(24)** showed non-significant

difference when compare to each other and Dose dependent response was observed for developed compounds.

DBP has showed [figure 4.10 (B)] elevated drastically in hypertensive control compare to NC (NC vs. DC, 83.50±2.24 vs. 149.97±4.68, p<0.0001). Administration of **(18)** [5mg/kg (85.73±14.32), p<0.0001 vs. DC] and [10mg/kg (83.11±8.72) p<0.0001 vs. DC]. Treatment with **(24)** [5 mg/kg (98.11±5.03), p<0.0001 vs. DC] and [10 mg/kg (79.87±4.40), p<0.0001 vs. DC] at both doses produce significant reduction DBP compare to DOCA salt treated rats. losartan and prazosin were able to nullify the effect of UNX+ DOCA salt evident by significant reduction BP.

Mean arterial pressure is considered as one of the definitive parameters for the evaluation of antihypertensive drug. Compound **(18)** [5mg/kg (115.09±9.11), p<0.0001 vs. DC] and [10mg/kg (103.62±10.58) p<0.0001 vs. DC] was able to ameliorate UNX+DOCA induced chronic rise in blood pressure. Treatment with **(24)** [5mg/kg (123.49±5.62), p<0.0001 vs. DC] and [10mg/kg (85.06±1.84), p<0.0001 vs. DC] also abolished the rise MAP evoked by DOCA alt and salt loading. Animals treated with compound with **(24)** has slightly reduced MAP than NC and SC animals however no statistical difference was observed. Combination of standard drugs also produced desired effect by reducing BP compare to DC (102.26±3.52, p<0.0001 vs. DC). It is evident of from detailed hemodynamic assessment that treatment with both the NCEs produced excellent anti-hypertensive effect. Treatment with lower dose (5mg/kg) produced comparable or slightly better action than combination of standard drugs it can be attributed to dual antagonistic potential.

Hear rate variability is associated with the UNX DOCA salt model of hypertension; However, in our study we did not find any significant difference amongst different groups. Treatment with compound **(18)** and **(24)** did not cause any bradycardic or tachycardic response with their chronic treatment. On the contrary, treatment with combination of standard drugs showed reduced heart rate, this can be attributed due to terazosin treatment, as terazosin treatment alone cause severe bradycardic response in animals.

DOCA administration along with salt intake is known to induce renal hypertension related to its sodium water retention effects(94).DOCA being the precursor to aldosterone, is converted to aldosterone *in-vivo* through the action of the enzymes 11β-hydroxylase and subsequently aldosterone synthase. This de novo formation of aldosterone from exogenously administered DOCA leads to sodium retention in the distal tubules of the kidney. Increase in blood pressure is mediated mainly through plasma volume expansion

accompanied by sympathoexcitation and increased vasopressin levels(95), increase central and peripheral RAAS system, Alteration of the central baroreflex involvement of NOX pathways and endothelin-I induced vasoconstriction are also signatory to DOCA-salt mediated hypertension.

Compound **(18)** and **(24)** exhibited marked effects at both doses of 5mg/kg and 10mg/kg revealed potent inhibition of two major governing systems and their cross talk involved in the pathogenesis of hypertension. Results showed non-significant difference between standard treatments and compounds under investigation.

4.5.4 Effect of compound (18) and (24) on articular reactivity in UNX+DOCA salt induced hypertension

Table 4.11: Articular reactivity of comp (18) and (24) in UNX+DOCA salt induced hypertension

Groups	ΔP(mmHg)		
	Phenylephrine	**Angiotensin II**	**Acetylcholine**
NC	30.5±2.17	66.56±1.38	-56.32±9.58
SC	33.71±1.51	67.88±1.33	-51.76±3.01
UNX+DOCA (DC)	54.42±3.72$^{\#}$	106.84±4.97$^{\#\#}$	-45.47±8.41
DC+ Compound (18) (5mg/kg)	42.83±12.11	57.15±14.22**	-71.38±7.89
DC+ Compound (18) (10mg/kg)	31.42±5.16*	35.83±5.33***	-80.87±0.95
DC+ Compound (24) (5mg/kg)	26.98±0.83**	65.59±6.33**	-51.96±2.96
DC+ Compound (24) (10mg/kg)	23.24±4.12**	49.85±5.99***	-63.73±6.32
DC+Los+Tera	41.14±2.73	45.80±7.59***	-53.20±3.49

ΔP= indicates the difference in blood pressure between before and after Phenylephrine or Ang-II i.v. bolus. #= compare to NC & SC control. *= compare to UNX+DOCA. *=p<0.05, ##, **=p<0.01, ###,***=p<0.001 ns= non-significant

Studies have reported increase sympathetic nerve activity, upregulation RAAS system and AT_1 receptor. To test these findings in this study; vasoactive agents such phenylephrine, Ang II and acetylcholine were injected as i.v. bolus. Hypertensive rats showed enhanced pressure response due to upregulation of SNS and RAAS system. While on the other hand, vasodilatory effect of ach is attenuated in disease control rats. This can be due to damaged

endothelium resulted into reduced nitric oxide release and eNOS action (96). These results displayed in table 4.11 are in line with observation and proposed hypothesis.

Articular reactivity to different agonist was assesses by i.v bolus administration of vasoactive agents via jugular vein. UNX+DOCA salt treated showed heightened responses to selective α_1 agonist phenylephrine (5 µg/kg). Disease control produced more pronounced increment ($p<0.001$) in ΔP compare to NC and SC rats as evident in table 4.11. Pre-treatment with (18) only at 10mg/kg showed significant inhibition of pressor response while both the doses of (24) produced significant inhibition when challenged against phenylephrine [Compound (24- 5mg/kg, $p>0.05$), 24-10 mg/kg), $p<0.05$)]. Combination of standard drug produced lesser response compare to DC rats however it was not significant ($p>0.05$). Current study showed enhanced response to phenylephrine revealed up-regulation of adrenergic receptor, specifically α_1 receptors. Reid et.al. showed increased sympathetic nerve activity is also involved in DOCA-salt hypertension during the early phase (1–5 days after starting treatment) and developed phase (2–6 weeks after starting treatment)(97).

Similarly, AngII evoked potent rise in BP (ΔP= 66.56±1.38 vs. 106.84± 4.97, NC vs. DC, $p<0.0001$) in hypertensive rats due to activation RAAS system. Treatment with NCEs and standard drugs abolished pressor response significantly. Current study highlights the impact of dual receptor inhibition on improvement of response to vasoactive agents.

Many studied have been reported regarding disturbed endothelial dysfunction in hypertension in *ex-vivo* conditions. We have studied effect of Ach on pressor response for indication of integrity and function of endothelial nitric oxide in *in-vivo*. Ach administration cause potent fall in normotensive animals while hypertensive rats showed abrogated responses to Ach (56.32±9.58 vs. 45.47±8.41, NC vs. DC). Treatment with compound (18) (10mg/kg, $p<0.05$) showed excellent response to exogenous Ach which leads to fall in blood pressure. Treatment with (24) and standard drugs were able to produce modest effect to Ach.

4.5.5 Effect of compound (18) and (24) on metabolic parameters in UNX+DOCA salt induced hypertension

Table 4.12: Effect of 179 on metabolic parameters in UNX+DOCA salt induced hypertension

Group	Glucose	TG	TC	HDL
NC	141.57±3.35	55.16±1.28	44.32±2.09	55.21±2.14
SC	145.12±4.10	54.86±3.85	40.62±2.44	54.19±2.93
UNX+DOCA (DC)	147.97±6.05	76.40±6.13$^{\#}$	56.14±5.83	39.74±2.66$^{\#\#}$
DC+ Compound (18) (5 mg/kg)	132.87±8.63	58.70±1.64	50.41±3.08	60.01±1.61***
DC+ Compound (18) (10 mg/kg)	134.40±7.78	54.57±2.90*	46.16±2.31	56.71±1.61**
DC+ Compound (24) (5 mg/kg)	142.37±1.56	76.10±2.84	52.99±6.49	57.35±0.66*
DC+ Compound (24) (10 mg/kg)	137.40±2.89	64.20±4.10	46.86±3.29	57.30±3.68*
DC+Los+Tera	144.08±5.92	64.30±4.96	42.84±4.43	52.51±3.61*

#= compare to NC & SC control. *= compare to UNX+DOCA. *=p<0.05, ##, **=p<0.01, ###,***=p<0.001
ns= non-significant

Hypertension and metabolic anomalies are often progressed hand in hand and they have cause-effect relationship and vice versa. DOCA salt treatment is believed to exhibit metabolic dysregulation because of overwhelming response of RAAS and SNS. As both these systems play vital role in the insulin signaling and mediated effects (98), (99). In addition, elevated level of mineralocorticoid levels is reported to hamper insulin signaling (100) and mineralocorticoid antagonist improve insulin sensitivity in animals (101). Hypertensive rats showed non-significant change in glucose level after UNX+DOCA treatment compare to sham control animals. Treatment with NCE or standard drugs did not produce any change in glucose hemostasis. DOCA salt treated rats showed elevated level of TG ($p<0.05$) compared to naïve animals while oral administration with compound (18) was effective in lowering of TG significantly. Treatment with other drugs was not able to alter this metabolic abnormality. HDL-C level was also dramatically decreased with DOCA treatment. All treatment regime produced beneficial effective to raise this good cholesterol significantly. Total cholesterol was unaffected in all the groups as there was no significant change amongst the groups.

4.5.6 Effect of compound (18) and (24) on Ach mediated endothelial relaxation and nitric oxide level in UNX+DOCA salt induced hypertension

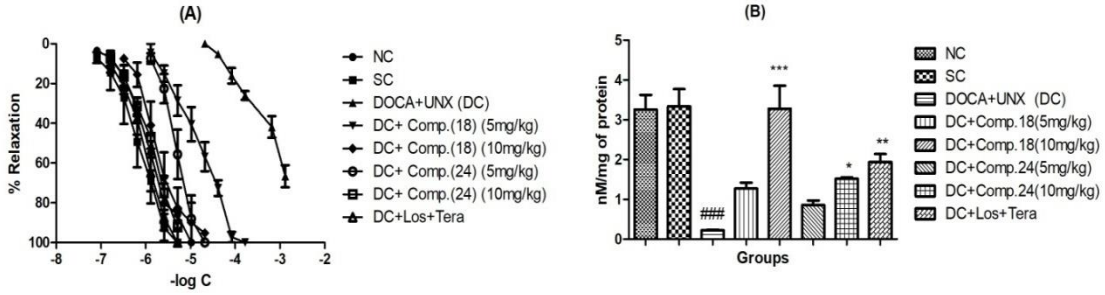

Figure 4.11: Effect of (18) and (24) on hemodynamic parameters. (A) Endothelial relaxation (B) Nitric oxide (values are expressed as mean±SEM (n=6). Data was analysed by one way ANOVA followed by Dunnet post hoc test. #= compare to sham control. *= compare to UNX+DOCA. *=p<0.05, ##, **=p<0.01, ###,***=p<0.001

Persistent hypertension leads to erosion of endothelium in blood vessel lining resulted into decrease nitric oxide bioavailability (102). Hypertensive rats showed marred relaxation to acetylcholine due to enhance blood response mediated by unilateral nephrectomy and DOCA salt. Normal control and sham control animals exhibited EC_{50} value of $1.076*10^{-6}$ µM. while hypertension cause massive shift in EC_{50} value as DOCA salt treated rats showed 691.9 µM. It is also noteworthy that aorta from the hypertensive rats were not able to produce 100% relaxation. This detrimental effect was reversed by novel entities under investigation as evident in figure 4.11. These data are in correlation with level of nitric oxide; a potent vasodilator. Hypertensive rats significantly reduced level of nitric oxide in plasma (3.25± 0.36 nM vs. 0.22±0.1 nM,p<0.0001) as compare to SC and NC rats. Treatment with compound **(18)** with 10 mg/kg was able to increase nitric oxide significantly compared to DC rats.

4.5.7 Effect of compound (18) and (24) on Protein Kinase C (PKC) and p-Akt protein expression in UNX+DOCA salt induced hypertension

Protein kinase C (PKC) expression in aorta of hypertensive rats was significantly elevated as compared to NC animals. PKC is implicated in basal vascular smooth muscle (VSM) tone and myocardial contraction. Studies have reported increased activity of PKC in hypertensive patients (Ref). It also acts as critical modulator of vascular contraction via

calcium dependent and calcium independent signalling through MAPK pathway. PKC can be upstream to the MAPK pathways that regulate the increment of basal tone in hypertensive rats(103). PKC is found to heteroedimerize between the croostalk of RAAS and SNS. Interactions between α_1R and AT_1R exist at the second messenger level (104). The proposed molecular interaction in the second messenger pathway between the α_1R and AT_1R is a consequence of both receptors coupling to Gq-proteins. Protein kinase C in turn is known to play a role in AngII induced potentiation of norepinephrine-induced effects on vascular tone(105).

Treatment with dual antagonists significantly reduced the expression of PKC in rat aorta by inhibiting the cross talk between α_1 and AT_1 receptor. This may result into decrease calcium mobilization and MAPK activation leading to reduced VSM contraction.

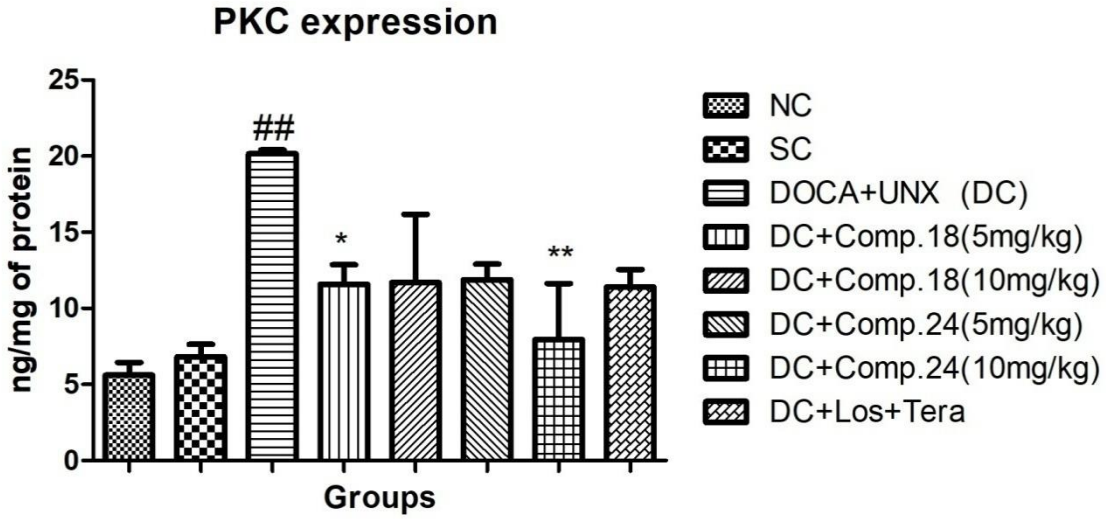

Figure 4.12: Effect of (18) and (24) on PKC expression in rat aorta of DOCA salt hypertensive rats (values are expressed as mean±SEM (n=6). Data was analysed by one way ANOVA followed by Dunnet post hoc test. #= compare to sham control. *= compare to UNX+DOCA. *=p<0.05, ##, **=p<0.01

On the other hand, increased activity of PKC leads to MAPK activation. MAPK activate several other second messenger such PI_3K, ERK1/2. PI_3K was found be expressed in DOCA salt hypertensive rats however its downstream component, p-Akt level was decreased(106). Current study showed decreased p-Akt level in rat aorta of hypertensive rat. Reduced p-Akt level is highly related to decreased eNOS enzyme and reduced NO production. Novel compound **(24)** showed increase p-Akt level in aorta after six week of treatment. Our results are in accordance with previous report where chronic blockade of RAAS increased p-Akt expression(107).

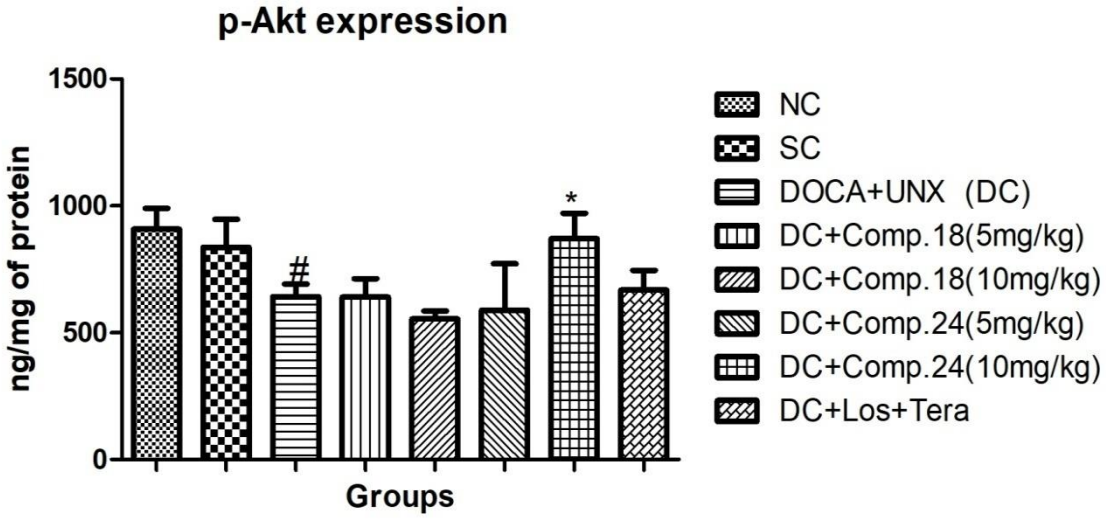

Figure 4.13: Effect of (18) and (24) on p-Akt expression in rat aorta of DOCA salt hypertensive rats (values are expressed as mean±SEM (n=6). Data was analysed by one way ANOVA followed by Dunnet post hoc test. #= compare to sham control. *= compare to UNX+DOCA. *,# = $p<0.05$

4.5.8 Effect of compound (18) and (24) on cytokine imbalance in UNX+DOCA salt induced hypertension

Table 4.13: Effect of (18) and (24) on cytokine levels in UNX+DOCA salt induced hypertension

Group	IL-6 (pg/ml)	TNF-α (pg/ml)	PRA (ng/ml)
NC	796.09±170.05	275.9±13.01	6.01±0.24
SC	936.06±219.58	269.40±13.81	5.78±0.34
UNX+DOCA (DC)	2766.05±447.98$^{\#\#}$	918.73±14.89$^{\#\#\#}$	2.51±0.79$^{\#\#}$
DC+ Compound (18) (5 mg/kg)	1106.41±263.46*	678.23±38.88**	5.17±0.23**
DC+ Compound (18) (10 mg/kg)	862.66±125.47**	466.9±55.76$^{***,\$\$\$}$	4.66±0.14*
DC+ Compound (24) (5 mg/kg)	1249.33±250.00	854.4±8.08	3.12±0.42*
DC+ Compound (24) (10 mg/kg)	572.66±17.40**	619.15±14.58***	4.37±0.39**
DC+Los+Tera	786.00±288.63**	376.40±10.69$^{***,\%\%}$	5.18±0.15**

#= compare to sham control. *= compare to UNX+DOCA. *=p<0.05, ##, **=p<0.01, ###,***=p<0.001 ns= non-significant

Several studies reported that hypertension is associated with many circulating inflammatory factors (108). Increased inflammatory factors are also related to the increased risk of hypertension in normotensive individuals. Inflammation in the brain has received increased attention as a cause of sympathoexcitation(109). Hence, an inflammatory-sympathetic mechanism is a key element in the pathogenesis of hypertension. On the other hand, overactive RAAS system, produce ROS and activate NAPDH oxidase, this oxidative stimulus caused activation and release of cytokine which further increase the blood pressure and induce inflammatory changes in heart and kidney.

Elevated cytokine level is responsible for initiation and sustenance of blood pressure in DOCA salt induced hypertension. TNF-α promotes sodium retention, vasoconstriction, hypertrophy and oxidative injury during the development of hypertension in DOCA-salt hypertension.(110) Hypertensive animals showed significant elevation in IL-6, ($p< 0.001$) and TNF- α($p<0.0001$) level compared to normal control animals. Treatment with (**18)** and **(24)** at both the doses produce beneficial effect by reducing cytokine imbalance. Combination of standard drug found to be more effective in reducing detrimental level of cytokine level in plasma as compared to hypertensive rats. Increase level of IL-6 and TNF-α caused decrease in NO bioavailability and further contributed to maintenance of blood pressure.(111)

Many lines of evidences suggest that DOCA salt induced hypertension is renin independent as it is marked by decreased plasma rennin activity(112). It is speculated that there is elevated renal perfusate pressure in solitary kidney in uninephrectomized rats which cause diminished renin release and subsequent activation of sympathetic nerve and spillover of norepinephrine. DMLs target both receptors together resulted into balance of the cytokine imbalance and helps to normalize the blood pressure.

4.5.9 Effect of compound (18) and (24) on urinary indices in UNX+DOCA salt induced hypertension

Table 4.14: Effect of (18) and (24) on urinary parameters in UNX+DOCA salt induced hypertension

Group	Urine output(ml)	Sodium (µmol/l)	Potassium (µmol/l)	Uric acid (µmol/l)	Urea (ng/ml)	Creatinine (mg/dl/day)	Creatinine Clearance	Albumin (µg/day)
NC	20.667 ± 1.76	268.361 ± 9.962	45.000 ± 1.426	306.480 ± 19.153	12.508 ± 1.547	22.167 ± 0.795	2.800 ± 0.208	12.153 ± 0.334
SC	19.333 ± 2.028	263.279 ± 5.658	44.360 ± 7.246	301.662 ± 17.096	10.274 ± 1.398	22.083 ± 0.961	2.683 ± 0.044	14.084 ± 0.220
UNX+DOCA (DC)	88.000 ± $4.726^{###}$	184.262 ± $11.858^{###}$	66.608 ± 1.986^{ns}	535.876 ± $16.836^{###}$	49.564 ± $4.552^{###}$	7.083 ± $0.417^{###}$	1.133 ± $0.145^{###}$	28.912 ± $4.481^{#}$
DC+ Compound (18) (5 mg/kg)	60.333 ± 2.333^{***}	268.852 ± 7.166^{**}	57.073 ± 6.497^{ns}	399.127 ± 10.683^{ns}	40.280 ± 4.099^{ns}	11.500 ± 1.127^{ns}	1.313 ± 0.144^{ns}	18.962 ± 0.759^{ns}
DC+ Compound (18) (10 mg/kg)	53.667 ± 3.844^{**}	264.590 ± 8.273^{***}	39.512 ± 7.617^{ns}	444.340 ± 17.954^{**}	15.888 ± 1.348^{***}	13.250 ± 0.661^{**}	2.250 ± 0.189^{*}	18.348 ± 1.535^{ns}
DC+ Compound (24) (5 mg/kg)	36.333 ± 2.906^{***}	228.033 ± 13.983^{***}	50.762 ± 2.688^{ns}	392.827 ± 24.037^{***}	21.900 ± 1.372^{***}	11.333 ± 0.982^{ns}	1.850 ± 0.202^{ns}	15.892 ± 2.830^{*}

Group	Urine output(ml)	Sodium (µmol/l)	Potassium (µmol/l)	Uric acid (µmol/l)	Urea (ng/ml)	Creatinine (mg/dl/day)	Creatinine Clearance	Albumin (µg/day)
DC+ Compound (24) (10 mg/kg)	27.667 ± 3.844***	222.459 ± 4.926**	31.829 ± 13.994*	369.480 ± 20.403***	13.956 ± 1.652***	17.417 ± 1.228***	2.393 ± 0.301**	12.966 ± 1.854**
DC+Los+Tera	35.667 ± 3.930*	258.853 ± 6.695ns	37.454 ± 3.155ns	465.463 ± 11.772ns	16.854 ± 3.789ns	15.817 ± 1.099**	1.943 ± 0.038ns	20.378 ± 0.303ns

#= compare to sham control. *= compare to UNX+DOCA. *=p<0.05, ##, **=p<0.01, ###,***=p<0.001 ns= non-significant

Urinary parameters are important while studying mineralocorticoid induced hypertension since the major affected organ is the kidney. Hypertension mediated overload leads to functional damage to the kidney which may be suggested by changes in excretion of electrolytes, creatinine, protein and glucose(113),(114) Accordingly, it was decided to evaluate a battery of parameters which provide an index of renal function.

UNX+DOCA (DC) treatment showed a significant ($P<0.001$) increase in urine output compared to both Normal control (NC) and Sham control (SC) groups It is known that mineralocorticoids like DOCA favors sodium/water retention and in turn supports excretion of potassium. In mild contrast to this finding, we found that urinary output was increased about 4-fold in DOCA-salt treated animals. This group was supplemented with 1% NaCl and 0.2% KCl in drinking water which increases the osmolarity of the drinking solution thus leading to increased volume intake and ultimately output.(115),(116) Compound (18) (5mg/kg & 10mg/kg) group showed significant ($P<0.001$) decrease in urine output when compared to UNX+DOCA (DC) treated rats. Compound (24) (5 mg/kg& 10 mg/kg) treatment showed significant ($p<0.001$) decrease in urine output when compared to UNX+DOCA (DC) animals. Los + tera showed significant ($p<0.001$) decrease in urine output when compared to UNX+DOCA (DC) animals.

UNX+DOCA (DC) treatment showed a significant ($p<0.001$) increase in urinary sodium levels when compared to sham control (SC) and normal control (NC) animals. Treatment with Compound (18) at 5mg/kg& 10 mg/kg showed a significant ($p<0.001$) increase in sodium when compared to UNX+DOCA salt-treated group. Compound (24) (5 mg/kg & 10 mg/kg) treatment showed significantly ($p<0.01$ & $p<0.001$ respectively) increased sodium levels when compared to UNX+DOCA (DC) animals. Treatment with losartan + terazosin showed significant ($p<0.001$) increase in the sodium levels when compared with UNX+DOCA (DC) group. This was suggestive of increased sodium retention in the positive control group which might contribute to increased vascular volume factoring the rise in blood pressure. This data is in agreement with the findings reported by investigators.(95),(117).

Kidneys are known to effectively excrete creatinine in the urine and block the spillage of glucose and proteins in the urine. However, when renal structure is marred due to mineralocorticoid insult which can consequently cause reduce creatinine excretion A decline in glomerular filtration rate was also evident from the creatinine clearance values which were reduced in the DOCA-salt group as compared to the control group(118).

UNX+DOCA (DC) treated rats showed significant ($p<0.001$) decrease in creatinine levels and increase in creatinine clearance compared to the normal control (NC) and sham control (SC) animals. Compound (18) at 10mg/kg showed significant ($p<0.01$) increase in creatinine levels when compared to UNX+DOCA (DC) treated rats. Compound (18) at 5mg/kg reflected non-significant increase in creatinine levels when compared to disease control (DC) rats. Compound **(24)** (10 mg/kg) treatment showed significant ($p<0.001$) increase in creatinine levels when compared to UNX+DOCA (DC) animals. Compound **(24)** (5 mg/kg) treatment showed non-significant increase in creatinine level when compared to disease control (DC) animals. The treatment with Los+ tera showed a significant ($p<0.001$) increase in creatinine levels when compared to UNX+ DOCA treated rats.

4.5.10 Effect on compound (18) and (24) on oxidative stress parameters in UNX+DOCA salt induced hypertension

4.5.10.1 Effect on compound (18) and (24) on oxidative stress parameters in heart of UNX+DOCA salt induced hypertension

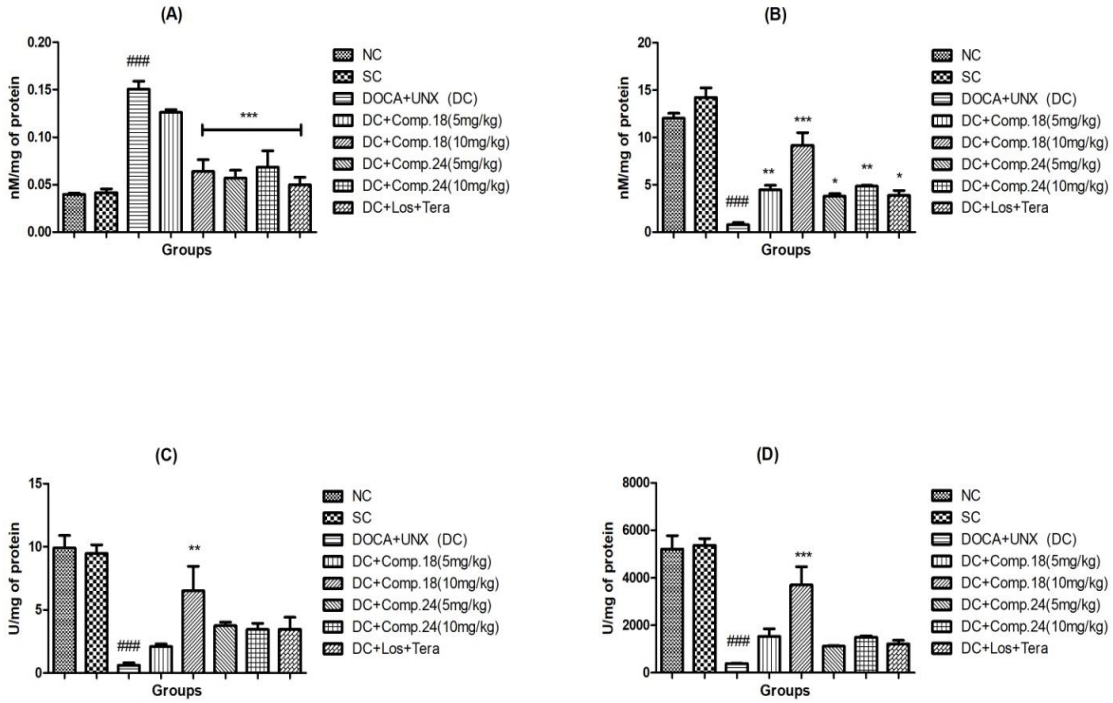

Figure 4.14: Effect of (18) and (24) on oxidative stress parameters in heart. (A) MDA (B) GSH (C) SOD (D) Catalase. Values are expressed as mean±SEM (n=6). Data was analyzed by one way ANOVA followed by Dunnet post hoc test. #= compare to sham control. *= compare to UNX+DOCA. *=p<0.05, **=p<0.01, ###,***=p<0.001 ns= non-significant.

UNX+DOCA salt induced significant lipid peroxidation evident by dramatic increase in MDA content in heart homogenate (p<0.001). Treatment with (18) (5 mg/kg) was found to be ineffective to reverse this effect however other treatments produced favorable effect by reducing MDA content significantly (p<0.001) figure 4.14 (A). Antioxidant protection was markedly affected as evident in figure 4.14 (B) by significant (p<0.001) low level of GSH in hypertensive rats compare to normal control. Treatment with (18), (24) and standard drugs caused significant (p<0.01) elevation in GSH content.

As depicted in figure 4.14 (C) and (D), UNX+DOCA treatment showed detrimental effects on antioxidant defense by significantly reduced SOD and catalase level in heart

homogenates ($p<0.001$). Treatment with (24) (10mg/kg) restored this balance by significantly increase ($p<0.001$) preventive enzyme in tissue samples.

4.5.10.2 Effect on compound (18) and (24) on oxidative stress parameters in kidney of UNX+DOCA salt induced hypertension

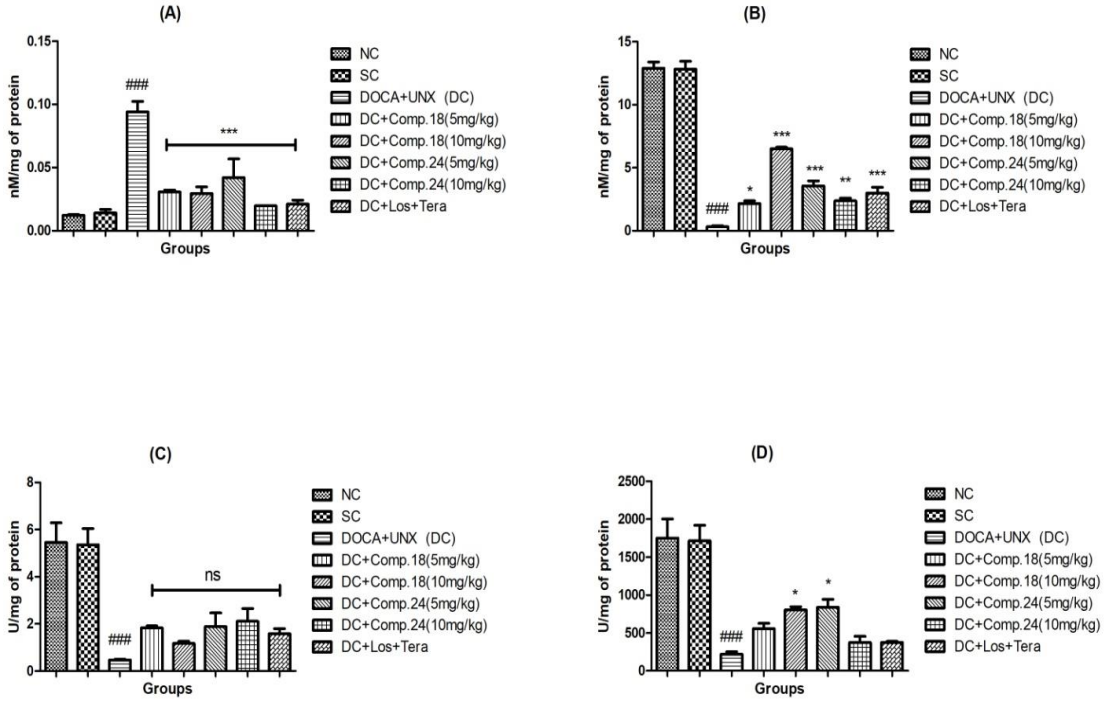

Figure 4.15: Effect of (18) and (24) on oxidative stress parameters in kidney. (**A) MDA (B) GSH (C) SOD (D) Catalase.** Values are expressed as mean±SEM (n=6). Data was analysed by one way ANOVA followed by Dunnet post hoc test. #= compare to sham control. *= compare to UNX+DOCA. *,#=$p<0.05$, **=$p<0.01$, ###,***=$p<0.001$ ns= non-significant

Analysis of kidney homogenates suggests elevated level of MDA and GSH, and reduced level of protective antioxidant such as SOD and catalase in hypertensive rats. Increased production of ROS, demonstrated in micropuncture studies in the kidney macula densa of spontaneously hypertensive rats (SHR) is attributed to a decrease in the bioavailability of nitric oxide. This may directly induce vasoconstriction and increase tubulo-glomerular feedback, resulting in enhanced renal vascular resistance and hypertension(119).. Lipid peroxidation is greatly increased in DOCA salt treated rats showed involvement of ROS

generation in pathogenesis of hypertension. Administration of standard drugs and NCEs reduced MDA content significantly after 45 days.

Antioxidant defence is severely affected by UNX+DOCA salt treatment evident by significant reduction in GSH, SOD, catalase. Compound (18) and (24) markedly reduce oxidative by increase GSH and catalase content. However, treatment was found be non-significant as far as elevation in SOD is concerned.

The mechanisms involved in angiotensin II-induced vascular O_2•− production is well characterized. ROS production by angiotensin II can be separated into an acute phase involving protein kinaseC (PKC), c-Src, growth factor receptors transactivation and translocation of cytosolic p47phox to the membrane(120) and a sustained phase involving up-regulation of NADPH oxidase subunits(121). Potent blockade of SNS and RAAS by compounds under investigation prevented generation of ROS mediated by AngII and epinephrine directly or by inhibiting the stimulation of endothelin release.

4.6 Pharmacological screening and evaluation of compound (14) and (50) for FXa inhibition

4.6.1 *In-vitro* FXa inhibition *and ex-vivo* assay for evaluation of antithrombotic activity

Series I: FXa inhibition, PT and aPTT time measurement of 2-Aminobenzamide derivatives (Benzyl substitutions)

In-vitro enzyme inhibition assay for FXa was performed for the synthesized compounds at a concentration of 100 µM by using a human Factor Xa enzyme and chromogenic substrate (S-2765). The enzyme inhibition was determined from the change in the absorbance at 405 nm with hydrolysis of the substrate by the enzyme. Those compounds with more than 50 % inhibition of FXa were chosen for determination of their IC_{50} values. IC_{50}, PT and aPTT time of 2-aminobenzamide derivatives are mentioned in table 4.15 and 4.16.

Table 4.15: IC_{50} values, PT and aPTT time of compounds (1-17)

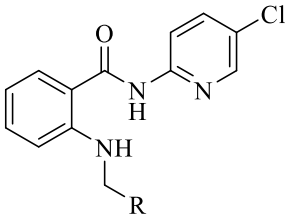

Compound	Where -*R* is	IC_{50} ± SEM (µM)	PT (sec)	aPTT (sec)
1	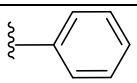	>100	22	19
2	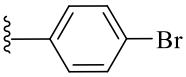	23.7 ± 3.4	22	15
3	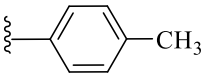	18.4 ± 2.6	21	30
4	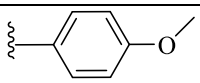	11.5 ± 1.3	22	34
5	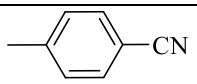	85.56±2.76	20	18
6	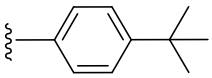	41.0 ± 3.2	21	30
7	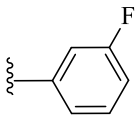	48.3 ± 2.9	24	30
8	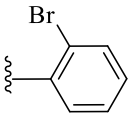	23.2 ± 8.4	23	37.5
9	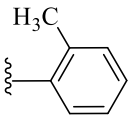	>100	20	19
10	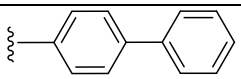	35.3 ± 2.3	22	35
11	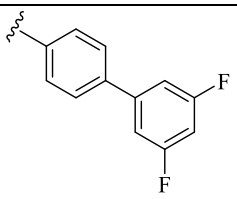	**5.4 ± 1.0**	24	**40**
12	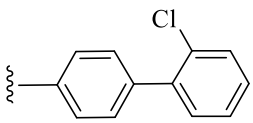	**1.3 ± 0.8**	24	**40**

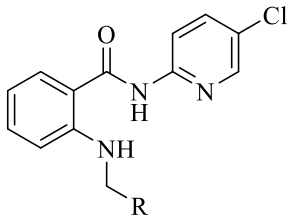

Compound	Where -*R* is	IC_{50} ± SEM (µM)	PT (sec)	aPTT (sec)
13	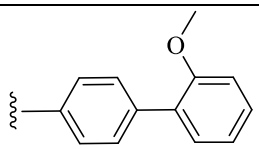	12.5 ± 2.2	22	35
14	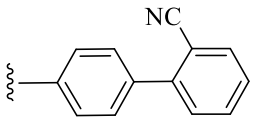	**0.7 ± 0.2**	25	**45**
15	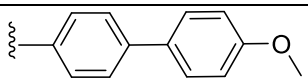	>100	21	28
16	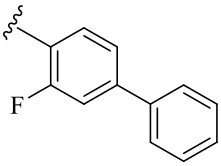	30.0 ± 6.4	23	30
17	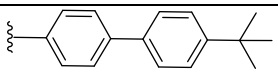	52.5 ± 5.7	9	35

Compounds exhibiting significant inhibition of the enzyme FXa in the preliminary screening were evaluated further by *ex-vivo* measurements of prothrombin time and aPTT time. These studies are important in development of anti-thrombotic agents as it is the reflection of efficacy of new agent on coagulation cascade and clot formation. Substitution at the 4th position of compound **(1)** resulted into compounds **(2-6)** with improvement of FXa inhibition however it was far higher than the standard drug. Substitution at 2nd and 3rd position also resulted into sub molar potency of compounds.

Increase in aromaticity by means of substituted benzyl replacement resulted into favorable results and IC_{50} of compounds were greatly improved **(11-15).** Compound **(14)** was found to be the most potent compound of synthesized compounds. *Ex-vivo* study by PT and aPTT time was showed considerable improvement in parameters as compound **(14)** exhibited highest prolonging activity.

Series II: FXa inhibition, PT and aPTT time measurement of 2-Aminobenzamide derivatives (Piperazinyl substitutions)

Table 4.16: IC_{50} values, PT and aPTT time of compounds (18-23)

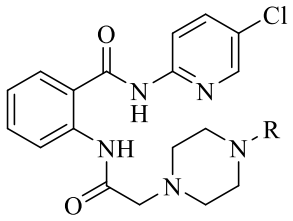

Compound	Where -*R* is	IC_{50} ± SEM (µM)	PT (sec)	aPTT (sec)
18	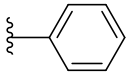	95.2± 5.21	21	44
19	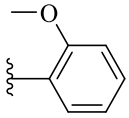	>100	20	39
20	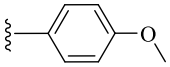	>100	19	41
21	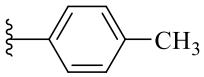	96.23 ± 6.78	24	35
22	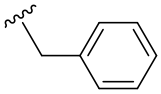	57.5 ± 8.6	25	52
23	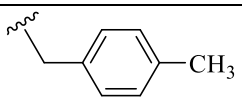	>100	22	44

Substitution of benzyl ring in series I with substituted piperazinyl resulted in compounds **(18-23)**. However, it is observed that insertion of heterocyclic ring produced detrimental effect on potency of compounds as evident in table 4.16. Compound exhibited very high IC_{50} values and showed poor activity against FXa. However newly synthesized compound retained their PT and aPTT prolongation properties.

Series III: FXa inhibition, PT and aPTT time measurement of 1,3,4 thiadiazole derivatives (Benzyl Substitutions)

Table 4.17: IC_{50} values, PT and aPTT time of compounds (24-30)

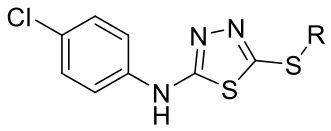

Compound	Where -*R* is	IC_{50} ± SEM (µM)	PT (sec)	aPTT (sec)
24	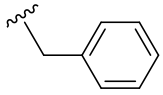	> 100	21.29	42.12
25	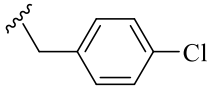	> 100	17.955	47.97
26	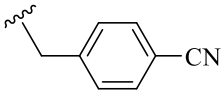	> 100	23.436	42.12
27	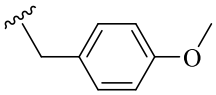	> 100	20.223	42.51
28	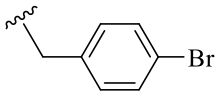	> 100	20.79	58.11
29	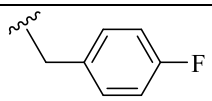	> 100	22.869	59.67
30	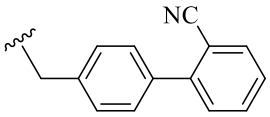	9.55 ± 1.3	30.996	56.16

Series IV: FXa inhibition, PT and aPTT time measurement of 1,3,4 thiadiazole derivatives (Aminoalkyl Substitutions)

Table 4.18: IC_{50} values, PT and aPTT time of compounds (31-39)

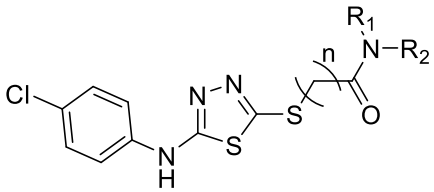

Compound	N	Where -NR_1R_2 is	IC_{50} ± SEM (µM)	PT (sec)	aPTT (sec)
31	1	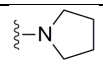	> 100	22.11	48.75
32	1	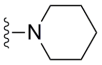	> 100	22.491	50.7

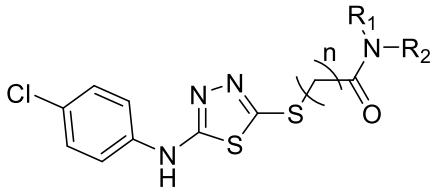

Compound	N	Where -NR_1R_2 is	IC_{50} ± SEM (µM)	PT (sec)	aPTT (sec)
33	1	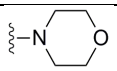	> 100	29.673	44.85
34	2		> 100	28.917	85.02
35	2	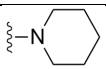	> 100	32.508	70.2
36	2	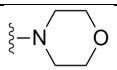	> 100	38.934	69.03
37	3		> 100	38.367	173.55
38	3	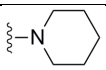	> 100	27.027	85.02
39	3	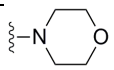	> 100	38.556	68.64

To check the antithrombotic potential of these 1,3,4-thiadiazole derivatives, all the synthesized compounds were screened against FXa at a concentration of 100 µM as per the previously reported procedure. Those compounds with more than 50 % of the FXa inhibition were chosen for determination of their IC_{50} values. Simple benzyl substituted compounds (**24-30**) and aminoalkyl derivatives (**31-39**) showed <50 % inhibition of the enzyme at a concentration of 100 µM (Table 4.17 and 4.18). Compound (**30**) having substituted biphenyl group as the P4 motif showed higher FXa inhibitory activity (IC_{50} = 9.55 µM) amongst the benzyl substituted compounds.

Series V: FXa inhibition, PT and aPTT time measurement of 1,3,4 thiadiazole derivatives (Heterocyclic Substitutions)

Table 4.19: IC_{50} values, PT and aPTT time of compounds (40-52)

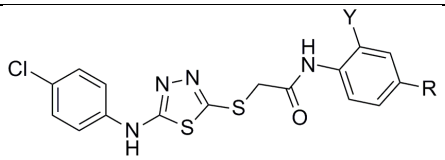

Compound	X	Where -*R* is	IC_{50} ± SEM (µM)	PT (sec)	aPTT (sec)
40	H		> 100	22.30	47.97
41	H		> 100	17.38	52.65
42	H		> 100	27.02	52.26
43	H	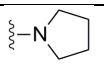	16.5 ± 2.7	28.16	62.79
44	H	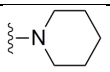	18.8 ± 1.8	27.02	59.28
45	H	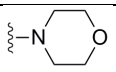	6.5 ± 1.1	37.04	80.34
46	H	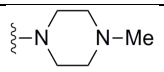	4.98 ± 1.0	24.57	64.74
47	H	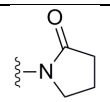	**2.05 ± 0.8**	51.97	92.04
48	H	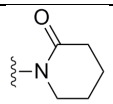	**0.79 ± 0.13**	55.94	117
49	H	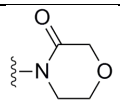	**0.35 ± 0.12**	125.30	246.87
50	H	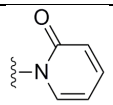	**0.22 ± 0.08**	110.94	173.55
51	H	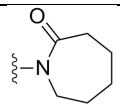	**2.56 ± 1.3**	38.36	85.02
52	F	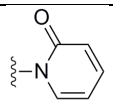	**0.47 ± 0.13**	125.30	120.12

Compounds (**40-42**) having 4-cholroaniline (**40**), 4-fluoroaniline (**41**) and 4-methoxyaniline (**42**) showed poor FXa inhibitory activity (IC_{50}>100 µM). These substitutions at *para* position of aniline were replaced by different heterocycles like pyrrolidine, piperidine, morpholine and *N*-methylpiperazine to get compounds (**43-46**).

These compounds (**43-46**) offered good FXa inhibitory activity with IC_{50} values of 16.5 µM, 18.8 µM, 6.5 µM and 4.9 µM, respectively (Table 4.19).

Replacement of simple pyrrolidine ring in compound (**43**, IC_{50} = 16.5 µM) with pyrrolidinone ring resulted in compound (**47**, IC_{50} = 2.05 µM) with much improved FXa inhibitory activity. Exchanging the pyrrolidinone to piperidinone and morpholinone resulted into compounds (**48**, IC_{50} = 0.79 µM) and (**49**, IC_{50} = 0.35 µM) enhancing the FXa inhibitory activity. Further replacement of piperidinone ring in compound (**48**) with caprolactam in compound (**51**) resulted in some loss of potency (IC_{50} = 2.56 µM). Aromatization of piperidinone ring in compound (**48**) resulted into the most potent compound (**50**) of the series. Compound (**50**, IC_{50} = 0.22 µM) showed even better FXa inhibitory activity than apixaban (IC_{50} = 0.32 µM). Incorporation of fluorine atom at ortho position of phenylpyridinone ring in compound (**50**) resulted into the compound (**52**) which exhibited 2-fold loss of FXa inhibitory activity.

Series VI: FXa inhibition, PT and aPTT time measurement of 1,3,4 thiadiazole derivatives (Heterocyclic Substitutions)

Table 4.20: IC_{50} values, PT and aPTT time of compounds (53-66)

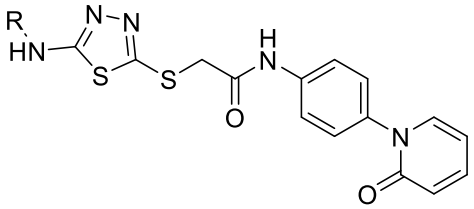

Compound	Where -*R* is	IC_{50} ± SEM (µM)	PT (sec)	aPTT (sec)
53	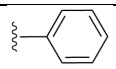	57 ± 4.8	29.106	82.68
54	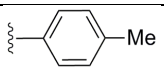	**3.11 ± 1.6**	27.027	59.28
55	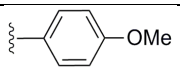	71.96 ± 4.1	23.436	52.26
56	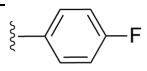	10.43 ± 1.2	39.312	89.31
57	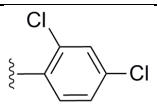	16.53 ± 2.1	28.539	63.18
58	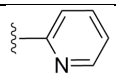	28.14 ± 3.8	33.642	73.71
59	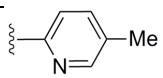	20.72 ± 2.9	36.099	64.74

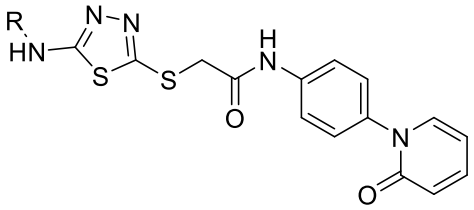

Compound	Where -*R* is	IC_{50} ± SEM (µM)	PT (sec)	aPTT (sec)
60	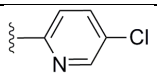	**1.72 ± 1.0**	43.281	109.98
61	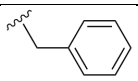	> 100	23.814	50.7
62	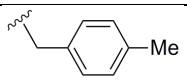	23.92 ± 3.1	24.759	63.18
63	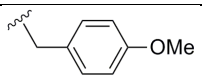	15.70 ± 2.1	29.862	65.91
64	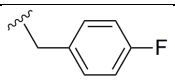	22.64 ± 3.6	38.367	69.42
65	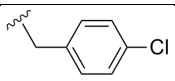	27.12 ± 2.4	28.917	54.21
66	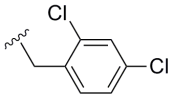	25.60 ± 2.1	26.649	53.04

Further modifications were carried out to explore favorable P1 motifs with pyridinone as the optimal P4 substituent, but all attempts proved unsuccessful (Table 4.20). Removal and replacement of chlorine atom of *p*-chlorophenyl group in compound (**50**) with methyl, methoxy and fluoro groups offered compounds (**53-56**) which exhibited significant loss of FXa inhibitory activity. Compound (**57**) containing additional chlorine atom at ortho position of *p*-chlorophenyl group showed a significant loss of activity (**57** vs **50**). 5-Chloro-2-pyridyl group as the P1 motif was expected to show better activity.the compound (**61)** (IC_{50} = 1.72 µM) having 5-chloro-2-pyridyl group exhibited excellent inhibition but lesser potency than compound (**50**). To gauge the distance between -Cl and Tyr228, compounds (**61-66)** with substituted benzyl groups as P1 motifs were synthesized. None of the compounds (**61-66**) from this series showed any improvement in the activity over compound (**50**).

Series VII: FXa inhibition, PT and aPTT time measurement of carbazole derivatives

Table 4.21: IC_{50} values, PT and aPTT time of compounds (67-78)

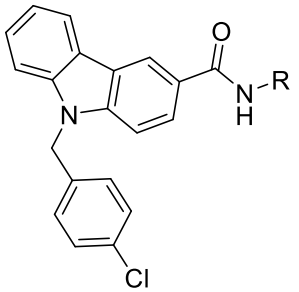

Compound	Where -*R* is	IC_{50} ± SEM (µM)	PT (sec)	aPTT (sec)
67	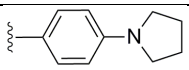	>100	22.1	40.8
68	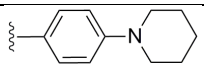	>100	20.7	41.1
69	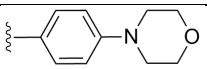	>100	21.5	43.1
70	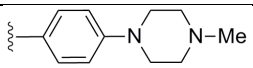	>100	20.02	44.2
71	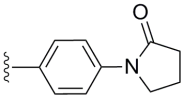	63.15 ± 3.6	23.4	42.7
72	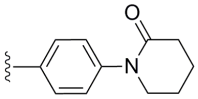	15.87 ± 1.8	**33.5**	**66.1**
73	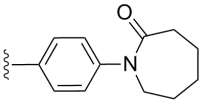	ND	21.76	41.0
74	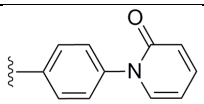	7.49 ± 0.9	**39.9**	**69.6**
75	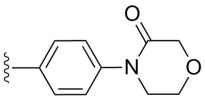	47.20 ± 4.2	29.7	62.6
76	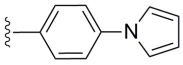	29.40 ± 2.2	22.6	42.8
77	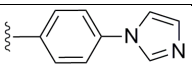	16.60 ± 1.4	24.1	47.7
78	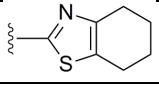	33.10 ± 2.6	29.7	49.8
	Apixaban	**0.35±0.1**	**>180**	**>180**
	Blank	-	18.9	39

The anticoagulation potential of the newly synthesized FXa inhibitors was assessed by measuring the prothrombin time (PT) and activated partial thromboplastin time (aPTT). PT

and aPTT estimate the effect of an inhibitor on the extrinsic and intrinsic pathways respectively. Significant prolongation in both PT and aPTT by inhibitors shows their effect on both the pathways and indicate selectivity towards FXa, which is common in both pathways. All the synthesized compounds were subjected to determination of PT and aPTT at a concentration of 1 mM in human plasma. The *in-vitro* anticoagulant activities of compounds (**67-78**) were given in Table 4.21.

All the synthesized compounds were evaluated for PT and aPTT time measurements. All the compounds exhibited moderate anticoagulant activity. Among the tested compounds, compound (**75**) having 2-oxopyridine moiety showed good activity with PT (39.6 sec) and aPTT (69.6 sec) time. Compound (**73**) has 2-piperidinone moiety also showed notable activity with PT (33.5 sec) and aPTT (66.1 sec) time.

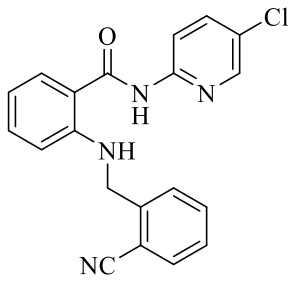

Compound (14)

N-(5-chloropyridin-2-yl)-2-((2-cyanobenzyl)amino)benzamide

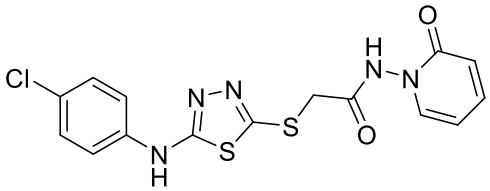

Compound (50)

2-((5-((4-chlorophenyl)amino)-1,3,4-thiadiazol-2-yl)thio)-N-(2-oxopyridin-1(2H)-yl)acetamide

From the extensive *in-vitro* evaluation, it was concluded that Compound **(14),** IC_{50} = **0.7 ± 0.2** and Compound (50), IC_{50} = **0.22 ± 0.08** have excellent interactions at P1 and P4 motif and possess excellent IC_{50} values. They are further explored for their selectivity over thrombin and other serine proteases and *in-vivo* activity.

4.6.2 Molecular modeling studies of compound (14) and (50) for FXa enzyme

To have a view of the molecular interactions of the synthesized compounds with the enzyme, docking studies were performed with FXa. Compound (**14**) offered the highest docking score which indicated its high binding interactions with the enzyme. The intermolecular interactions of the highest binding of compound (**14**) are displayed in figure 4.16 (A). The chloro group of pyridine in compound (**14**) was observed to be stabilized at 3.82 Å from the centroid of Tyr228 aromatic ring which indicated high stability of the ligand-enzyme complex. Compound (**14**), the –C=O and -NH of the amide interacted with -NH of Gln192 (2.12 Å) and –C=O of Gly219 (1.92 Å), respectively by hydrogen bonding to form a stable complex. The aromatic ring of 2-aminobenzamide exhibited the strong π-cation interactions with the Arg222. Generally, the π-cation interaction is considered stronger than hydrogen bond or any other physical interactions, and this has been observed here to impart ligand receptor stability. Further, the *ortho* substituted biphenyl group in compound (**14**) exhibited excellent π-π interaction with Tyr99, Phe174 and Trp215 triad in the S4 pocket. From the obtained results we clearly get an idea that occupying S1 and S4 sites by specific lipophilic functionalities is of utmost importance for enhanced binding affinity of the ligands within the enzyme active site.

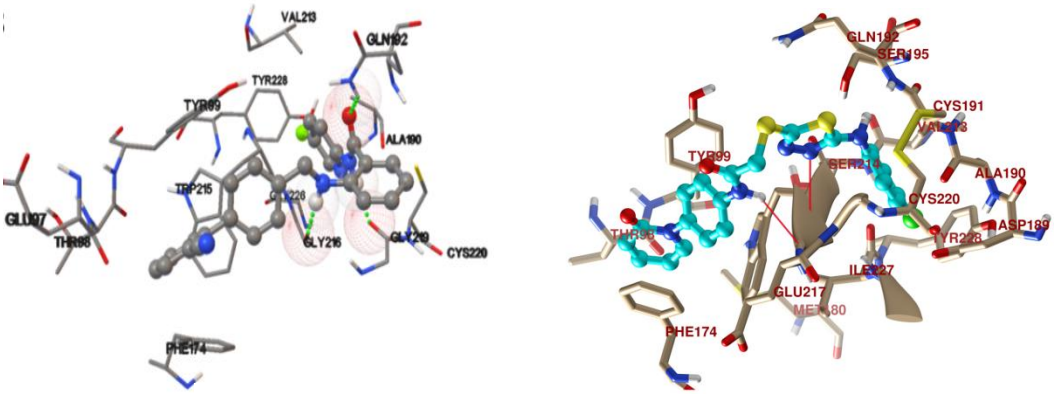

Figure 4.16: Docking pose and representation of interactions between compounds **(A) (14)** and **(B) (50)** and the active site of FXa enzyme.

The most active compound (**50**) offered the highest docking score which indicated its high affinity with the enzyme. The molecular interactions of the compound (**50**) are shown in figure 4.16 (B). The *p*-chlorophenyl group occupied the S1 binding site with promising hydrophobic interactions. Also, the chloro was observed in establishing non-covalent interactions with Tyr228. Further –NH- of acetamide and one of the =N- of thiadiazole ring

of **(50)** interacted with Gly216 by forming hydrogen bonds that imparted stability to the ligand receptor complex. The phenylpyridinone system was observed to occupy S4 binding site, wherein the pyridinone ring of phenylpyridinone formed strong pi-pi interactions with Phe174 and Trp215.

4.6.3 Selectivity of compound (14) and (50) for FXa

4.6.3.1 Thrombin (FIIa) inhibition assay

Selectivity is a significant issue in the development of factor Xa inhibitors. Factor Xa and other enzymes in the coagulation cascade belong to the trypsin-like serine protease family, the various members of which are involved in numerous physiological functions in the body. Hence, to avoid toxicity and adverse side effects, it is important to selectively inhibit the target enzyme (122). Achieving the needed selectivity has proved challenging due to the high degree of structural homology around the active site of this class of enzymes (123). Among many serine proteases, inhibition of thrombin has been vigorously investigated as an approach to identifying novel anticoagulants. As the generator of fibrin monomers, thrombin is vital for thrombosis and hemostasis. Thrombin, unlike factor Xa, is a multifunctional protein (124). It has been implicated in atherosclerosis, inflammation and neurodegenerative diseases. It is also involved in inhibition of platelet function thus poses high risk of bleeding. These off-target effects are mainly responsible for toxicity and side effects.

After screening of developed NCEs for their FXa inhibitor potential and *ex-vivo* activity, compounds which showed IC_{50} > 5µM were screened for their thrombin inhibition to evaluate their specificity and selectivity. Compounds (11, 12, 14, 46-52, 54, 60, apixaban) were selected for the study. All the compounds showed high IC_{50} values, while apixaban showed IC_{50}= 12.8 ± 2.2 µM for thrombin. 2-Aminobenzamide derivatives (11, 12 and 14) showed IC_{50}> 100µM. Compounds from 1,3,4 thiadiazole derivatives also exhibited poor selectivity for thrombin as IC_{50} were more than >80µM. These compounds showed high potency for FXa (IC_{50}= 5.4 to 0.22µM for FXa) suggesting excellent candidates for development of novel FXa inhibitors.

4.6.3.2 Selectivity of novel Factor Xa inhibitors over other serine proteases

To check further selectivity and specificity, we also performed docking study of the most active compound (**14)** and **(50)** with other serine proteases which are involved in blood

homeostasis. Binding of novel compounds with FIXa and FXIa was studied by docking study. For this purpose, the protein structures were obtained from RCSB database (PDB code: 1SL3, 3CL5, 5QCK respectively). The docking scores suggest the selectivity of compound **(14), (50)** for FXa over thrombin, FIXa and FXIa. Docking scores and IC_{50} values of compound **(14), (50)** and apixaban over other serine proteases were represented in table 4.22.

Table 4.22: Docking score and IC_{50} values of compound (14) and (50) and apixaban over other serine proteases

Enzyme	14		50		Apixaban	
	Glide XP docking score	IC_{50} value (µM)[a]	Glide XP docking score	IC_{50} value (µM)[a]	Glide XP docking score	IC_{50} value (µM)[a]
FXa	-10.43	0.7 ± 0.2	-11.34	0.22 ± 0.08	-9.075	0.35 ± 0.1
Thrombin (FIIa)	-7.88	> 100	-7.90	>100	-5.284	12.8 ± 2.2
FIXa	-6.98	ND	-6.5	ND	-4.626	ND
FXIa	-8.07	ND	-7.92	ND	-5.584	ND

IC_{50} values shown are the mean of triplicate measurements. ND = Not determined

To evaluate the specificity of developed specific Factor Xa inhibitors, compound **(14)** and **(50)** were studied for their affinity for thrombin and other serine proteases in coagulation cascade. It was found that compound **(14)** and **(50)** have IC_{50} value more than 100 µM while Apixaban has IC_{50} value of 12.8 µM. Docking studies showed that compound **(14)** and **(50)** do not possess noteworthy interaction for other serine proteases. This result summarizes the specificity and advantage of developed molecule over available drugs.

4.6.4 Cytotoxicity assay of compound (14) and (50) in H9C2 cardiacmyocytes cells

After confirming FXa inhibitory activity and selectivity over other serine proteases, compounds were subjected to cytotoxic potential by MTT assay. H9C2 cardiac myocytes were selected for the study and it was found that at different concentrations (0.001 µM-1000µM) compound **(14)** and **(50)** did not exhibit cytotoxicity as evident in figure 4.17. Hence it is safe to study these compounds for toxicology and *in-vivo* model of thrombus formation.

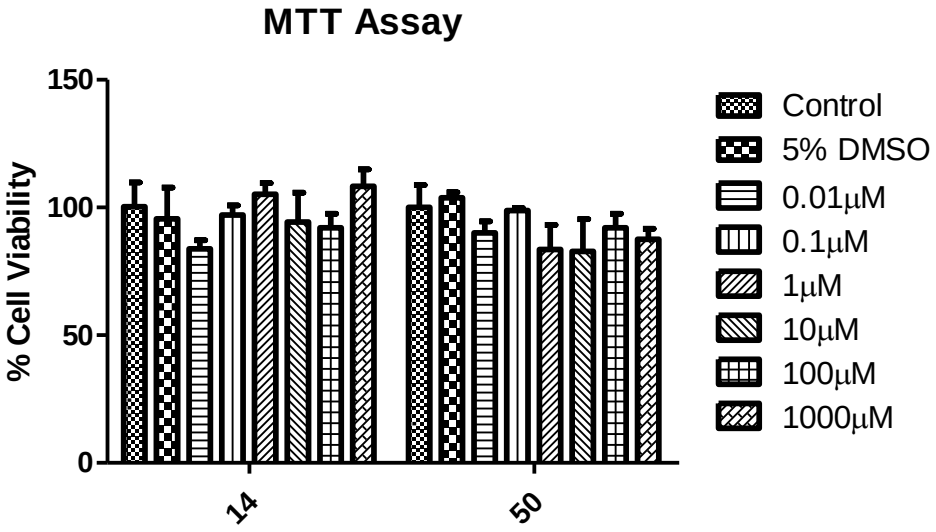

Figure 4.17: Survival of cells post-incubation with different concentrations of compounds **(14), (50)**, 5% DMSO (vehicle) and control cells in H9C2 cells (n=3). Statistical analysis did not find any significant difference between the groups.

4.6.5 Antithrombotic activity of compound (14) and (50) against *in-vivo* $FeCl_3$ induced arterial thrombosis

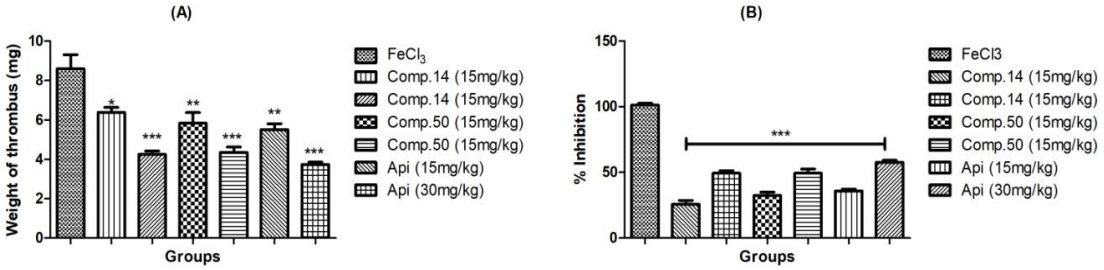

Figure 4.18: Effect of compound 14, 50 and apixaban (15 and 30 mg/kg) on thrombus weight ($FeCl_3$ induced arterial thrombosis model). Statistical analysis was performed by One way ANOVA using Graph-pad prism 5.0.

$^{*}p < 0.05$, $^{**}p < 0.001$, $^{***}p < 0.0001$ vs. $FeCl_3$. (n = 5).

The topical application of ferric chloride ($FeCl_3$) to the vasculature is one of the most commonly used experimental approaches to induce thrombosis. As depicted in figure 4.18 application of 35% $FeCl_3$ soaked filter paper strip on carotid artery caused thrombus formation. It is proposed that physiochemical effect of $FeCl_3$ on blood cells is the primary instigator driving blood cell adhesion to the endothelium(125). Vascular endothelial cells (VECs) are extensively involved in blood homeostasis by synthesis and secretion of many

active substances to regulate platelet activation, coagulation, and fibrinolysis. VEC damage is an initial stage of $FeCl_3$induced thrombus formation. TF is released and further activate FXa enzyme. FXa binds to clots during clot formation and contributes to the pro-coagulant growth of thrombi. VEC destruction initiates the extrinsic coagulation process, leading to fibrin clot and thrombus formation.

The "secondary" phase of $FeCl_3$ injury is initiated with red cell aggregates and damaged endothelium providing a reactive surface for the accumulation of platelets and initiation of blood coagulation, necessary for stable thrombus formation (126), (127), (128). Administration of compounds **(14)** and **(50)** at both doses significantly reduce thrombus formation against $FeCl_3$ challenge. Compound **(14)** exhibited 25% and 49% of inhibition at 15 mg/kg and 30 mg/kg respectively while Compound **(50)** displayed excellent anti-thrombotic activity by 33% and 51% inhibition at 15 mg/kg and 30 mg/kg respectively. Apixaban also showed significant inhibition against $FeCl_3$ insult by showing significant reduction in thrombus weight. Antithrombotic activity of compound **(14)** and **(50)** were comparable to standard drug.

REFERENCES

1. Grundy SM. Metabolic syndrome: a multiplex cardiovascular risk factor. The Journal of Clinical Endocrinology & Metabolism. 2007;92(2):399-404.

2. Roth GA, Mensah GA, Fuster V. The global burden of cardiovascular diseases and risks: a compass for global action. American College of Cardiology Foundation Washington DC; 2020.

3. Roth GA, Mensah GA, Johnson CO, Addolorato G, Ammirati E, Baddour LM, et al. Global burden of cardiovascular diseases and risk factors, 1990–2019: update from the GBD 2019 study. Journal of the American College of Cardiology. 2020;76(25):2982-3021.

4. Jose AP, Prabhakaran D. World Hypertension Day: Contemporary issues faced in India. The Indian journal of medical research. 2019;149(5):567.

5. Hess PL, Al-Khalidi HR, Friedman DJ, Mulder H, Kucharska-Newton A, Rosamond WR, et al. The metabolic syndrome and risk of sudden cardiac death: the atherosclerosis risk in communities study. Journal of the American Heart Association. 2017;6(8):e006103.

6. Mazloomzadeh S, Zarandi FK, Shoghli A, Dinmohammadi H. Metabolic syndrome, its components and mortality: A population-based study. Medical journal of the Islamic Republic of Iran. 2019;33:11.

7. Collaborators GRF. Global, regional, and national comparative risk assessment of 84 behavioural, environmental and occupational, and metabolic risks or clusters of risks for 195 countries and territories, 1990–2017: a systematic analysis for the Global Burden of Disease Study 2017. Lancet (London, England). 2018;392(10159):1923.

8. Hajjar I, Kotchen JM, Kotchen TA. Hypertension: trends in prevalence, incidence, and control. Annual review of public health. 2006;27:465-90.

9. Unger T, Borghi C, Charchar F, Khan NA, Poulter NR, Prabhakaran D, et al. 2020 International Society of Hypertension global hypertension practice guidelines. Hypertension. 2020;75(6):1334-57.

10. Chopra S, Baby C, Jacob JJ. Neuro-endocrine regulation of blood pressure. Indian journal of endocrinology and metabolism. 2011;15(Suppl4):S281.

11. L. Izzo J. Sympathoadrenal activity, catecholamines, and the pathogenesis of vasculopathic hypertensive target-organ damage. American journal of hypertension. 1989;2(12_Pt_2):305S-12S.

12. Chopra S, Baby C, Jacob JJ. Neuro-endocrine regulation of blood pressure. Indian journal of endocrinology and metabolism. 2011;15 Suppl 4(Suppl4):S281-8.

13. Rupp H, Jäger B. The renin-angiotensin system and the sympathetic nervous system in hypertension and congestive heart failure: implications for therapeutic interventions. Journal of Clinical and Basic Cardiology. 2001;4(1):47-51.

14. Du Y, Qiu J, Nelson SH, Wang DH. Regulation of type 1 ANG II receptor in vascular tissue: role of alpha1-adrenoreceptor. Am J Physiol. 1997;273(4 Pt 2):R1224-9.

15. Li HT, Long CS, Gray MO, Rokosh DG, Honbo NY, Karliner JS. Cross talk between angiotensin AT1 and alpha 1-adrenergic receptors: angiotensin II downregulates alpha 1a-adrenergic receptor subtype mRNA and density in neonatal rat cardiac myocytes. Circ Res. 1997;81(3):396-403.

16. Hall JE, Brands MW, Henegar JR. Angiotensin II and long-term arterial pressure regulation: the overriding dominance of the kidney. J Am Soc Nephrol. 1999;10 Suppl 12:S258-65.

17. Wolff DW, Buckalew VM, Jr., Strandhoy JW. Renal alpha 1- and alpha 2-adrenoceptor mediated vasoconstriction in dogs: comparison of phenylephrine, clonidine, and guanabenz. J Cardiovasc Pharmacol. 1984;6 Suppl 5:S793-8.

18. Zimmerman BG, Sybertz EJ, Wong PC. Interaction between sympathetic and renin-angiotensin system. J Hypertens. 1984;2(6):581-7.

19. Reid IA. Interactions between ANG II, sympathetic nervous system, and baroreceptor reflexes in regulation of blood pressure. Am J Physiol. 1992;262(6 Pt 1):E763-78.

20. Starke K. Regulation of noradrenaline release by presynaptic receptor systems. Rev Physiol Biochem Pharmacol. 1977;77:1-124.

21. Rantala A, Kauma H, Lilja M, Savolainen M, Reunanen A, Kesäniemi Y. Prevalence of the metabolic syndrome in drug-treated hypertensive patients and control subjects. Journal of internal medicine. 1999;245(2):163-74.

22. Srivastava AK. Challenges in the treatment of cardiometabolic syndrome. Indian Journal of Pharmacology. 2012;44(2):155.

23. Ke C, Zhu X, Zhang Y, Shen Y. Metabolomic characterization of hypertension and dyslipidemia. Metabolomics. 2018;14(9):1-11.

24. Das UN. Renin–angiotensin–aldosterone system in insulin resistance and metabolic syndrome. Journal of translational internal medicine. 2016;4(2):66-72.

25. Kishi T, Hirooka Y. Sympathoexcitation associated with Renin-Angiotensin system in metabolic syndrome. International Journal of Hypertension. 2013;2013.

26. Huggett RJ, Burns J, Mackintosh AF, Mary DA. Sympathetic neural activation in nondiabetic metabolic syndrome and its further augmentation by hypertension. Hypertension. 2004;44(6):847-52.
27. Esler M, Straznicky N, Eikelis N, Masuo K, Lambert G, Lambert E. Mechanisms of sympathetic activation in obesity-related hypertension. Hypertension. 2006;48(5):787-96.
28. Salvetti A, Brogi G, Di Legge V, Bernini G. The inter-relationship between insulin resistance and hypertension. Drugs. 1993;46(2):149-59.
29. Zhou M-S, Schulman IH, Zeng Q. Link between the renin–angiotensin system and insulin resistance: Implications for cardiovascular disease. Vascular medicine. 2012;17(5):330-41.
30. Ormazabal V, Nair S, Elfeky O, Aguayo C, Salomon C, Zuñiga FA. Association between insulin resistance and the development of cardiovascular disease. Cardiovascular diabetology. 2018;17(1):1-14.
31. Poulter NR, Borghi C, Parati G, Pathak A, Toli D, Williams B, et al. Medication adherence in hypertension. Journal of hypertension. 2020;38(4):579-87.
32. Oparil S, Calhoun DA. Managing the patient with hard-to-control hypertension. American family physician. 1998;57(5):1007.
33. Tikkanen I, Tikkanen T, Cao Z, Allen TJ, Davis BJ, Lassila M, et al. Combined inhibition of neutral endopeptidase with angiotensin converting enzyme or endothelin converting enzyme in experimental diabetes. Journal of hypertension. 2002;20(4):707-14.
34. Battistini B, Daull P, Jeng AY. CGS 35601, a triple inhibitor of angiotensin converting enzyme, neutral endopeptidase and endothelin converting enzyme. Cardiovascular drug reviews. 2005;23(4):317-30.
35. Murugesan N, Gu Z, Fadnis L, Tellew JE, Baska RAF, Yang Y, et al. Dual angiotensin II and endothelin A receptor antagonists: synthesis of 2 ‘-substituted N-3-isoxazolyl biphenylsulfonamides with improved potency and pharmacokinetics. Journal of medicinal chemistry. 2005;48(1):171-9.
36. Palaniswamy C, Selvaraj DR, Palaniappan D. Dual angiotensin II and endothelin receptor antagonists. American Journal of Therapeutics. 2011;18(3):e67-e70.
37. Ramsay RR, Popovic-Nikolic MR, Nikolic K, Uliassi E, Bolognesi ML. A perspective on multi-target drug discovery and design for complex diseases. Clinical and translational medicine. 2018;7(1):3.

38. Hopkins AL. Network pharmacology: the next paradigm in drug discovery. Nature chemical biology. 2008;4(11):682-90.
39. Bottegoni G, Favia AD, Recanatini M, Cavalli A. The role of fragment-based and computational methods in polypharmacology. Drug discovery today. 2012;17(1-2):23-34.
40. Lakka H-M, Laaksonen DE, Lakka TA, Niskanen LK, Kumpusalo E, Tuomilehto J, et al. The metabolic syndrome and total and cardiovascular disease mortality in middle-aged men. Jama. 2002;288(21):2709-16.
41. Meigs JB, Wilson PW, Nathan DM, D'Agostino RB, Williams K, Haffner SM. Prevalence and characteristics of the metabolic syndrome in the San Antonio Heart and Framingham Offspring Studies. Diabetes. 2003;52(8):2160-7.
42. Malone P, Agutter P. The aetiology of deep venous thrombosis. Journal of the Association of Physicians. 2006;99(9):581-93.
43. Russo I. The prothrombotic tendency in metabolic syndrome: focus on the potential mechanisms involved in impaired haemostasis and fibrinolytic balance. Scientifica. 2012;2012.
44. Ozkul A, Turgut ET, Akyol A, Yenisey C, Kadikoylu G, Tataroglu C, et al. The relationship between insulin resistance and hypercoagulability in acute ischemic stroke. European neurology. 2010;64(4):201-6.
45. Mao X, Ait-Aissa K, Lagrange J, Youcef G, Louis H. Hypertension, hypercoagulability and the metabolic syndrome: A cluster of risk factors for cardiovascular disease. Biomedical materials and engineering. 2012;22(1-3):35-48.
46. Stewart LK, Kline JA. Metabolic syndrome increases risk of venous thromboembolism recurrence after acute deep vein thrombosis. Blood advances. 2020;4(1):127-35.
47. Lee A. The role of rheological and haemostatic factors in hypertension. Journal of human hypertension. 1997;11(12):767-76.
48. Vayá A, Mira Y, Ferrando F, Contreras M, Estelles A, España F, et al. Hyperlipidaemia and venous thromboembolism in patients lacking thrombophilic risk factors. British journal of haematology. 2002;118(1):255-9.
49. Deguchi H, Pecheniuk NM, Elias DJ, Averell PM, Griffin JH. High-density lipoprotein deficiency and dyslipoproteinemia associated with venous thrombosis in men. Circulation. 2005;112(6):893-9.

50. Sevinsky JR, Rao L, Ruf W. Ligand-induced protease receptor translocation into caveolae: a mechanism for regulating cell surface proteolysis of the tissue factor-dependent coagulation pathway. The Journal of cell biology. 1996;133(2):293-304.
51. Chen Y-J, Lin-Chao S, Huang T-S, Yang M-L, Lu F-J. Humic acid induced growth retardation in a Sertoli cell line, TM4. Life sciences. 2001;69(11):1269-84.
52. Gallus A, Lee L, Coghlan D. New aspects of the blood coagulation cascade, anticoagulants and vein thrombosis in Asia. Annals of the Academy of Medicine, Singapore. 2002;31(6):685-96.
53. Stein P, Grandison D, Hua T, Slettehaugh P, Henry J, Turlapaty P, et al. Therapeutic level of oral anticoagulation with warfarin in patients with mechanical prosthetic heart valves: review of literature and recommendations based on international normalized ratio. Postgraduate medical journal. 1994;70:S72-S83.
54. Alquwaizani M, Buckley L, Adams C, Fanikos J. Anticoagulants: a review of the pharmacology, dosing, and complications. Current emergency and hospital medicine reports. 2013;1(2):83-97.
55. Blossom DB, Kallen AJ, Patel PR, Elward A, Robinson L, Gao G, et al. Outbreak of adverse reactions associated with contaminated heparin. New England Journal of Medicine. 2008;359(25):2674-84.
56. Spinler SA, Willey VJ. A patient's guide to taking dabigatran etexilate. Circulation. 2011;124(8):e209-e11.
57. Eriksson BI, Quinlan DJ, Weitz JI. Comparative pharmacodynamics and pharmacokinetics of oral direct thrombin and factor Xa inhibitors in development. Clinical pharmacokinetics. 2009;48(1):1-22.
58. Graff J, Harder S. Anticoagulant therapy with the oral direct factor Xa inhibitors rivaroxaban, apixaban and edoxaban and the thrombin inhibitor dabigatran etexilate in patients with hepatic impairment. Clinical pharmacokinetics. 2013;52(4):243-54.
59. Ufer M. Comparative efficacy and safety of the novel oral anticoagulants dabigatran, rivaroxaban and apixaban in preclinical and clinical development. Thrombosis and haemostasis. 2010;103(03):572-85.
60. ARUNLAKSHANA Ot, Schild H. Some quantitative uses of drug antagonists. British journal of pharmacology and chemotherapy. 1959;14(1):48-58.

61. Iglarz M, Binkert C, Morrison K, Fischli W, Gatfield J, Treiber A, et al. Pharmacology of macitentan, an orally active tissue-targeting dual endothelin receptor antagonist. Journal of Pharmacology and Experimental Therapeutics. 2008;327(3):736-45.
62. Parasuraman S, Raveendran R. Measurement of invasive blood pressure in rats. Journal of pharmacology & pharmacotherapeutics. 2012;3(2):172.
63. O'Sullivan J, Finnie SL, Teenan O, Cairns C, Boyd A, Bailey MA, et al. Refining the Mouse Subtotal Nephrectomy in Male 129S2/SV Mice for Consistent Modeling of Progressive Kidney Disease With Renal Inflammation and Cardiac Dysfunction. Frontiers in Physiology. 2019;10(1365).
64. Kumar MS, Singh A, Jaryal AK, Ranjan P, Deepak K, Sharma S, et al. Cardiovascular autonomic dysfunction in patients of nonalcoholic fatty liver disease. International journal of hepatology. 2016;2016.
65. Vizioli EO, Spadin MD, Correa FM, Viaro F, Evora PR, Chies AB. Acetylcholine-induced aortic relaxation studied in salbutamol treated rats. Journal of smooth muscle research = Nihon Heikatsukin Gakkai kikanshi. 2005;41(5):271-81.
66. Trinder P. Estimation of blood glucose by GOD-POD method. Ann Clin Bio Chem. 1969;6:24.
67. Warnick GR, Wood PD. National Cholesterol Education Program recommendations for measurement of high-density lipoprotein cholesterol: executive summary. The National Cholesterol Education Program Working Group on Lipoprotein Measurement. Clinical chemistry. 1995;41(10):1427-33.
68. Stein A, Mayer G. Triglycerides: GPO-Pap, End point Assay. Clin Chern. 1995;41:1421-6.
69. Toro G, Ackermann PG. Practical clinical chemistry: Little Brown & Company; 1975.
70. Fossati P, Prencipe L, Berti G. Use of 3, 5-dichloro-2-hydroxybenzenesulfonic acid/4-aminophenazone chromogenic system in direct enzymic assay of uric acid in serum and urine. Clinical chemistry. 1980;26(2):227-31.
71. Schoenfeld R, Lewellan C. A colorimetric method for determination of serum chloride. Clinical Chemistry. 1964;10(6):533-9.
72. Lowry OH, Rosebrough NJ, Farr AL, Randall RJ. Protein measurement with the Folin phenol reagent. Journal of biological chemistry. 1951;193:265-75.
73. Miranda KM, Espey MG, Wink DA. A rapid, simple spectrophotometric method for simultaneous detection of nitrate and nitrite. Nitric oxide. 2001;5(1):62-71.

74. Slater T, Sawyer B. The stimulatory effects of carbon tetrachloride and other halogenoalkanes on peroxidative reactions in rat liver fractions in vitro. General features of the systems used. Biochemical Journal. 1971;123(5):805-14.

75. Moron MS, Depierre JW, Mannervik B. Levels of glutathione, glutathione reductase and glutathione S-transferase activities in rat lung and liver. Biochimica et Biophysica Acta (BBA)-General Subjects. 1979;582(1):67-78.

76. Misra HP, Fridovich I. The role of superoxide anion in the autoxidation of epinephrine and a simple assay for superoxide dismutase. Journal of Biological chemistry. 1972;247(10):3170-5.

77. Aebi H. Catalase in vitro. Methods in enzymology. 1984;105:121-6.

78. Zhao Y, Jiang M, Zhou S, Wu S, Zhang X, Ma L, et al. Design, synthesis and structure–activity relationship of oxazolidinone derivatives containing novel S4 ligand as FXa inhibitors. European Journal of Medicinal Chemistry. 2015;96:369-80.

79. Wang Y, Sun X, Yang D, Guo Z, Fan X, Nie M, et al. Design, synthesis, and structure–activity relationship of novel and effective apixaban derivatives as FXa inhibitors containing 1, 2, 4-triazole/pyrrole derivatives as P2 binding element. Bioorganic & medicinal chemistry. 2016;24(21):5646-61.

80. Yamamoto Y, Koike K. Characterization of α1-adrenoceptor-mediated contraction in the mouse thoracic aorta. European journal of pharmacology. 2001;424(2):131-40.

81. Dale M, Haylett D. Pharmacology Condensed. 1st Edn. Chirchill Livingston. Elsevier Ltd., UK. pp; 2004.

82. Liles JT, Dabisch PA, Hude KE, Pradhan L, Varner KJ, Porter JR, et al. Pressor responses to ephedrine are mediated by a direct mechanism in the rat. Journal of Pharmacology and Experimental Therapeutics. 2006;316(1):95-105.

83. Padia SH, Howell NL, Siragy HM, Carey RM. Renal angiotensin type 2 receptors mediate natriuresis via angiotensin III in the angiotensin II type 1 receptor–blocked rat. Hypertension. 2006;47(3):537-44.

84. Smith SA, Williams MA, Leal AK, Mitchell JH, Garry MG. Exercise pressor reflex function is altered in spontaneously hypertensive rats. The Journal of physiology. 2006;577(3):1009-20.

85. Guyenet PG. The sympathetic control of blood pressure. Nature Reviews Neuroscience. 2006;7(5):335-46.

86. Bae EH, Kim IJ, Park JW, Ma SK, Lee JU, Kim SW. Renoprotective effect of rosuvastatin in DOCA–salt hypertensive rats. Nephrology Dialysis Transplantation. 2010;25(4):1051-9.

87. Basting T, Lazartigues E. DOCA-salt hypertension: an update. Current hypertension reports. 2017;19(4):32.

88. Gomes PM, Sá RWM, Aguiar GL, Paes MHS, Alzamora AC, Lima WG, et al. Chronic high-sodium diet intake after weaning lead to neurogenic hypertension in adult Wistar rats. Scientific reports. 2017;7(1):1-14.

89. Stachenfeld NS. Acute effects of sodium ingestion on thirst and cardiovascular function. Current sports medicine reports. 2008;7(4 Suppl):S7.

90. Brooks VL, Scrogin KE, McKEOGH DF. The interaction of angiotensin II and osmolality in the generation of sympathetic tone during changes in dietary salt intake: an hypothesis. Annals of the New York Academy of Sciences. 2001;940(1):380-94.

91. Brooks VL, Haywood JR, Johnson AK. Translation of salt retention to central activation of the sympathetic nervous system in hypertension. Clinical and experimental pharmacology and physiology. 2005;32(5-6):426-32.

92. Wang D, Luo Y, Myakala K, Orlicky DJ, Dobrinskikh E, Wang X, et al. Serelaxin improves cardiac and renal function in DOCA-salt hypertensive rats. Scientific reports. 2017;7(1):1-10.

93. Loch D, Hoey A, Morisseau C, Hammock BO, Brown L. Prevention of hypertension in DOCA-salt rats by an inhibitor of soluble expoxide hydrolase. Cell biochemistry and biophysics. 2007;47(1):87-97.

94. Seifi B, Kadkhodaee M, Karimian SM, Zahmatkesh M, Xu J, Soleimani M. Evaluation of renal oxidative stress in the development of DOCA-salt induced hypertension and its renal damage. Clinical and experimental hypertension. 2010;32(2):90-7.

95. Yemane H, Busauskas M, Burris SK, Knuepfer MM. Neurohumoral mechanisms in deoxycorticosterone acetate (DOCA)–salt hypertension in rats. Experimental physiology. 2010;95(1):51-5.

96. Basting T, Lazartigues E. DOCA-salt hypertension: an update. Current hypertension reports. 2017;19(4):1-8.

97. Reid JL, Zivin JA, Kopin IJ. Central and peripheral adrenergic mechanisms in the development of deoxycorticosterone-saline hypertension in rats. Circulation research. 1975;37(5):569-79.

98. Patil CN, Ritter ML, Wackman KK, Oliveira V, Balapattabi K, Grobe CC, et al. Cardiometabolic effects of DOCA-salt in male C57BL/6J mice are variably dependent on sodium and nonsodium components of diet. American Journal of Physiology-Regulatory, Integrative and Comparative Physiology. 2022;322(6):R467-R85.

99. Grobe JL, Buehrer BA, Hilzendeger AM, Liu X, Davis DR, Xu D, et al. Angiotensinergic signaling in the brain mediates metabolic effects of deoxycorticosterone (DOCA)-salt in C57 mice. Hypertension. 2011;57(3):600-7.

100. Bender SB, McGraw AP, Jaffe IZ, Sowers JR. Mineralocorticoid receptor–mediated vascular insulin resistance: an early contributor to diabetes-related vascular disease? Diabetes. 2013;62(2):313-9.

101. Garg R, Adler GK. Role of mineralocorticoid receptor in insulin resistance. Current Opinion in Endocrinology, Diabetes and Obesity. 2012;19(3):168-75.

102. Favero G, Paganelli C, Buffoli B, Rodella LF, Rezzani R. Endothelium and its alterations in cardiovascular diseases: life style intervention. BioMed research international. 2014;2014.

103. Kim J, Lee YR, Lee C-H, Choi W-H, Lee C-K, Kim J, et al. Mitogen-activated protein kinase contributes to elevated basal tone in aortic smooth muscle from hypertensive rats. European journal of pharmacology. 2005;514(2-3):209-15.

104. Barnes PJ. Receptor heterodimerization: a new level of cross-talk. The Journal of clinical investigation. 2006;116(5):1210-2.

105. Henrion D, Laher I, Laporte R, Bevan JA. Angiotensin II amplifies arterial contractile response to norepinephrine without increasing Ca++ influx: Role of protein kinase C. Journal of Pharmacology and Experimental Therapeutics. 1992;261(3):835-40.

106. Northcott CA, Hayflick JS, Watts SW. PI3-Kinase upregulation and involvement in spontaneous tone in arteries from DOCA-salt rats: is p110δ the culprit? Hypertension. 2004;43(4):885-90.

107. Northcott CA, Poy MN, Najjar SM, Watts SW. Phosphoinositide 3-kinase mediates enhanced spontaneous and agonist-induced contraction in aorta of deoxycorticosterone acetate-salt hypertensive rats. Circulation research. 2002;91(4):360-9.

108. Kim K-I, Lee J-H, Chang H-J, Cho Y-S, Youn T-J, Chung W-Y, et al. Association between blood pressure variability and inflammatory marker in hypertensive patients. Circulation Journal. 2008;72(2):293-8.

109. Santisteban MM, Ahmari N, Carvajal JM, Zingler MB, Qi Y, Kim S, et al. Involvement of bone marrow cells and neuroinflammation in hypertension. Circulation research. 2015;117(2):178-91.

110. Harrison D. Sy 17-2 inflammation, immunity and hypertension. Journal of hypertension. 2016;34:e535.

111. Tanase DM, Gosav EM, Radu S, Ouatu A, Rezus C, Ciocoiu M, et al. Arterial hypertension and interleukins: potential therapeutic target or future diagnostic marker? International journal of hypertension. 2019;2019.

112. Song K, Stuart D, Abraham N, Wang F, Wang S, Yang T, et al. Collecting duct renin does not mediate DOCA-salt hypertension or renal injury. PLoS One. 2016;11(7):e0159872.

113. Artunc F, Amann K, Nasir O, Friedrich B, Sandulache D, Jahovic N, et al. Blunted DOCA/high salt induced albuminuria and renal tubulointerstitial damage in gene-targeted mice lacking SGK1. Journal of molecular medicine. 2006;84(9):737-46.

114. Blasi ER, Rocha R, Rudolph AE, Blomme EA, Polly ML, McMahon EG. Aldosterone/salt induces renal inflammation and fibrosis in hypertensive rats. Kidney international. 2003;63(5):1791-800.

115. Jia Z, Aoyagi T, Yang T. mPGES-1 protects against DOCA-salt hypertension via inhibition of oxidative stress or stimulation of NO/cGMP. Hypertension. 2010;55(2):539-46.

116. Quigley R, Chakravarty S, Zhao X, Imig JD, Capdevila JH. Increased renal proximal convoluted tubule transport contributes to hypertension in Cyp4a14 knockout mice. Nephron Physiology. 2009;113(4):p23-p8.

117. Jennings GL. Recent clinical trials of hypertension management. Hypertension. 2013;62(1):3-7.

118. Sahan-Firat S, Jennings BL, Yaghini FA, Song CY, Estes AM, Fang XR, et al. 2, 3′, 4, 5′-Tetramethoxystilbene prevents deoxycorticosterone-salt-induced hypertension: contribution of cytochrome P-450 1B1. American Journal of Physiology-Heart and Circulatory Physiology. 2010;299(6):H1891-H901.

119. Seifi B, Kadkhodaee M, Karimian SM, Zahmatkesh M, Xu J, Soleimani MJC, et al. Evaluation of renal oxidative stress in the development of DOCA-salt induced hypertension and its renal damage. 2010;32(2):90-7.

120. Li J-M, Shah AM. Mechanism of endothelial cell NADPH oxidase activation by angiotensin II: role of the p47phox subunit. Journal of Biological Chemistry. 2003;278(14):12094-100.

121. Laplante M-A, De Champlain J. The interrelation of the angiotensin and endothelin systems on the modulation of NAD (P) H oxidase. Canadian journal of physiology and pharmacology. 2006;84(1):21-8.

122. Rai R, Sprengeler P, Elrod K, Young W. Perspectives on factor Xa inhibition. Current medicinal chemistry. 2001;8(2):101-19.

123. Pinto DJ, Smallheer JM, Cheney DL, Knabb RM, Wexler RR. Factor Xa inhibitors: next-generation antithrombotic agents. Journal of medicinal chemistry. 2010;53(17):6243-74.

124. De Cristofaro R, De Candia E. Thrombin domains: structure, function and interaction with platelet receptors. Journal of thrombosis and thrombolysis. 2003;15(3):151-63.

125. Barr JD, Chauhan AK, Schaeffer GV, Hansen JK, Motto DG. Red blood cells mediate the onset of thrombosis in the ferric chloride murine model. Blood, The Journal of the American Society of Hematology. 2013;121(18):3733-41.

126. Tseng MT, Dozier A, Haribabu B, Graham UM. Transendothelial migration of ferric ion in FeCl3 injured murine common carotid artery. Thrombosis research. 2006;118(2):275-80.

127. Eckly A, Hechler B, Freund M, Zerr M, Cazenave JP, Lanza F, et al. Mechanisms underlying FeCl3-induced arterial thrombosis. Journal of Thrombosis and Haemostasis. 2011;9(4):779-89.

128. Li W, McIntyre TM, Silverstein RL. Ferric chloride-induced murine carotid arterial injury: A model of redox pathology. Redox biology. 2013;1(1):50-5.